34340

National Library of Canada / Bibliothèque nationale du Canada

CANADIAN THESES ON MICROFICHE / *THÈSES CANADIENNES SUR MICROFICHE*

NAME OF AUTHOR/*NOM DE L'AUTEUR* EARL JAMES FINDLAY

TITLE OF THESIS/*TITRE DE LA THÈSE* PHOSPHOLIPID PHASE STRUCTURE IN PROTHROMBIN ACTIVATION

UNIVERSITY/*UNIVERSITÉ* UNIVERSITY OF ALBERTA

DEGREE FOR WHICH THESIS WAS PRESENTED/ *GRADE POUR LEQUEL CETTE THÈSE FUT PRÉSENTÉE* PH D

YEAR THIS DEGREE CONFERRED/*ANNÉE D'OBTENTION DE CE GRADE* 1977

NAME OF SUPERVISOR/*NOM DU DIRECTEUR DE THÈSE* DR. P. G. BARTON

Permission is hereby granted to the NATIONAL LIBRARY OF CANADA to microfilm this thesis and to lend or sell copies of the film.

The author reserves other publication rights, and neither the thesis nor extensive extracts from it may be printed or otherwise reproduced without the author's written permission.

L'autorisation est, par la présente, accordée à la BIBLIOTHÈQUE NATIONALE DU CANADA de microfilmer cette thèse et de prêter ou de vendre des exemplaires du film.

L'auteur se réserve les autres droits de publication; ni la thèse ni de longs extraits de celle-ci ne doivent être imprimés ou autrement reproduits sans l'autorisation écrite de l'auteur.

DATED/*DATÉ* 21 Sep 77 SIGNED/*SIGNÉ* E J Findlay

PERMANENT ADDRESS/*RÉSIDENCE FIXÉ* 26 Hummingbird Road
Sherwood Park, Alberta
T8A 0A2

NL-91 (3-74)

National Library of Canada

Cataloguing Branch
Canadian Theses Division

Ottawa, Canada
K1A 0N4

Bibliothèque nationale du Canada

Direction du catalogage
Division des thèses canadiennes

NOTICE

The quality of this microfiche is heavily dependent upon the quality of the original thesis submitted for microfilming. Every effort has been made to ensure the highest quality of reproduction possible.

If pages are missing, contact the university which granted the degree.

Some pages may have indistinct print especially if the original pages were typed with a poor typewriter ribbon or if the university sent us a poor photocopy.

Previously copyrighted materials (journal articles, published tests, etc.) are not filmed.

Reproduction in full or in part of this film is governed by the Canadian Copyright Act, R.S.C. 1970, c. C-30. Please read the authorization forms which accompany this thesis.

THIS DISSERTATION
HAS BEEN MICROFILMED
EXACTLY AS RECEIVED

AVIS

La qualité de cette microfiche dépend grandement de la qualité de la thèse soumise au microfilmage. Nous avons tout fait pour assurer une qualité supérieure de reproduction.

S'il manque des pages, veuillez communiquer avec l'université qui a conféré le grade.

La qualité d'impression de certaines pages peut laisser à désirer, surtout si les pages originales ont été dactylographiées à l'aide d'un ruban usé ou si l'université nous a fait parvenir une photocopie de mauvaise qualité.

Les documents qui font déjà l'objet d'un droit d'auteur (articles de revue, examens publiés, etc.) ne sont pas microfilmés.

La reproduction, même partielle, de ce microfilm est soumise à la Loi canadienne sur le droit d'auteur, SRC 1970, c. C-30. Veuillez prendre connaissance des formules d'autorisation qui accompagnent cette thèse.

LA THÈSE A ÉTÉ
MICROFILMÉE TELLE QUE
NOUS L'AVONS REÇUE

THE UNIVERSITY OF ALBERTA

PHOSPHOLIPID PHASE STRUCTURE IN PROTHROMBIN ACTIVATION

by

© Earl James Findlay

A THESIS

SUBMITTED TO THE FACULTY OF GRADUATE STUDIES AND RESEARCH IN PARTIAL FULFILMENT OF THE REQUIREMENTS FOR THE DEGREE OF DOCTOR OF PHILOSOPHY

DEPARTMENT OF BIOCHEMISTRY

EDMONTON, ALBERTA

FALL 1977

THE UNIVERSITY OF ALBERTA

FACULTY OF GRADUATE STUDIES AND RESEARCH

The undersigned certify that they have read, and recommend to the Faculty of Graduate Studies and Research, for acceptance, a thesis entitled "Phospholipid Phase Structure in Prothrombin Activation" submitted by Earl James Findlay in partial fulfilment of the requirements for the degree of Doctor of Philosophy.

Peter G Dalton
.....
Supervisor

Ronald N. McElhaney
.....

Cyril M. Kay
.....

Mark Pozsgay
.....

Julian M. Stuertevant
.....
External Examiner

This thesis is dedicated to

Ora, Matthew and Valerie

ABSTRACT

The physicochemical properties of dioleoylphosphatidylglycerol (DOPG), dimyristoylphosphatidylglycerol (DMPG) and dipalmitoylphosphatidylglycerol (DPPG) in the presence and absence of Ca^{++} and Mg^{++} were examined using differential thermal analysis and light scattering. The thermal behaviour of the sodium salts of the phosphatidylglycerols (PG) was identical to that of the corresponding phosphatidylcholines. Increasing the divalent cation:PG ratio up to 1:2 resulted in a progressive increase in transition temperature to a maximum 20°C above the transition temperature of the PG sodium salt. A similar increase in transition temperature was observed on conversion of the PG sodium salts to their protonated forms. Hysteretic behaviour observed during acid-base titrations of DMPG-Na^{+} was attributed to restricted accessibility of the polar head groups to the bulk aqueous environment under titration conditions.

At greater than a 1:2 ratio of Ca^{++}:PG, DPPG and DMPG formed thermally stable complexes with transition temperatures of 87°C (DMPG-Ca^{++}) and 89°C (DPPG-Ca^{++}). The effect of Ca^{++} (>1:2) on DOPG was less dramatic and resulted in only a 6°C increase in transition temperature. Mg^{++} was not as effective as Ca^{++} in forming stable complexes with DMPG and DPPG. The rate of formation was slower and the PG-Mg^{++} complexes were less stable than PG-Ca^{++} complexes. The rate of Ca^{++} conversion of DMPG and DPPG to stable high-melting complexes

was inversely related to the length of the acyl chains.

The thermal behaviour of binary mixtures of synthetic phosphatidylglycerol sodium salts ($PG\text{-}Na^{+}$) with various synthetic phosphatidylcholines (PC) was examined by differential thermal analysis and light scattering. When the acyl chains of the PGNa and PC components were identical, highly cooperative gel-liquid crystalline transitions were observed at all proportions, indicative of almost ideal miscibility throughout the phase diagram. In contrast, mixing of $PG\text{-}Na^{+}$ and PC with different chain lengths increased the transition width. In the presence of Ca^{2+}, cooperatively melting mixtures were formed when the chain length of the PG was equal to or two carbon atoms shorter than the PC but cooperativity was decreased when the chain length of the PG was two carbon atoms longer than the PC. Greater differences in chain length or mixing saturated and unsaturated chains induced phase separations.

Binary mixtures with identical head group composition but differing in acyl chain composition and phase structure were examined for activity in the reaction:

$$\text{prothrombin} \xrightarrow[\text{phospholipid, } Ca^{++}]{\text{factor } X_a\text{, factor V}} \text{thrombin}$$

Phospholipid mixtures in the gel phase at the reaction temperature were inert. Higher activity was manifested by liquid-crystalline mixtures but optimal activity was observed with mixtures which exhibited lateral phase separation behaviour. Correlation of these results with established

information on lipid-protein (lipid-Ca^{++}-prothrombin, lipid-Ca^{++}-Xa, lipid-V) and protein-protein (Xa-prothrombin, Xa-V, prothrombin-V) interactions in prothrombin activation suggested that orientation of the proteins in an effective catalytic unit was facilitated by the presence of the lateral interfaces at the boundaries between PG-enriched and PC-enriched domains.

ACKNOWLEDGEMENTS

I would like to thank the following people:

Dr. P.G. Barton for his assistance, supervision and tolerance throughout this work, Dr. Helena Horak, Cliff Gibbs and Marina To for their participation in maintaining a friendly working environment conducive to productive research, John Silvius for thought-provoking discussions on a variety of topics, the members and ex-members of the Royal Canadian Mounted Police responsible for the decisions which permitted me to continue this research, and Mrs. Mae Wylie for efficient typing of this thesis under less than ideal conditions.

Financial support by the Royal Canadian Mounted Police is gratefully acknowledged.

TABLE OF CONTENTS

	Page
CHAPTER I - THE PROTHROMBIN ACTIVATION SYSTEM ..	1
A. INTRODUCTION	1
B. PROTHROMBIN	4
1. Structural aspects of prothrombin activation	4
2. Calcium-binding properties of prothrombin	7
3. The nature of the vitamin K-dependent Ca^{++}-binding sites	8
4. Functional significance of vitamin K-dependent Ca^{++}-binding sites	9
C. FACTOR X AND FACTOR Xa	10
1. Structure of Factor X and Factor Xa	10
2. Calcium-binding properties of Factor X (X_a)	10
3. Requirement for intact disulfide bridges for Ca^{++} binding	11
D. FACTOR V	12
1. Structure and activation of Factor V	12
2. Interaction of Factor Va with prothrombin	13
E. THE PHOSPHOLIPID REQUIREMENTS OF PROTHROMBIN ACTIVATION	13
1. The requirement for an acidic lipid component	13
2. Phospholipid requirements for binding the vitamin K-dependent proteins	14
3. Factor V-phospholipid interactions	14
4. Requirement for a liquid-crystalline lipid phase	15

Page

F. RATIONALE FOR USE OF PHOSPHATIDYLGLYCEROLS IN THIS STUDY 16

CHAPTER II - PHYSICOCHEMICAL PROPERTIES OF SYNTHETIC PHOSPHATIDYLGLYCEROLS 17

A. INTRODUCTION 17

B. THERMOTROPIC PROPERTIES OF DLPG 18

1. Effect of pH 18

2. Effect of Ca^{++} 18

3. Effect of Mg^{++} 18

C. FREEZE-FRACTURE STRUCTURES OF DLPG-CORRELATION WITH THERMOTROPIC BEHAVIOUR 21

1. Effect of NaCl on freeze-fracture structure 21

2. Effect of Ca^{++} on freeze-fracture structure 21

3. Effect of Mg^{++} on freeze-fracture structure 21

D. TRANSITION ENTHALPY OF DLPG 22

E. THERMOTROPIC PROPERTIES OF DMPG 23

1. Effect of pH 23

2. Effect of Ca^{++} 23

3. Effect of Mg^{++} 26

F. THERMOTROPIC PROPERTIES OF DPPG 27

G. DMPG:DMPC MIXTURES - THE EFFECTS OF Ca^{++} 27

H. Ca^{++} - ANIONIC PHOSPHOLIPID INTERACTIONS 28

I. Ca^{++}-INDUCED FUSION OF PS-CONTAINING VESICLES 30

J. EFFECTS OF Ca^{++} ON PS VESICLE PERMEABILITY .. 31

K. LATERAL DOMAIN FORMATION - PHASE BOUNDARY LIPID 32

Page

L. THE PURPOSE OF THIS STUDY 34

CHAPTER III - MATERIALS AND METHODS 35

A. MATERIALS 35

B. METHODS 37

1. Chemical Synthesis of DMPG 37

2. Preparation of diacyl phosphatidyl-glycerols 37

3. Extraction procedure for DMPG 38

4. Extraction procedure for DPPG 40

5. Column chromatography purification of DMPG and of DPPG 40

6. Extraction procedure for DOPG 41

7. Preparative thin layer chromatography - DOPG 42

8. General comment on these preparative procedures for the diacyl PGs 42

9. Atomic absorption spectrophotometry 42

10. Phosphorus determinations 43

11. Fatty acid analyses 43

12. Differential thermal analysis 43

(a) Na^{+}-salt of diacyl PGs 43

(b) Protonated diacyl PG 43

13. Nuclear magnetic resonance ^{13}C, ^{1}H 45

(a) Sample preparation 45

14. Sonication of lipids 45

15. Titrations of DMPG 45

16. Clotting assays 46

(a) Reagents 46

Page

(b) Lipid samples 46

(c) Standard 37°C assay 47

(d) Clotting assay at 30°C 48

(e) Clotting assay at 44°C 48

17. Light scattering experiments 48

CHAPTER IV - PHYSICOCHEMICAL STUDIES OF LIPIDS .. 49

A. PROTON MAGNETIC RESONANCE SPECTRUM OF DMPG .. 49

B. ^{13}C NUCLEAR MAGNETIC RESONANCE SPECTRUM OF DMPG .. 49

C. DIFFERENTIAL THERMAL ANALYSIS 54

1. Differential thermal analysis of the sodium salts of synthetic phosphatidylglycerols 54

2. Differential thermal analysis of mixtures of phosphatidylglycerol sodium salts and phosphatidylcholines with identical acyl chains 57

3. Differential thermal analysis of mixtures of phosphatidylglycerol sodium salts and phosphatidylcholines with non-identical acyl chains 57

4. Differential thermal analysis of mixtures of phosphatidylglycerol calcium salts and phosphatidylcholines 67

5. Differential thermal analysis of DPPG-Ca^{++} 77

6. Differential thermal analysis of DMPG-Ca^{++} .. 80

7. Differential thermal analysis of DPPG-Mg^{++} 87

8. Differential thermal analysis of DMPG-Mg^{++} 87

9. Effect of cholesterol on the thermal behaviour of phosphatidylglycerols 92

Page

10. Differential thermal analysis of phosphatidylcholine:phosphatidylglycerol-Ca^{++} mixtures in the presence of cholesterol 103

11. Thermal behaviour of mixtures of phosphatidylglycerol-Na^{+} and phosphatidylglycerol-H^{+} 103

D. TITRATIONS OF DMPG IN AQUEOUS DISPERSION 110

E. THERMAL BEHAVIOUR OF SYNTHETIC PHOSPHOLIPIDS EXAMINED BY LIGHT SCATTERING 118

1. Temperature dependence of light scattering properties of phosphatidylcholines 118

2. Temperature dependence of the light scattering properties of PG:PG mixtures 123

F. DISCUSSION OF THE PHYSICOCHEMICAL STUDIES 138

1. Phosphatidylglycerol-Na^{+} salts 138

2. The effect of Ca^{++} on the thermal behaviour of DMPG and DPPG 140

3. Summary of Ca^{++} effects on thermal behaviour of DLPG, DMPG and DPPG 141

4. The effect of Mg^{++} on the thermal behaviour of DMPG and DPPG 141

5. Postulated mechanisms for Ca^{++}-PG interactions 143

6. Summary of the postulated mechanism for the effects of Ca^{++} on the thermal behaviour of DMPG and DPPG 146

7. The effects of Ca^{++} on the thermal behaviour of PG:PC mixtures 149

8. Effects of cholesterol on DMPG-Na^{+} and DPPG-Na^{+} in the absence of Ca^{++} 155

9. Effects of cholesterol on PG:PC mixtures in the presence of Ca^{++} 155

Page

10. Effects of cholesterol on DPPG-Ca^{++} and DMPG-Ca^{++} 156

CHAPTER V - COAGULATION ASSAY RESULTS 159

1. Calibration with a lipid standard 159

2. Requirement for an acidic lipid component 162

3. Requirement for a liquid-crystalline (fluid) component 166

4. Cooperative and non-cooperative phase transitions 168

5. Fluid phase and fluid-fluid phase separation 169

6. Gel-fluid phase separation 174

7. Lipid composition of the active phase .. 178

A. COMMENT ON THE B & A CEPHALIN CALIBRATION CURVES 179

CHAPTER VI - DISCUSSION - A LIPID PHASE SEPARATION MODEL FOR PROTHROMBIN ACTIVATION 183

A. DESCRIPTION OF THE MODEL 183

B. IMPLICATIONS OF THE MODEL 186

BIBLIOGRAPHY 191

LIST OF TABLES

Table	Description	Page
I	Chemical Shift Assignments-Proton Magnetic Resonance Spectrum of DMPG	51
II	^{13}C Chemical Shift Assignments-DMPG and some Related Compounds	53
III	Transition Temperature of Various Phospholipids in Multilamellar Suspension	58
IV	Thermal Transitions in Synthetic Phosphatidylglycerols and Phosphatidylcholines as Detected by Light Scattering	137
V	Physical States of Lipid Mixtures at Different Temperatures	167

LIST OF FIGURES

Figure		Page
1.	Cascade model for blood coagulation	3
2.	Schematic structure for prothrombin	6
3.	Differential scanning calorimetry of DLPG	20
4.	Effect of Ca^{++} on the phase transition of DMPG	25
5.	Effect of Mg^{++} on the phase transition of DMPG	25
6.	Metastable transition behaviour of DMPG in the presence of high concentrations of Mg^{++}	25
7.	Proton magnetic resonance spectrum of DMPG	50
8.	^{13}C nuclear magnetic resonance spectrum of DMPG	52
9.	Differential thermal analysis thermograms for pure phosphatidylglycerols and pure phosphatidylcholines	56
10.	Differential thermal analysis thermogram of DMPG-Na^{+}:DMPC mixtures	60
11.	Differential thermal analysis thermograms of DOPG-Na^{+}:DOPC and DPPG-Na^{+}: DPPC mixtures	62
12.	Differential thermal analysis thermograms of equimolar mixtures of DMPG-Na^{+} and phosphatidylcholines.	64
13.	Differential thermal analysis thermograms of equimolar mixtures of DPPG-Na^{+} and phosphatidylcholines	66
14.	Differential thermal analysis thermograms of equimolar mixtures of DPPG: DPPC and DPPG:DSPC in the presence of Ca^{++}	69

Figure		Page
15.	Differential thermal analysis thermograms of equimolar mixtures of DPPG:DMPC, DPPG:DLPC and DPPG:DOPC in the presence of Ca^{++}	71
16.	Differential thermal analysis data for mixtures of DMPG and phosphatidylcholines in the presence of Ca^{++}	74
17.	Differential thermal analysis thermograms of mixtures of DOPG with phosphatidylcholines in the presence of Ca^{++}	76
18.	Differential thermal analysis thermograms of DPPG-Ca^{++}	79
19.	Differential thermal analysis thermograms of DPPG-Ca^{++}	82
20.	Differential thermal analysis thermograms of DPPG-Ca^{++}	84
21.	Differential thermal analysis thermogram of DMPG-Ca^{++}	86
22I.	Differential thermal analysis of DPPG	89
22II.	Differential thermal analyses of DPPG-Mg^{++}	89
23.	Differential thermal analysis of DMPG-Mg^{++}	91
24.	Differential thermal analysis of DMPG:cholesterol (3:1)	94
25.	Differential thermal analysis of DPPG:cholesterol (3:1)	96
26.	Differential thermal analysis of DMPG:cholesterol (2:1)	100
27.	Differential thermal analysis of DPPG:cholesterol mixtures	102
28.	Effect of cholesterol on the thermal behaviour of DPPG-Ca^{++}:DLPC mixtures	105
29.	Differential thermal analysis of mixtures of DPPG-Na^{+} and DPPG-H^{+}	107

Figure		Page
30.	Differential thermal analysis of mixtures of DMPG-Na^+ and DMPG-H^+	109
31.	Differential thermal analysis of a mixture of DMPG-Na and DMPG-H^+	112
32.	Hysteretic effect during titration of DMPG	114
33.	Titration curves of DMPG-Na^+	116
34.	Temperature dependence of intensity of light scattered at 90°C (I_{90}) from DMPC aqueous dispersion	120
35.	Temperature dependence of intensity of light scattered at 90° from a DPPC aqueous dispersion	122
36.	Temperature dependence of intensity of light scattered at 90° from a DMPG:DMPC aqueous dispersion	125
37.	Temperature dependence of intensity of light scattered at 90° from a DPPG:DPPC aqueous dispersion	127
38.	Temperature dependence of intensity of light scattered at 90° from a DMPG:DLPC aqueous dispersion	129
39.	Temperature dependence of intensity of light scattered at 90° from a DMPG:DLPC aqueous dispersion	132
40.	Temperature dependence of intensity of light scattered at 90° from a DPPG:DLPC aqueous dispersion	134
41.	Effect of phospholipid concentration on the gel-liquid-crystalline transition temperature	136
42.	Effect of dehydration on thermal behaviour of DPPG-Ca^{++}	148
43.	Differential thermal analysis of DMPG-Ca^{++}:DMPC	151
44.	Schematic illustration of thermal transition events during heating of DPPG-Ca^{++}:DOPC	154

Figure		Page
45.	Clotting times as a function of Bell & Alton cephalin concentration	161
46.	Clotting activity-composition profiles for DMPG:PC mixtures at T = 30°C	163
47.	Clotting activity-composition profiles for DMPG:PC mixtures at T = 37°C	164
48.	Clotting activity-composition profiles for DMPG:PC mixtures at T = 44°C	165
49.	Clotting activity-composition profiles for DMPG:DLPC and DOPG:DOPC	171
50.	Clotting activity-composition profiles for DOPG:DOPC and DPPG:DLPC mixtures	176
51.	Clotting activity-composition profiles for DOPG:DSPC and DPPG:DOPC mixtures	177
52.	Effect of sonication on clotting times	182
53.	Schematic illustration of prothrombin activation model	185
54.	Effect of cholesterol on the clotting activity of PG:PC mixtures	189

LIST OF ABBREVIATIONS

γ-carboxyglutamic acid	- 3-aminopropane-1,1,3-tricarboxylic acid
diC_n	- notation for describing the acyl chain lengths of diacyl phospholipids. C_n refers to the number of methylene groups in the hydrocarbon chains
DSC	- differential scanning calorimetry
DTA	- differential thermal analysis
DLPC	- dilauroylphosphatidylcholine
DMPC	- dimyristoylphosphatidylcholine
DOPC	- dioleoylphosphatidylcholine
DPPC	- dipalmitoylphosphatidylcholine
DSPC	- distearoylphosphatidylcholine
DOPE	- dioleoylphosphatidylethanolamine
DLPG	- dilauroylphosphatidylglycerol
DMPG	- dimyristoylphosphatidylglycerol
DOPG	- dioleoylphosphatidylglycerol
DPPG	- dipalmitoylphosphatidylglycerol
DSPS	- distearoylphosphatidylserine
e.s.r.	- electron spin resonance
g.l.c.	- gas-liquid chromatography
Δ^H	- phase transition enthalpy
$I_{90°}$	- intensity of light scattered at 90° to incident light beam
Na_2EDTA	- disodium salt of ethylenediaminetetraacetic acid
NMR	- nuclear magnetic resonance
PC	- phosphatidylcholine (1,2-diacyl-sn-glycero-3-phosphocholine)

PE	- phosphatidylethanolamine (1,2-diacyl-sn-glycero-3-phosphoethanolamine)
PG	- phosphatidylglycerol (1,2-diacyl-sn-glycero-3-phospho-1-glycerol)
PI	- phosphatidylinositol (1,2-diacyl-sn-glycerol-3-phosphoinositol)
PS	- phosphatidylserine (1,2-diacyl-sn-glycero-3-phospho-L-serine
T_c	- phospholipid phase transition temperature
$_{s}T_{90}^{10}$	- phospholipid phase transition width determined by light scattering
t.l.c.	- thin layer chromatography
Tempo	- 2,2,6,6-tetramethylpiperidine-1-oxyl. An electron spin resonance probe

CHAPTER I

THE PROTHROMBIN ACTIVATION SYSTEM

A. INTRODUCTION

Coagulation of mammalian blood is the end result of a series of complex, interrelated, biochemical reactions. With the exceptions of the conversion of fibrinogen* to fibrin and the subsequent cross-linking of the fibrin monomers, these reactions primarily involve conversion of inactive enzyme precursors to active proteolytic enzymes (Fig. 1). In mammals, two separate pathways leading to blood coagulation converge with the activation of Factor X. The first reaction common to both pathways is the proteolytic cleavage of prothrombin by activated Factor X (Factor Xa) to form thrombin. This reaction is a focal event in blood coagulation and the reaction product, thrombin, may also be involved in other hemostatic processes such as platelet aggregation and serotonin release (8).

Optimal conversion of prothrombin to thrombin *in vitro* requires at least four components in addition to prothrombin. Factor Xa is the only one of these components that can activate prothrombin (9-12). However, the inclusion of an additional plasma coagulation factor (Factor V) and phospholipid to a Factor Xa-Ca^{++} mixture causes a dramatic increase in the rate of prothrombin activation (13,14).

* The nomenclature used for the blood coagulation system components is that recommended by the Task Forces of the International Society of Thrombosis and Haemostasis. Unless otherwise specified the clotting factors discussed are of bovine origin.

Figure 1. Cascade model for blood coagulation (1). Except for the two initial stages of intrinsic and extrinsic systems, an enzyme in conjunction with accessory components of the activation complex converts the substrate from an inactive to a highly active proteolytic enzyme which then becomes the proteinase in the subsequent stage. Four of the coagulation factors are "vitamin K-dependent" proteins: Factor VII, Factor IX, Factor X and prothrombin. Recent discussions of the two initial stages can be found in the monograph edited by Reich et al. (2). Participation of accessory components in the early stages is less well defined than in late stages. Accessory component labelled 1 could be the surface activator of Factor XII. A plasma activity has been described but not chemically characterized (3) that participates in Factor XI activation. Evidence has been presented (4,5,6) that indicates platelet involvement in the stages involving Factors XII, XI, and IX may be of primary importance. For a review of the entire coagulation process see Davie and Fujikawa (7).

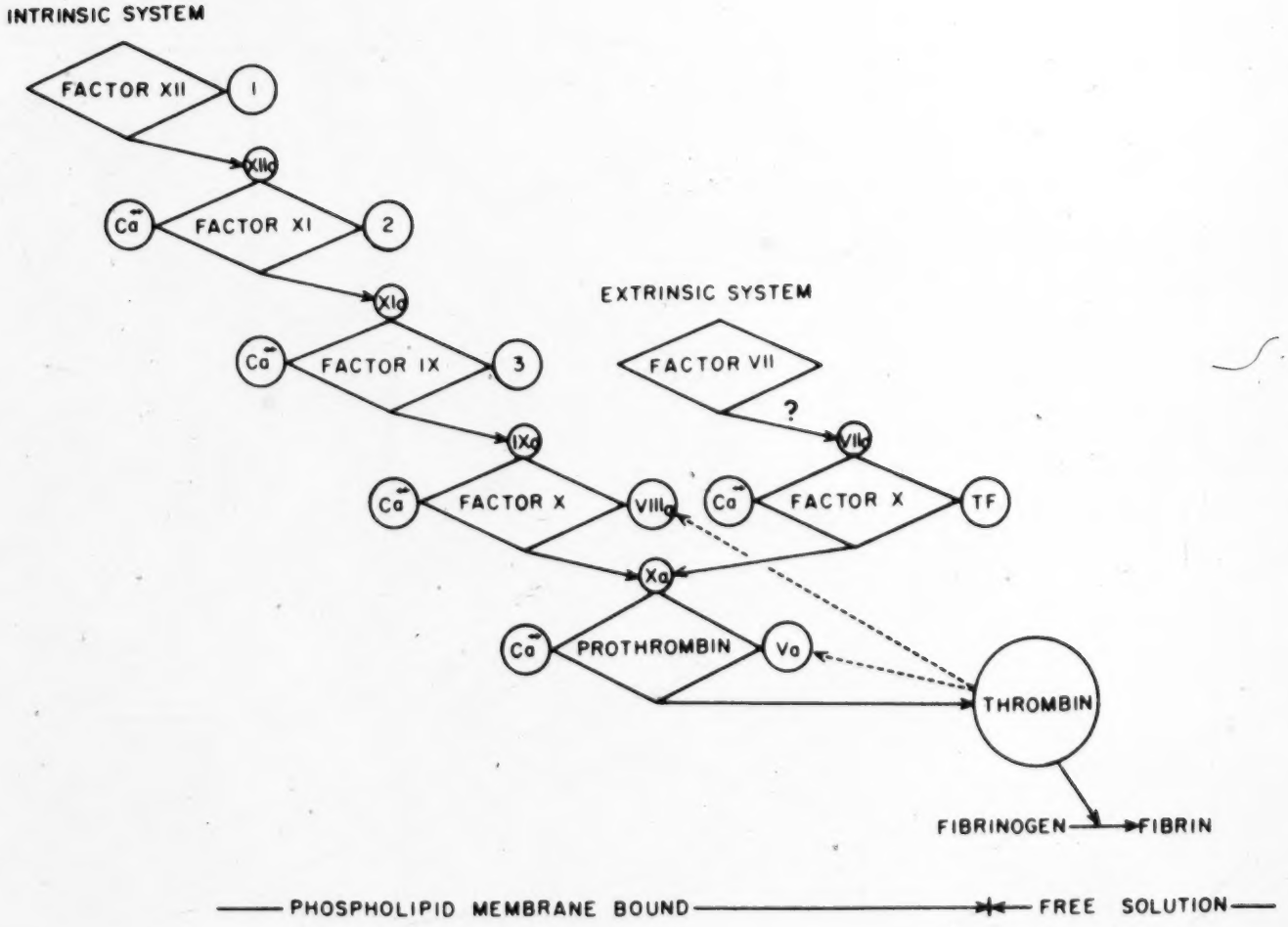
INTRINSIC SYSTEM
FACTOR XII
I
XIIa
Ca
FACTOR XI
2
XIa
Ca
FACTOR IX
3
IXa
Ca
FACTOR X
VIIIa
EXTRINSIC SYSTEM
FACTOR VII
?
VIIa
Ca
FACTOR X
TF
Xa
Ca
PROTHROMBIN
Va
THROMBIN
FIBRINOGEN
FIBRIN
PHOSPHOLIPID MEMBRANE BOUND
FREE SOLUTION

This increases the rate of thrombin production to at least 1,000 times (14) and as much as 19,000 times (13) that observed with Factor Xa alone.

Sufficient evidence has now accumulated to show Factor Xa, Factor V, phospholipid and Ca^{++} can combine to form a particulate complex, termed 'prothrombinase', capable of binding prothrombin and converting it to thrombin (8). As much of the recently published information concerning the nature of the lipid-protein and protein-protein interactions during prothrombin activation is pertinent to the work contained in this thesis it will be briefly reviewed.

B. PROTHROMBIN

1. Structural aspects of prothrombin activation

Prothrombin is a plasma glycoprotein with a molecular weight of approximately 72,000 (15,16). It consists of a single polypeptide chain with five intra-chain disulfide bridges. The amino acid composition and sequence have been determined (17,18).

During activation, prothrombin is converted to thrombin plus smaller polypeptide segments called activation fragments (Fig. 2). The number of activation fragments formed varies with the activation conditions. These proteolysis products have been characterized in detail by several laboratories (19,20,21). The total mass of the prothrombin molecule can be accounted for in the two usually observed fragments (prothrombin fragment 1, prothrombin fragment 2)

Figure 2. Schematic structure for prothrombin. Prethrombin implies that the amino acid sequence ultimately giving rise to thrombin is contained in the polypeptide: fragment implies that the polypeptide is not finally associated with thrombin. The three peptide bonds cleaved during prothrombin activation are designated 1, 2 and 3. If bond 1 is cleaved two products are formed: Prothrombin Fragment 1 and Prethrombin 1. Prothrombin Fragment 1 consists of the region from the amino terminus to bond 1 (Arg 156, Ser 157). Prethrombin 1 is the polypeptide from bond 1 to the carboxyl terminus of prothrombin. Cleavage of bond 2 (Arg 274, Thr 275) yields Prothrombin fragment 1-2 and Prethrombin 2. Cleavage of bond 1 in Fragment 1-2 yields Prothrombin Fragment 1 and Prothrombin Fragment 2. Cleavage of bond 3 (Arg 323, Ile 324) in Prethrombin 2 yields thrombin, a disulfide linked two chain enzyme in which the polypeptide chain between bonds 2 and 3 is designated the A chain and the polypeptide from bond 3 to the carboxyl terminus is designated the B chain. In human prothrombin, an additional bond, 2' is cleaved which results in formation of an A chain of human thrombin which is 13 amino acid residues shorter than the A chain of bovine thrombin. Numbers in parentheses are molecular weights x 10^{-3} (1).

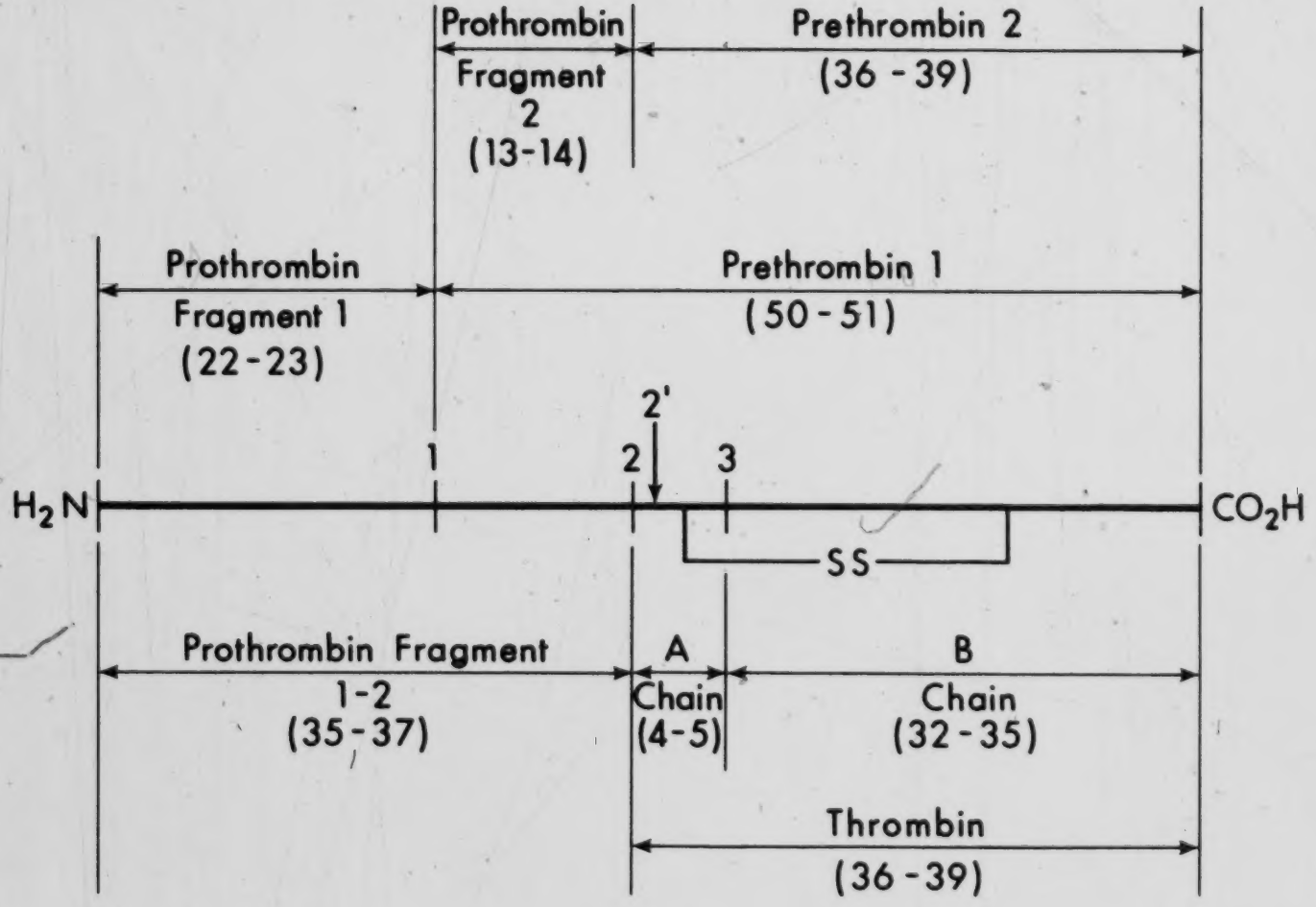
Prothrombin
Fragment
2
(13-14)
Prethrombin 2
(36 - 39)
Prothrombin
Fragment 1
(22-23)
Prethrombin 1
(50 - 51)
2'
1
2
3
H2N
CO2H
SS
Prothrombin Fragment
1-2
(35-37)
A
Chain
(4-5)
B
Chain
(32-35)
Thrombin
(36-39)

and thrombin.

2. Calcium binding properties of prothrombin

The first quantitative analysis of Ca^{++} binding to prothrombin (22) reported the existence of two classes of binding sites with characteristics n = 4, log K_{assoc} = 4.0 and n = 12, log K_{assoc} = 2.57. More recently, Mann et al. (23) reported 10 to 11 binding sites. Six of these sites, located in fragment 1, had log K_{assoc} = 3.5. Five weaker binding sites with log K_{assoc} = 2.7 were present in the fragment 2 region. Stenflo and Ganrot (24) reported binding of 10 to 12 moles of Ca^{++} per mole of prothrombin with three high affinity sites (log K_{assoc} = 4.3) that exhibited positive cooperativity.

A conformational change associated with Ca^{++} binding could be demonstrated by circular dichroism (25), ultraviolet spectral changes (26) and sedimentation velocity analytical centrifugation (27). Similar Ca^{++} binding behaviour and conformational changes were observed for isolated prothrombin fragment 1 (26) whereas binding to prethrombin 1 was weak and did not show positive cooperativity (23).

Qualitatively there is general agreement that prothrombin contains two types of Ca^{++} binding sites. However, the quantitative disparity among the data from various Ca^{++}-binding studies implies that the binding probably does not fit any simple model. Benson et al. (28,29), for example,

have interpreted their data as indicating no positive co-operativity in Ca^{++} binding to either prothrombin or isolated fragment 1.

Recently Henricksen and Jackson (26) have described changes in Ca^{++} binding isotherms, resulting from changes in buffer systems, that have no doubt complicated the correlation of results from the various studies.

3. The nature of the vitamin K-dependent Ca^{++} binding sites

In 1974, Stenflo succeeded in isolating a tetrapeptide with the apparent composition leu-glu-glu-val from the amino terminal region of prothrombin (30). This tetrapeptide had an inordinately high anodal electrophoretic mobility relative to a chemically synthesized tetrapeptide of the same sequence. A combination of mass spectrometry, proton magnetic resonance and chemical modification demonstrated that the glutamic acid residues of the tetrapeptide each had an additional carboxyl group attached to the gamma carbon. The structure of these γ-carboxyglutamic acid residues (3-aminopropane-1,1,3-tricarboxylic acid) was confirmed by several other groups (31,32,33). Magnusson *et al.* (33) have shown that all of the first 10 glutamic acid residues of prothrombin fragment 1 are modified to γ-carboxyglutamic acid.

The γ-carboxyglutamic acid residues appear to be formed post-ribosomally as a consequence of a vitamin K-dependent carboxylation process (31,34).

4. Functional significance of vitamin K-dependent Ca^{++}-binding sites

In mammals, deficiency of vitamin K, or administration of vitamin K antagonists results in biosynthesis of abnormal prothrombin which cannot be activated by prothrombinase (24,35). This abnormal prothrombin does not contain the γ-carboxyglutamate residues present in normal prothrombin (30,36), does not bind Ca^{++} (27,37), and does not bind to phospholipids (38,39).

In the absence of phospholipid, the rate of activation of abnormal prothrombin by Factor Xa-Ca^{++} is the same as that of normal prothrombin (39). Addition of phospholipid to Factor Xa-Ca^{++} results in a 50-fold increase in the activation rate of normal prothrombin while the rate for abnormal prothrombin remains the same (39).

Activation of prethrombin 1 (prothrombin minus fragment 1) is not accelerated by phospholipid and binding of this intermediate to phospholipid cannot be demonstrated (40). Fragment 1 does bind to phospholipid in the presence of Ca^{++} (26,40,41). These data are consistent with the idea that the vitamin K-dependent γ-carboxyglutamate residues of fragment 1 are required for the Ca^{++}-mediated binding of prothrombin to the phospholipid component of the prothrombinase complex.

C. FACTOR X AND FACTOR Xa

1. Structure of Factor X and Factor Xa

Factor X, a glycoprotein, has a molecular weight of 55,000 and contains 10% carbohydrate including 3.8% neuraminic acid, 2.9% hexose and 3.6% hexoseamine (42). It consists of two polypeptide chains, a light chain of M.W. 17,000 and a heavy chain with M.W. 38,000, linked by disulfide bridges. During activation a polypeptide of M.W. 11,000 is cleaved from the heavy chain to yield Factor Xa with M.W. 44,000 (43). Activation can occur via the intrinsic pathway (IXa, phospholipid, Ca^{++}) or via a number of extrinsic routes including proteolysis by Russell viper venom, trypsin (44) or Factor VIIa (Fig. 1).

2. Calcium-binding properties of Factor X(Xa)

Like prothrombin, Factor X(Xa) has two classes of Ca^{++} binding sites. The site characteristics are n = 2-3, $\log K_{assoc}$ = 3.5 - 3.6 and n = 25, $\log K_{assoc}$ = 2.6 (45). Factor X(Xa) also undergoes a conformational change upon binding Ca^{++} (46). The Ca^{++}-binding properties of Factor X(Xa) are vitamin K-dependent (47).

The presence of γ-carboxyglutamic acid residues in the light chain (48) and the striking homology in the primary structure of the 44 amino terminal residues of the light chain of Factor X(Xa) and the 45 amino terminal residues of prothrombin (1) support the proposal that the light chain contains the phospholipid binding sites (49). The intact

Factor Xa molecule binds to phospholipid in the presence of Ca^{++} (50). However, in contrast to prothrombin fragment 1, the isolated light chain of Factor X(Xa) does not bind to phospholipid.

3. Requirement for intact disulfide bridges for Ca^{++} binding

Henricksen and Jackson (26) recently studied the effect of reduction of the intra-chain disulfide bridges on the Ca^{++}- and phospholipid-binding properties of prothrombin fragment 1 and Factor X(Xa). They reported loss of positive cooperativity and lowered affinity for Ca^{++} when the disulfide bridges were reduced and postulated a secondary and/or tertiary structure involvement in maintaining the Ca^{++} binding groups in an optimal spatial arrangement, similar to the situation with chelating agents. These observations have been confirmed by Nelsestuen *et al*. (51).

Prothrombin fragment 1 and the light chain of Factor X, both with intra-chain disulfide bridges reduced, had very similar Ca^{++}-binding isotherms (26,51). Failure to demonstrate cooperative 'tight' binding of Ca^{++} to the isolated light chain of Factor X(Xa) under 'non-reducing' conditions may have been due to failure to obtain the light chains with intra-chain disulfide bridges intact (26,51).

D. FACTOR V

1. Structure and activation of Factor V

Factor V is the least well characterized of the prothrombin activation system components. Attempts at purification have been complicated by a complex sub-unit structure, a propensity to aggregate and a well documented instability (52,53).

The native form of Factor V in bovine plasma has a molecular weight of about 400,000 and is converted to an active species (Factor Va) with a molecular weight of approximately 250,000 (52,53). Factor V(Va) has no proteolytic activity in the prothrombin activation system. However, activation enhances the ability of Factor V to interact with prothrombin (see below).

Activation can occur by exposure to thrombin (54), Russell viper venom (55), or cellulose phosphate (52). A recent study (56) suggests activation by non-enzymatic methods results in a dissociated form of native Factor V(Vd) with M.W. 276,000 while enzymatic activation results in Factor Va with M.W. 213,000. Thrombin inactivated by diisopropylfuorophosphate does not activate Factor V (57), suggesting the molecular mechanisms involved in Factor V activation by the enzymatic and non-enzymatic means are quite different. Papahadjopoulos *et al*. (58) proposed that activation of Factor V involved splitting a bond between two subunits, one or both of which were more active when separated. It is possible the enzymatic activation involves

separation of subunits in association with minor proteolysis. However this mechanism remains to be elucidated.

2. Interaction of Factor Va with prothrombin

Jackson et al. (59) have reported that activation of Factor V converted it from a form incapable of binding prothrombin to an activated form capable of binding quantitatively and reversibly to a prothrombin-sepharose column. Subsequently it was found that Factor Va acceleration of prothrombin activation required, in addition to Ca^{++}, fragment 2 or fragment 1-2 either covalently or non-covalently associated with prethrombin 2 (23,60). Mann et al. (23) concluded that the 'strong' binding sites of fragment 1 were phospholipid binding sites and the 'weak' sites of fragment 2 were the Factor Va binding sites. However, Hanahan et al. (50) have reported failure to demonstrate any stable complex formation between Factor Va and prothrombin in the absence of phospholipid.

E. THE PHOSPHOLIPID REQUIREMENTS OF PROTHROMBIN ACTIVATION

1. The requirement for an acidic lipid component

Studies of the correlation between negative surface charge density and coagulant activity of phospholipid dispersions have indicated an apparent requirement for an 'optimal surface charge' (61,62). However, it was later postulated that this requirement might merely reflect the need for interfacial groups capable of binding Ca^{++} in a specified lattice complementary to the spatial arrangement

of the γ-carboxyglutamic acid residues of the coagulant proteins (63).

2. Phospholipid requirements for binding the vitamin K-dependent proteins

The binding of the vitamin K-dependent proteins to phospholipids requires Ca^{++} and negatively charged phospholipid functional groups. Prothrombin in the presence of Ca^{++} forms stable complexes with phosphatidylserine (PS), phosphatidic acid (PA) (64), phosphatidylglycerol (PG) (40) and mixtures of these anionic lipids with phosphatidylcholine (PC) and phosphatidylethanolamine (PE), but not with PC or PE alone (40,50,64). Chelation of the Ca^{++} with EDTA results in dissociation of the complexes (54). Similar results have been obtained with Factor X(Xa) (50,54).

The data available are consistent with a mechanism that involves a Ca^{++}-mediated interaction between the negatively charged phospholipid polar head groups and the γ-carboxyglutamate residues of the proteins. However, the stoichiometry of these interactions has not been determined.

3. Factor V - phospholipid interactions

In contrast to the well-defined interactions of the vitamin K-dependent proteins with phospholipids, the molecular details of the Factor V-phospholipid association are not clear.

Association of Factor V with phospholipid does not require added Ca^{++} (50,65,66) and has been reported to

involve hydrophobic effects (66,67). Factor V binds to mixtures of zwitterionic and acidic phospholipids (65,66) and Hanahan et al. (50) have reported a mandatory requirement for acidic phospholipid. However, Colman et al. (53) have reported formation of Factor V-phosphatidylethanolamine (PE) complexes. Complexes containing Factor V and catalytically hydrogenated PE had very low clotting activity relative to complexes formed with naturally occurring PE, indicating a possible requirement for a liquid-crystalline lipid state (53) for catalytically effective Factor V-phospholipid complexes.

4. Requirement for a liquid-crystalline lipid phase

Sterzing and Barton (68) had demonstrated that a liquid-crystalline lipid phase was required for high clotting activity. Catalytically hydrogenated PS was found to be inactive at 37°C but activity could be restored by the addition of cholesterol. Cholesterol eliminated the phase transition of the PS (Tc = 72°C), as detected by differential thermal analysis and presumably 'fluidized' the lipid.

Apart from this study, the main thrust of the research in this area had been directed toward defining the lipid chemical properties and the optimal ratio of anionic to zwitterionic phospholipid necessary for procoagulant activity. No systematic study had been done to correlate the physical state of the lipids with their ability to function in the prothrombin activation system.

F. RATIONALE FOR USE OF PHOSPHATIDYLGLYCEROLS IN THIS STUDY

Phospholipids with a net negative charge at physiological pH include PA, PS and PG. Barton et al. (64) had shown that PA-PC mixtures, while capable of forming complexes with prothrombin in the presence of Ca^{++}, showed little clotting activity.

Mixtures of PS-PC demonstrate high clotting activity. However, it was felt that synthesis of PS, by current methods, in quantities adequate for the planned physical studies, would be prohibitively time consuming.

Phosphatidylglycerols on the other hand had been shown to be relatively easy to prepare from synthetic PCs by the transphosphatidylase function of phospholipase D (EC 3.1.4.4) (70) and PG-PC mixtures had demonstrated the ability to form complexes with prothrombin which were effective in thrombin generation. As the physical characterization of the lipid system used would require relatively large amounts of acidic lipid, it was felt that the PGs were most amenable to investigation.

CHAPTER II

PHYSICOCHEMICAL PROPERTIES OF SYNTHETIC PHOSPHATIDYLGLYCEROLS

A. INTRODUCTION

The transphosphatidylase function of phospholipase D (phosphatidylcholine phosphatidohydrolase EC 3.1.4.4) was first investigated, in detail, by Yang, Freer and Benson (70). They suggested it offered a useful route for synthesis of a variety of phosphatidylesters including phosphatidylglycerols. The configuration of the glycerol moiety in the phosphatidylglycerol produced was a racemic mixture of 1-sn-glycerol and 3-sn-glycerol indicating the phosphatidylation step was not stereospecific (70,71).

Although phosphatidylglycerol, prepared by the action of phospholipase D on egg lecithin, was used for studies involving black-film bilayers (72) and cation permeability of liposomes (73,74), very little detailed information concerning the ionic and thermotropic properties of the phosphatidylglycerols was available prior to 1973. Since that time studies of synthetic phosphatidyl glycerols (DLPG, DMPG, DPPG) have done much to characterize the properties of this class of phospholipid. These studies are directly relevant to the work in this thesis so their results will be discussed.

B. THERMOTROPIC PROPERTIES OF DLPG

1. Effect of pH

The gel to liquid-crystalline transition of DLPG in NaCl (0.1M, pH 6), as detected by DSC, was reported to occur at 3°C (75). A later paper (76) reported a double peaked transition for DLPG in NaCl (0.1M, pH 7) centered at 0°C. At pH 3, a broad double transition centered at approximately 10°C was observed.

2. Effect of Ca^{++}

Addition of Ca^{++}, up to a ratio of Ca^{++}:DLPG of 1:2, resulted in a single DSC peak at 18°C. With Ca^{++}:DLPG ratios greater than 1:2, the transition temperature was raised to about 75°C (76).

3. Effect of Mg^{++}

Similar to Ca^{++}, addition of Mg^{++} up to a 1:2 ratio of Mg^{++}:DLPG resulted in a single DSC endotherm at 18°C (77). Ratios of Mg^{++}:DLPG greater than 1:2 resulted in a complex thermogram (Fig. 3) with endothermic transitions at 20°C and 75°C. The 20°C transition was followed immediately by an exotherm. These calorimetric results were interpreted as indicating: (1) a metastable gel phase below 20°C; (2) a stable gel phase between 20°C and 75°C; (3) a liquid-crystalline phase above 75°C which could exhibit substantial supercooling (77).

Figure 3. Differential scanning calorimetry of DLPG.

(a) Heating scan of DLPG in the presence of Mg^{++} (Mg^{++}:DLPG > 1:2).

(b) Rescanning from +30°C to +90°C after cooling to +30°C.

(c) Heating curve between -20°C and +50°C.

(d) Rescanning from -20°C to +90°C after cooling the sample from +50°C to -20°C.

Reference 76.

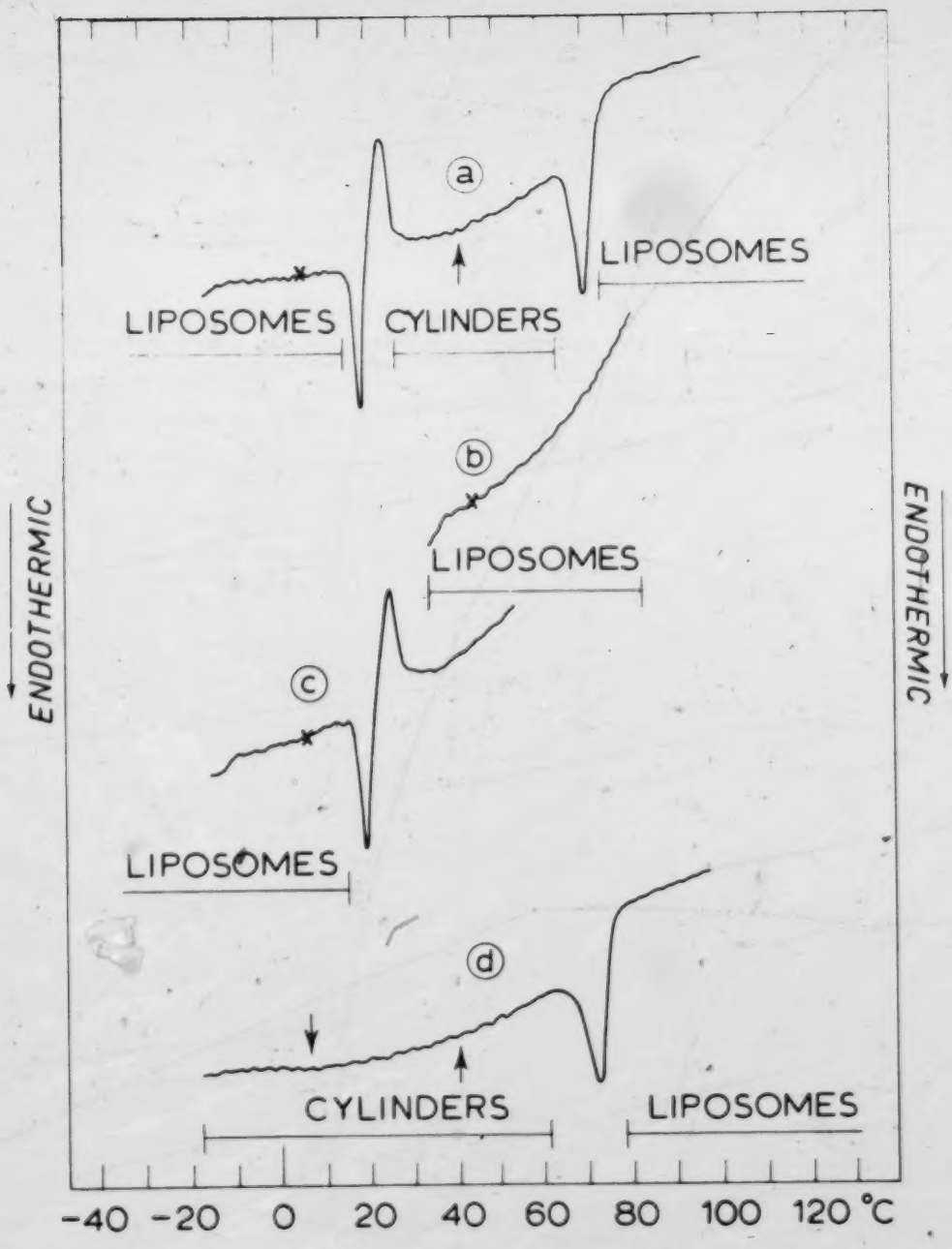
a
LIPOSOMES
LIPOSOMES
CYLINDERS
b
LIPOSOMES
ENDOTHERMIC
ENDOTHERMIC
c
LIPOSOMES
d
CYLINDERS
LIPOSOMES
-40 -20 0 20 40 60 80 100 120 °C

C. FREEZE-FRACTURE STRUCTURES OF DLPG-CORRELATION WITH THERMOTROPIC BEHAVIOUR

1. Effect of NaCl on freeze-fracture structure

In excess distilled water, DLPG formed a transparent suspension with no definite structures detectable by freeze-fracture electron microscopy (75). When NaCl was present (0.1M, pH 6) the suspension became opalescent and small vesicle-like structures were visible.

2. Effect of Ca^{++} on freeze-fracture structures

With Ca^{++}:DLPG ratios less than 1:2, liposomal structures were observed (76). Increasing the Ca^{++}:DLPG ratio to greater than 1:2 resulted in formation of large cylinders of tightly packed lamellae termed cochleate cylinders (76). It was postulated that these cochleate cylinders resulted from formation of a DLPG-Ca-DLPG complex which stabilized the bilayer structure resulting in the high transition temperature (T_c = 75°C).

3. Effect of Mg^{++} on freeze-fracture structures

The structures of the three Mg^{++}:DLPG (1:2) phases detected by DSC were examined by quenching samples rapidly from different points within the DSC scan (Fig. 3). The metastable gel phase (below 20°C) and the liquid crystalline phase (above 75°C-supercooling to 20°C) revealed liposomal structures while the stable gel phase was characterized by the presence of cochleate cylinders (76). The conversion of

the liposomal structures to the more highly ordered cylindrical structures presumably accounts for the exotherm observed immediately following the gel-liquid crystalline transition of the liposomes.

D. TRANSITION ENTHALPY OF DLPG

The latent heat of transition for DLPG in NaCl (0.1M, pH 6) was reported as 4.5 kcal/mole (77), which was similar to the 4.3 kcal/mole observed for DLPC. This value for DLPG is considerably higher than the 1.7 kcal/mole determined by high-sensitivity DSC (78). However, it compares favourably with the 4.77 kcal/mole which corresponds to the area under the total broad (-4°C to 10°C) transition curve observed with DLPC (78). The sharp DLPC peak at -1.8°C seen with high sensitivity DSC and used to determine the 1.7 kcal/mole value (78) was not resolvable with standard DSC methods (77). However, determined under identical experimental conditions, the transition enthalpies for DLPC and DLPG-Na^+ appear to be very similar (77). An analogous observation has been made for DMPG-Na^+ (6.8 kcal/mole) and DMPC (6.7 kcal/mole) (79).

Addition of Mg^{++} or Ca^{++} (Mg^{++} or Ca^{++}:DLPG less than 1:2) increased the transition enthalpy to 5.5 kcal/mole (77). This was interpreted as indicating a stabilization of the hydrophobic regions of the liposomal systems due to cation induced changes in polar head group spacing. This interpretation was supported by monolayer studies which indicated a decrease in the average area per molecule from 62$Å^2$ (NaCl,

0.1M, pH 6) to 54Å^2 in $CaCl_2$ (0.1M pH 6) (75).

The cochleate cylinders formed at high Mg^{++} or Ca^{++} concentrations melted with an unusually high enthalpy change (ΔH = 10 kcal/mole) (77). It was suggested that this high enthalpy change reflected the simultaneous disruption of the highly ordered lattice structure of the cylinders and melting of the hydrocarbon chains.

E. THERMOTROPIC PROPERTIES OF DMPG

1. Effect of pH

The gel to liquid-crystalline transition of DMPG in NaCl (0.12M, pH 7) as detected by DSC occurred at 23°C (79). Little change in transition temperature was observed when the pH was lowered to 3. However, the DSC peak was slightly broadened.

2. Effect of Ca^{++}

As the Ca^{++}:DMPG ratio was increased to 1:2 a gradual increase in transition temperature was observed. The maximum increase obtained was approximately 18°C. This increase was accompanied by a rise in transition enthalpy from 6.8 to 7.9 kcal/mole (79). Freeze-fracture electron microscopy indicated liposomal structures were present at low Ca^{++} concentrations. When the Ca^{++}:DMPG ratio was greater than 1:2, the transition temperature was raised to 89°C with an enthalpy change of 15.2 kcal/mole accompanying the transition (Fig. 4). Freeze-fracture electron microscopy of this high melting form showed

Figure 4. Effect of Ca^{++} on the phase transition of DMPG (79).

(a) Heating scan (DSC) of sample dispersed in 120 mM NaCl at pH 7.

(b) DMPG dispersed in 24mM $CaCl_2$ at pH 7.

(c) DMPG heating scan in 48 mM $CaCl_2$ at pH 7.

(d) Heating scan in 120mM $CaCl_2$ at pH 7.

Figure 5. Effect of Mg^{++} on the phase transition of DMPG (79).

(a) DSC heating scan of DMPG in 120mM NaCl at pH 7.

(b) DSC heating scan in 24mM $MgCl_2$ at pH 7.

(c) DSC heating scan in 48mM $MgCl_2$ at pH 7.

(d) DSC heating scan in 120mM $MgCl_2$ at pH 7.

Figure 6. Metastable transition behaviour of DMPG in the presence of high concentrations of Mg^{++} (79).

(1) Complete cooling curve; (2) complete heating curve;
(3) cooling curve to 50°C, followed by (4) heating;
(5) heating to 40°C, followed by cooling and
(6) complete reheating.

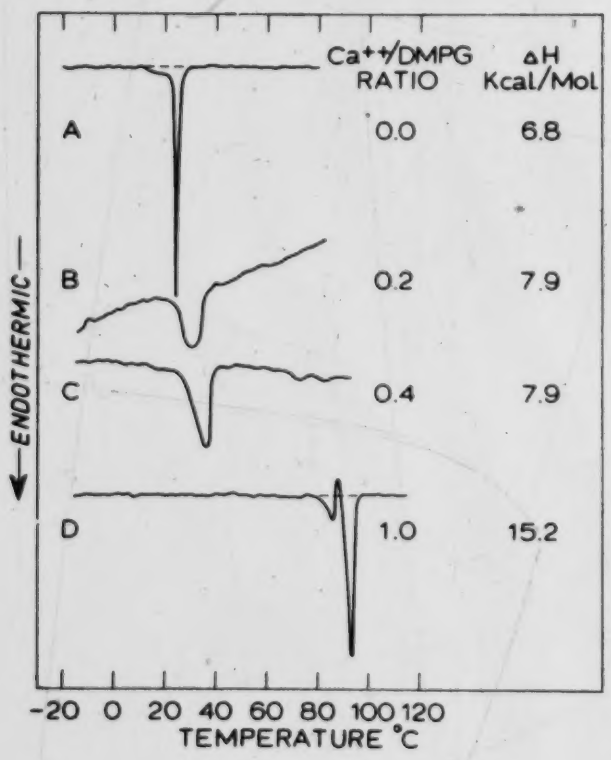

Figure 4.

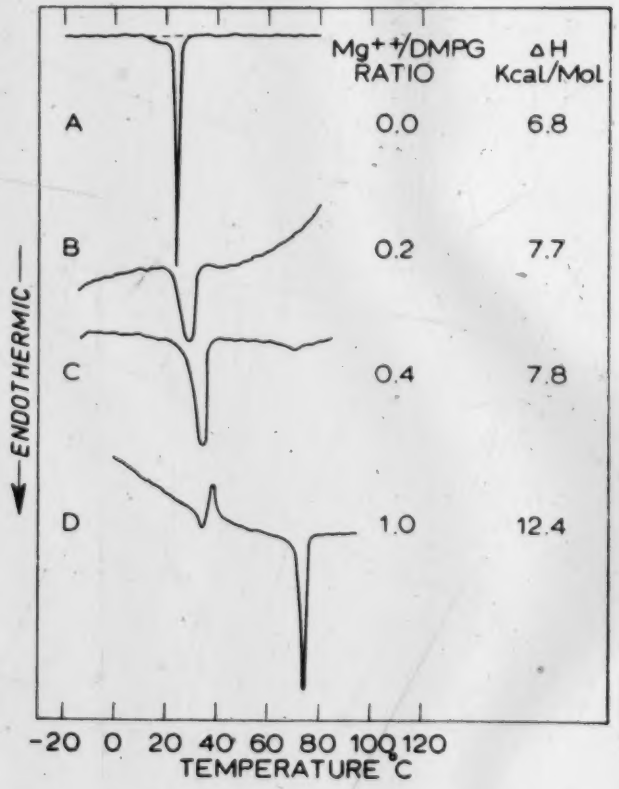

Figure 5.

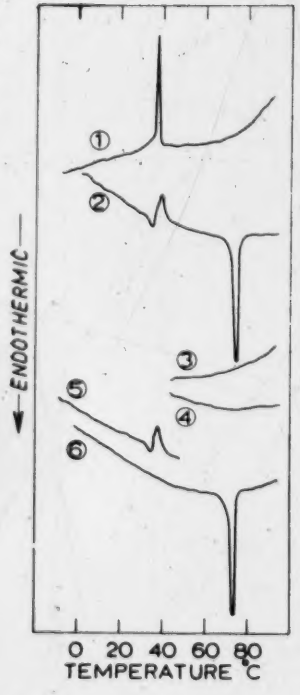

Figure 6.

discrete lamellar stacks. Some cochleate cylinders were observed but this morphological form did not predominate as it did with DLPC (75).

3. Effect of Mg^{++}

The effects of Mg^{++} on DMPG were analogous to those observed with DLPG. Ratios of Mg^{++}:DMPG up to 1:2 raised the transition temperature to about 38°C (79). Higher concentrations of Mg^{++} resulted in the complex thermogram illustrated in Fig. 5. The metastable thermal behaviour of DMPG (Fig. 6) in the presence of Mg^{++} was correlated to the freeze-fracture structure as follows. Below 30°C gel phase liposomes existed. Heated to 32°C, the liposomes underwent a gel to liquid-crystalline transition. The liquid-crystalline liposomal structure immediately underwent rearrangement to more stable 'crystal structures' (exotherm at 32°C). At 71°C the acyl chains of the lipid melted accompanied by simultaneous formation of liquid-crystalline liposomes which could be supercooled to below 40°C (79).

The transition enthalpy of the Mg^{++}- induced 'crystal' structures was 12.4 kcal/mole compared to 15.2 kcal/mole for the Ca^{++}:DMPG which indicated the high-melting structures formed with Ca^{++} were more stable than their Mg^{++} counterpart (79).

F. THERMOTROPIC PROPERTIES OF DPPG

The phase transition temperature for DPPG in NaCl (0.1M, pH 7.4) has been reported as 41°C (80). A pre-transition at 35 ± 1°C was also observed. Details of the effect of pH changes on the transition temperature of DPPG have not been reported.

The transition enthalpy of DPPG-Na^+ was 7.9 kcal/mole compared with 7.7 kcal/mole for DPPC (80).

Freeze-fracture electron microscopy has revealed that DPPG, dispersed in $MgCl_2$ (0.02M, pH 6) or $CaCl_2$ (0.01M, pH 6), forms closely packed multilamellar structures (81) similar to those observed with DMPG (79).

The effects of Mg^{++} and Ca^{++} on the thermotropic behaviour of DPPG have not been well documented but absence of any transition between 20°C and 70°C in the presence of high concentrations of either Mg^{++} or Ca^{++} has been reported (80).

G. DMPG:DMPC MIXTURES - THE EFFECTS OF Ca^{++}

Van Dijck *et al*. (79) reported that Ca^{++} (0.12M) raised the transition temperature of a DMPG:DMPC (1:1 mol/mol) mixture from 24°C to approximately 40°C. No phase separation detectable by DSC occurred in the presence of Ca^{++}. Freeze-fracture electron microscopy of the DMPG-Ca^{++}:DMPC mixture revealed only liposomal structures. No cochleate cylinders were observed (79).

Although comparatively little information is available in the literature concerning PG:PC mixtures and the effects of Ca^{++} on them, lipid mixtures containing other anionic phospholipids, particularly PS and PA, have been relatively well studied. For comparison purposes some of the current literature concerning acidic phospholipid-divalent cation interactions and the effects of these interactions on the properties of binary lipid mixtures will be briefly reviewed.

H. Ca^{++} - ANIONIC PHOSPHOLIPID INTERACTIONS

The ionic properties of PS both in aqueous dispersion (82,83,84,85) and in monolayers (86,87,88) have been studied extensively. Biochemically, the most interesting manifestations of these properties are related to the ability of PS to form chelation complexes with Ca^{++}. The physiological importance of these complexes results from (1) the ability to form mixed Ca^{++} chelates which can stabilize structural arrangements such as the lipid-protein complex involved in prothrombin activation (1,7) and (2) Ca^{++}-regulated alterations in lipid physical properties due primarily to lateral condensation (decreased surface area/molecule of PS) (88). The condensation effect of Ca^{++} binding to PS combined with high association constants ($\log K_a = 4$) for Ca^{++} - PS (84,85) relative to soluble Ca^{++} - organic ligand salts (e.g. Ca^{++} - $(COOH)_2$; $\log K_a = 3$) (89) indicated that the lattice array of negatively charged PS polar head groups at

the lipid-water interface must contribute to the binding ability. On the basis of this, Papahadjopoulos (88) suggested that Ca^{++} - PS formed a linear polymeric lattice. A similar polymeric lattice arrangement was also proposed for Ca^{++} - PA (88).

Evidence that the effect of Ca^{++} involves more than reduction of the charge repulsion between PS polar head groups or formation of Ca^{++}-chelated dimers (PS-Ca-PS) has been presented by Ohnishi and Ito (90,91). They studied the structural effects of Ca^{++} on PS:PC mixtures using a nitroxide spin label attached to a PC acyl chain (PC*). Addition of Ca^{++} to mixtures of PS:PC* resulted in formation of aggregates of fluid (liquid-crystalline) PC*. It was concluded that Ca^{++} bound to the PS to form closely packed PS clusters resulting in exclusion of most of the PC* from the PS-enriched domains. Similar behaviour, resulting in separation of rigid clusters of Ca^{++} - PA from fluid PC, was observed with PA:PC:Ca^{++} mixtures (92,93) but not with mixtures of phosphatidylinositol (PI):PC and Ca^{++} (91). This led to the conclusion that two chelating sites per polar head group were required to propagate the polymeric chelated structure. Further evidence for this was presented by Jacobson and Papahadjopoulos (80) who used DSC to examine the ability of Ca^{++} to segregate domains of acidic lipid from PS:PC and PA:PC mixtures. Neutralization of a PS:DPPC mixture by decreasing the pH or by adding Mg^{++} did not produce a detectable phase separation. Furthermore, a Ca^{++}-induced

phase separation was observed with DPPA:DPPC mixtures only at pH 8 and not at pH 6 indicating a requirement for two negative charges per acidic lipid headgroup.

Ohnishi and Ito (91) commented that the surface properties of the Millipore filters used to concentrate the PS:PC* mixtures changed from hydrophilic to hydrophobic concomitantly with formation of Ca^{++} chelated PS aggregates.

Recent NMR and X-ray diffraction studies of the Ca^{++} - PS complex by Hauser et al. (94) indicated that interaction of PS with Ca^{++} ($>10^{-3}$M) at 23°C resulted in formation of an essentially dehydrated ('hydrophobic') Ca^{++} - PS complex with highly immobilized hydrocarbon chains. The X-ray diffraction pattern for the Ca^{++} - PS, which closely resembled the pattern for gel phase DSPS, indicated that Ca^{++} binding induced, isothermally, a phase transition similar to that obtained by cooling the sodium salt of PS below the thermal transition temperature.

While the 'hydrophobic' effects seen by Ohnishi and Ito (91) and those reported by Hauser et al. (94) may not have resulted from the same Ca^{++} - PS molecular interactions, both pieces of data indicated a marked alteration in the lipid head group and Ca^{++} hydration patterns as a result of Ca^{++} - PS complex formation.

I. Ca^{++}-INDUCED FUSION OF PS CONTAINING VESICLES

Papahadjopoulos et al. (95) observed that the ability of phospholipid vesicles to induce cell fusion was

dependent upon the presence of acidic lipid and Ca^{++} and postulated a Ca^{++} bridge between negatively charged surface groups on the vesicles and cell membrane surface as an initial event in the fusion process. At low Ca^{++} concentrations (<1mM), or in the presence of Mg^{++} (2-5mM), PS vesicles formed large aggregates but did not fuse (96). At higher Ca^{++} concentrations (10mM) fusion of unilamellar PS vesicles occurred (97). Freeze-fracture electron micrographs indicated fusion of the vesicles resulted in formation of long cochleate cylinders similar to those observed with DLPG and DMPG in the presence of Ca^{++} (76,79).

J. EFFECTS OF Ca^{++} ON PS VESICLE PERMEABILITY

In 1966, Papahadjopoulos and Bangham (98) demonstrated that the permeability of PS vesicles increased sharply when Ca^{++} was added to the external bulk aqueous phase. The release rate of ^{22}Na from sonicated PS vesicles was low at low Ca^{++} concentrations (<0.5mM, T = 24°C) (96) but increased dramatically (500-1000 fold) at Ca^{++} concentrations between 0.5 and 2.0mM. The efflux of ^{14}C-sucrose from PS vesicles containing the Ca^{++} ionophore A23187 showed a greatly reduced response to changes in Ca^{++} concentrations (96). The ionophore permitted rapid equilibration of Ca^{++} across the bilayers and the reduced response to externally added Ca^{++} was interpreted as indicating that asymmetry of Ca^{++} distribution across the bilayer contributed to the increase in permeability observed in PS vesicles without

A23187. The large permeability change induced by Ca^{++} (>1mM) was accompanied by fusion of unilamellar vesicles into large multilamellar cochleate cylinders (99).

The high degree of correlation between conditions required to increase PS vesicle permeability (96), to induce vesicle fusion (97) and to cause isothermal phase transitions and phase separations (81) led Papahadjopoulos et al. to conclude that the key event leading to membrane fusion was the Ca^{++}-induced isothermal phase transition with its accompanying changes in molecular packing and formation of a gel phase stable up to at least 70°C (91,80). As the Ca^{++} - PS complex forms a highly ordered (94,80), thermally stable bilayer, it was proposed that the Ca^{++}-induced changes resulted from a transient disruption of the bilayer and formation of phase boundaries within the plane of the bilayer. These transient domain boundaries have been proposed as regions highly susceptible to fusion and to increased permeability.

K. LATERAL DOMAIN FORMATION - PHASE BOUNDARY LIPID

The permeability properties of vesicles of a number of synthetic phospholipids, including DPPC (100,80), DPPG (100) DMPG (79) and DMPC (101,102), have been examined as a function of temperature. In all cases, a transient large increase in permeability was observed at a temperature corresponding to approximately the mid-point of the gel to liquid-crystalline transition. The permeability during the lipid

phase transition was greater than that observed either above or below the phase transition temperature range. This increased permeation rate has been attributed to the presence of disorder (100) or mismatch regions (101) which occur at the interfaces of the gel and liquid-crystalline domains formed during the phase transition. Marsh et al. (101) calculated the ratio of domain boundary or interfacial lipid to gel phase plus liquid-crystalline lipid was maximal at the mid point of the phase transition for DMPC vesicles and they demonstrated that the maximum permeability of DMPC vesicles to Tempo-choline occurred at that same temperature (101).

According to the model proposed by Marsh et al. (101), lipid mixtures which display a low degree of cooperativity, or phase separation behaviour, would be expected to have a greater proportion of interfacial lipid than that calculated for a pure phospholipid undergoing a cooperative gel to liquid-crystalline transition. Tsong et al. (103) have attributed the lidocaine-induced increase in permeability to ANS (8-amlino-1-napthalenesulfonate) to a decrease in transition cooperativity (smaller cooperative unit) which resulted in an increase in the amount of phase boundary lipid.

Papahadjopoulos et al. (100) reported that ^{22}Na diffusion rates through vesicles composed of DOPG (T_c = -18°C) and DPPG (T_c = 42°C) at temperatures below the DPPC transition temperature (0-10°C) were higher than those observed for pure DOPG or pure DPPG vesicles.

The effects of Ca^{++} on the permeability of PS

vesicles (96) may also reflect the formation of highly permeable interfacial regions during the Ca^{++}-induced isothermal phase transition.

In conclusion, it would appear that the properties of a lipid bilayer can be greatly altered by the presence of interfacial regions occurring as boundaries between different compositional domains or as a result of a gel to liquid-crystalline phase transition. These interfacial regions could be physiologically important in the functioning of biological membranes with a heterogeneous lipid composition.

L. THE PURPOSE OF THIS STUDY

One aim of this study was to prepare and carefully characterize a series of anionic:zwitterionic phospholipid mixtures, which could be used to examine the effects of the lipid physical state on lipid-protein interactions. For reasons previously discussed phosphatidylglycerols were selected as the anionic lipid component. A second goal was to use these well-characterized lipid systems to establish a structure-function relationship for the lipid requirements of the prothrombin activation system.

CHAPTER III

MATERIALS AND METHODS

A. MATERIALS

Inorganic chemicals and reagents used in preparation of buffers were obtained from J.T. Baker Chemical Co., or Fisher Scientific Co., and were ACS reagent grade or better.

Michaelis (veronal-acetate) buffer was prepared as follows: Na-acetate (4.85g), Na-diethylbarbiturate (7.36g) and NaCl (8.5g) were dissolved in 975 ml of distilled water. The pH was adjusted to 7.35 with concentrated HCl and the volume made up to 1.0ℓ.

All organic solvents were glass distilled. Water was deionized and glass distilled.

Silicic acid used for column chromatography was 'Unisil' (200-325 mesh) from Clarkson Chemical Co., Williamsport, Pa., or 'Sorbsil' from Joseph Crossfield and Sons, Warrington, England.

Plates used in thin layer chromatography were obtained, pre-coated with Silica Gel 60 F254, from Brinkmann Instruments, Rexdale, Ontario.

L-α-Lecithin (β,γ-dilauryl) (Lot 400203) and L-α-Lecithin (β,γ-distearoyl) (Lot 400204) were obtained from Calbiochem, San Diego, California. L-α-phosphatidylcholine-dipalmitoyl and L-α-phosphatidylcholine-dimyristoyl were obtained from Sigma Chemical Co., St. Louis, Missouri.

The dioleoyl phosphatidylcholine, supplied by

Dr. P.G. Barton, was prepared by the method of Barton and Gunstone (104).

All synthetic phosphatidylcholines used were >98% pure as determined by micro t.l.c. and g.l.c. analysis of their fatty acid methyl esters.

Egg phosphatidylcholine was isolated from hen egg yolk by silicic acid (Sorbsil) chromatography by the method of Lea et al. (105) as modified by Hanahan et al. (106) and chromatographed as a single spot on micro t.l.c. analysis.

Phosphatidylserine was prepared from beef brains by Sanders' modification (107) of the method of Rouser et al. (108).

Egg phosphatidylcholine and phosphatidylserine were stored in solution in $CHCl_3$ at -20°C.

Brain lipid extract (cephalin) was prepared from beef brains according to Bell and Alton (109) and stored as a stock solution containing 118 µg of phosphorus per ml. For use in clotting assays, the stock solution was diluted with Michaelis buffer at pH 7.35.

Standard Normal Plasma (SNP) was obtained from DADE (Miami, Fla). Lot #757 was used for all clotting assays.

Russell viper venom (Burroughs-Wellcome 'Stypven') was obtained from Warner-Chillcott (Scarborough, Ontario).

Phospholipase D from cabbage leaves was obtained from Sigma. The enzyme was supplied as a desiccated powder and was made up to the required concentration in 0.1M Na-acetate buffer at pH 5.6.

B. METHODS

1. Chemical Synthesis of DMPG

Several attempts were made to chemically synthesize DMPG following the method of Baer and Buchnea (110). This involves phosphorylation of 1,2-dimyristoyl glycerol (111, 112) with phosphorus oxychloride ($POCl_3$), in the presence of pyridine, followed by esterification of 1,2-isopropylidene glycerol (112) to the activated phosphate group. Acid hydrolysis then cleaves the isopropylidene group from the isopropylidene glycerol to yield DMPG.

In spite of precautions taken to ensure pure, anhydrous reagents, all the reactions attempted yielded numerous by-products to an extent precluding isolation of DMPG in any appreciable yield. The phosphorylation step using $POCl_3$ seemed particularly prone to by-product formation.

In view of the unsatisfactory results obtained using this synthetic route, the transphosphatidylation reaction catalyzed by Phospholipase D was examined as an alternate method (70).

2. Preparation of Diacyl phosphatidylglycerols

The method used to synthesize the diacyl phosphatidyl glycerols from the corresponding diacyl phosphatidylcholines was essentially that of Dawson (113).

One mmole of the phosphatidylcholine was shaken in 60 ml of 0.1M Na-acetate buffer (pH 5.6). The suspension was sonicated briefly to break up coarse particles yielding

an opalescent dispersion. Glycerol (8.0 ml) was added dropwise to the combined sonicates in a 500 ml round bottom flask and mixed thoroughly. Next 10 ml of 1.0M $CaCl_2$ was added with stirring. Then 30 ml of a solution containing 100 mg of Phospholipase D (Sigma) in Na-acetate buffer was added followed by 15 ml of diethyl ether. The reaction mixture was incubated at 27°C and was monitored by thin layer chromatography until the PC spot had practically disappeared. Longer incubation was avoided to reduce the extent of phospholipase D - catalyzed hydrolysis of the product (PG). Finally, 100 ml of diethyl ether was added to the reaction mixture, which was then shaken and placed in a 250 ml separatory funnel and cooled to 4°C to terminate the reaction.

3. Extraction procedure for DMPG

The extraction procedure outlined below was designed to provide information regarding partitioning of the reaction products into the aqueous and organic phases.

After separation, the reaction mixture consisted of an aqueous phase, an ether phase and an insoluble interfacial band containing a substantial amount of yellowish-white solid material. This material was separated from the aqueous phase by filtration (Whatman #4 paper) to give a clear aqueous phase, a solid residue on the filter paper, and a clear diethyl ether phase. The solid residue and the filter paper were refluxed for 1/2 hour in 180 ml of $CHCl_3$:MeOH (2:1 v/v), then filtered through Whatman #4 filter paper. The residue

was washed with 100 ml of hot $CHCl_3$:MeOH (2:1 v/v). In the DMPG preparation the filtrate from the interfacial solid material contained approximately 80% of the total lipid phosphorus. The remaining lipid phosphorus was in the aqueous fraction (15-20%) and the ether fraction (<2%).

The lipid present in the aqueous phase could be extracted by adding enough solid Na_2EDTA to chelate the Ca^{++} present in the reaction mixture (10 mmoles), adjusting the solution to pH 9.0 with 1.0M NaOH, then following the Bligh and Dyer (114) extraction procedure.

The main fraction of lipid in $CHCl_3$:MeOH (2:1 v/v) was dried on a rotary evaporator, 80 ml of aqueous 0.05M NaCl, 0.1M Na_2EDTA at pH 8.5 were added, then 200 ml MeOH and 100 ml $CHCl_3$ were added to form a monophasic Bligh and Dyer solution. This was placed in a separatory funnel and 100 ml of $CHCl_3$ plus 100 ml 0.05M NaCl were added to make the mixture biphasic. Typically, 90% of the lipid partitioned into the lower $CHCl_3$ layer. Quantitative extraction could be achieved by re-extraction of the aqueous-methanolic phase with 5% methanol in chloroform.

It was usually necessary to do a second Bligh and Dyer extraction of the main lipid fraction in order to remove final traces of glycerol.

The main lipid fraction was dried on a rotary evaporator then redissolved in a minimum volume of $CHCl_3$ prior to column chromatography.

4. Extraction procedure for DPPG

With the DPPG preparation, 90-95% of the lipid was in the interfacial portion of the reaction mixture. Less than 2% was in the ether phase and less than 5% of the lipid partitioned into the aqueous layer. Consequently, the extraction procedure followed was identical to the procedure used for DMPG except it was not necessary to do the Bligh and Dyer extraction of the aqueous portion of the reaction mixture.

5. Column chromatography purification of DMPG and of DPPG

100g of Unisil were activated by heating overnight at 110°C. A column (3 cm x 60 cm packed height) was poured in $CHCl_3$ and washed with 200 ml of $CHCl_3$. The sample was applied in a minimum volume of $CHCl_3$ and allowed to equilibrate on the column for 1/2 hour before starting elution.

The elution was done using a stepwise $CHCl_3$:MeOH gradient. The column effluent was monitored by t.l.c. The PG eluted between 12-20% MeOH in $CHCl_3$. Considerable overlap occurred in the elution of the PA and PG from the column.

The overall yield from starting material was 20-30%.

It was later found that the conditions used to extract the lipid samples from the reaction mixture would result in a mixture of the Na^+ salt and the protonated form of the PG. Conversion of the PG completely to the Na^+ form (see d.t.a. sample preparation) prior to column chromatography

should increase the efficiency of the column.

6. Extraction procedure for DOPG

The distribution of DOPG in the aqueous-ether mixture was: H_2O ~ 1%; interfacial 30-40%; ether 60-70%. Due to the smaller volume of reaction mixture used in the DOPG preparations (50 ml) and the greater solubility of the dioleoyl phospholipids in non-polar solvents, the subsequent extraction procedure differed from that used for DMPG and DPPG.

After addition of excess ether and cooling to 4°C, the aqueous layer and the interface material were separated from the ether layer and centrifuged in an IEC PR-6 centrifuge for five minutes (T = 4°C) at 1000 rpm. The interface material became pelleted allowing easy separation of the aqueous and interface material. The solid interface pellet was suspended in 50 ml ether, stirred then filtered and the filtrate combined with the original ether fraction. Greater than 95% of the total lipid phosphorus was found in this combined ether fraction. After removal of ether in vacuo, 16 ml of 0.1M Na_2EDTA, 40 ml MeOH and 20 ml $CHCl_3$ were added and the solution titrated to pH 9.2 with 1.0M NaOH. The solution was then made biphasic according to Bligh and Dyer (114) and the lower ($CHCl_3$) layer dried by rotary evaporation. The residue was redissolved in a minimum volume (~1 ml) for application in preparative t.l.c.

7. Preparative thin layer chromatography - DOPG

The plates used were pre-coated (5 x 10 cm) silica gel plates (Merck). The sample was applied as single spots across the width of the plates to a total of 3-4 mg per plate. The solvent system was: $CHCl_3$:MeOH; NH_3:H_2O (65/35/2.5/2.5 by volume).

After developing and drying, the plates were observed under short wave UV light. The zone containing the PG ($R_f \sim 0.75$) was just detectable. This zone was scraped from the plates, suspended in $CHCl_3$:MeOH (2:1 v/v) and transferred to a plugged buret. The DOPG was eluted with $CHCl_3$:MeOH (2:1 v/v). Overall yield from starting material was approximately 30%.

8. General comment on these preparative procedures for the diacyl PGs

Considerable variation was observed in the distribution of the lipids among the organic, aqueous and interface material as well as in the relative amounts of PG:PA:PC present in each preparation. These variations necessitated close monitoring of the extraction procedures by t.l.c. and phosphorus determinations to minimize loss of product.

9. Atomic absorption spectrophotometry

Atomic absorption measurements were done using a Unicam SP 90A Series spectrophotometer with a 10 cm acetylene burner. Procedures outlined in the Pye Unicam Method Sheets

Ca2 and Mg2 were followed for Ca^{++} and Mg^{++} determinations, respectively.

10. Phosphorus determinations

Phospholipid phosphorus was determined by the method of King (115). For synthetic lipids, calculations were based on the anhydrous molecular weight. For naturally occurring phospholipids an average molecular weight of 775 was assumed.

11. Fatty acid analysis

Fatty acid methyl esters were prepared and isolated by the method of Brockerhoff (116).

The methyl esters were analysed using a Hewlett-Packard 5700A gas chromatograph equipped with a diethylene glycol succinate column. Quantitation of peaks was by Hewlett-Packard 3370B Integrator. Peaks were identified by reference to standards from Applied Science Laboratories, State College, Pa.

12. Differential thermal analysis

(a) Na^+ - salt of diacyl PGs. The Na^+ salt of PG was obtained by making a Bligh and Dyer (114) monophasic solution (Ca^{++} removed by prior EDTA wash) in which the aqueous component consisted of 0.1M Tris-HCl then titrating the solution to pH 9.5 with 1.0M NaOH. The standard Bligh and Dyer procedure was then followed to extract the PG into the $CHCl_3$ layer.

(b) Protonated diacyl PG. This form of the PG was obtained in a manner analogous to that used for the Na^+ salt except the monophasic Bligh and Dyer solution was titrated to pH 2.5 with 1.0M HCl prior to extraction into $CHCl_3$.

Aliquots of stock lipid solution were dried under N_2 to remove all visible solvent, then stored under vacuum at room temperature for 10-12 hours to remove final traces of solvent.

The dried lipid, usually 2-3 mg, was placed in a 2 mm diameter capillary tube and H_2O or 1.0M $CaCl_2$ added with a Hamilton microliter syringe. Water was usually present in approximately a 100 fold molar excess. The tube was then sealed and the lipid sample hydrated by the method of Ladbrooke et al. (117).

When mixtures of lipids were required, the lipids were mixed, in the required molar amounts in $CHCl_3$, before drying under N_2.

The analysis was carried out with a DuPont 900 Thermal Analyzer using the micro heating block. Rate of heating and cooling was approximately 10°C/min. Anhydrous N_2, cooled by passage through a copper coil submerged in liquid N_2, was used for cooling.

Thermograms were recorded on graph paper corrected for non-linearity of the Chromel-Alumel thermocouples.

13. Nuclear magnetic resonance ^{13}C, ^{1}H

(a) Sample preparation. Samples were dried under N_2, then in vacuo to remove solvents. They were redissolved in $CDCl_3$ with traces of MeOD added if necessary for complete solubilization of the lipid. TMS was used as an internal reference. Sample size was approximately 50 mg for ^{1}H spectra and approximately 400 mg for ^{13}C spectra.

Proton N.M.R. spectra were obtained on a Varian Ha-100-12 at a frequency of 100.1 MHz and T = 35°C.

The ^{13}C spectra were obtained on a Bruker WP-60 spectrophotometer at a frequency of 15.08 MHz.

Assignments of the resonances for the ^{1}H spectra were based on comparison with values published by Tocanne et al. (118) for dilauroylphosphatidylglycerol. The ^{13}C assignments were determined with reference to Birdsall et al. (119).

14. Sonication of lipids

Sonication of lipid samples was done with a Bronwill Biosonik IV ultrasonicator with a titanium tip. Low intensity sonication was used to disperse lipids in aqueous solutions. For short bursts of sonication (0-60 sec) the samples were at room temperature. If prolonged sonication was required, the samples were placed in an ice bath or in a water-cooled cell.

15. Titrations of DMPG

Titrations were done in a glass vessel designed so

that the titration solutions could be continuously stirred and the temperature in the vessel controlled by use of a water circulator. The pH was monitored continuously by means of a Radiometer GK-2302-C combination electrode in conjunction with a PHM 22 meter.

Sample preparation and the titration procedure were as previously described (83). The titrants were standardized by titration with primary standard Na_2CO_3. The DMPG titrations were done at 25°C.

For titrations in which the solutions were sonicated, the following procedure was used. Titrant was added with a microliter syringe (10 µl or 50 µl capacity) and the pH recorded. The mixture was then sonicated for 2 minutes at room temperature and the pH recorded again once the reading had stabilized.

16. Clotting assays

(a) Reagents. Standard Normal Plasma (SNP) from DADE was reconstituted with distilled water (1 ml/vial).

A 1/55,000 solution of Russell viper venom (RVV) was made in Michaelis buffer at pH 7.35.

The $CaCl_2$ solution was 0.025M.

(b) Lipid samples. Mixed phospholipid solutions were made by combining the required molar amounts of the lipid components in $CHCl_3$ then removing the solvent under N_2 and subsequently in vacuo. Michaelis buffer was then added and the

mixtures sonicated briefly (30 sec) to disperse the lipids. The samples were vortexed vigorously immediately prior to use in the assays. Unless otherwise noted the total lipid phosphorus concentration was 8 µg/ml.

Phosphatidylserine and egg phosphatidylcholine samples were prepared similarly to the synthetic lipids.

Bell and Alton cephalin was diluted from stock solution with Michaelis buffer to give a range of concentrations (usually 2.0-6.01 µgP/ml) suitable for defining a standard clotting activity curve.

(c) Standard 37°C assay. The one stage RVV test as described by Hjört et al. (120) and Bachmann et al. (121) was modified to permit evaluation of the effect of the lipid component on clotting activity. The SNP, RVV, and $CaCl_2$ were maintained at constant and near-optimal concentrations.

Reagents in active use were incubated at 37°C. For each assay, 0.1 ml of SNP, 0.1 ml of lipid or B & A cephalin and 0.1 ml of RVV solution were mixed in a clotting tube at 37°C. Then 0.1 ml of 0.025M $CaCl_2$ was added and rapidly mixed by shaking. The tube was then tilted back and forth so that the assay mixture flowed along the wall of the tube. Clotting times were measured, by stopwatch, starting with the addition of the $CaCl_2$, until clot formation impeded the flow of the assay mixture. A minimum of three assays was performed with each lipid sample to check reproducibility.

Clotting times were converted to "equivalent B & A

cephalin units" (μgP/ml) by reading from a calibration curve of log clotting time (sec) versus log Bell and Alton cephalin concentration (μgP/ml).

(d) Clotting assay at 30°C. This assay was identical to the above except all the reagents were stored and manipulations performed at 30°C.

(e) Clotting assay at 44°C. For this assay, the lipid component and the $CaCl_2$ were incubated at 44°C but the SNP and RVV were incubated at 37°C until being placed in a clotting tube at 44°C immediately before starting an assay. This allowed the assay mixture to warm to 44°C prior to addition of the $CaCl_2$ without exposing the heat labile SNP and RVV to the higher temperature for extended periods.

17. Light scattering experiments

The light scattering experiments were performed in a Perkin-Elmer MPF-4 Fluorescence Spectrophotometer with a circulating water bath providing the heating/cooling modes. The temperature of the sample was monitored by a thermocouple in direct contact with the sample solution and equipped with digital readout.

CHAPTER IV

PHYSICOHEMICAL STUDIES OF LIPIDS

A. PROTON MAGNETIC RESONANCE SPECTRUM OF DMPG

The ^{1}H nuclear magnetic resonance spectrum (Fig. 7) obtained for DMPG corresponded well with the spectrum published for didodecanoyl phosphatidylglycerol (DLPG) (118). On the basis of chemical shifts, the resonance bands could be assigned as indicated in Table I.

Methylene protons β to the carbonyl functions of the acyl chains (C2') were shifted slightly down field and appeared as a broad shoulder on the main methylene peak centered at 1.6 ppm (119). They were integrated together with the protons from C4' to C13'.

The complex pattern observed between 3.63 and 4.44 ppm could not be first order analysed at 100 MHz. However, the integral accounts for the eight methylene protons associated with C1, C1'', C3 and C3'' plus the methyne proton from C2''.

B. ^{13}C NUCLEAR MAGNETIC RESONANCE SPECTRUM OF DMPG

The ^{13}C spectrum (Fig. 8) and chemical shift values obtained for DMPG corresponded well with data reported (119) for DPPC and other model compounds (Table II).

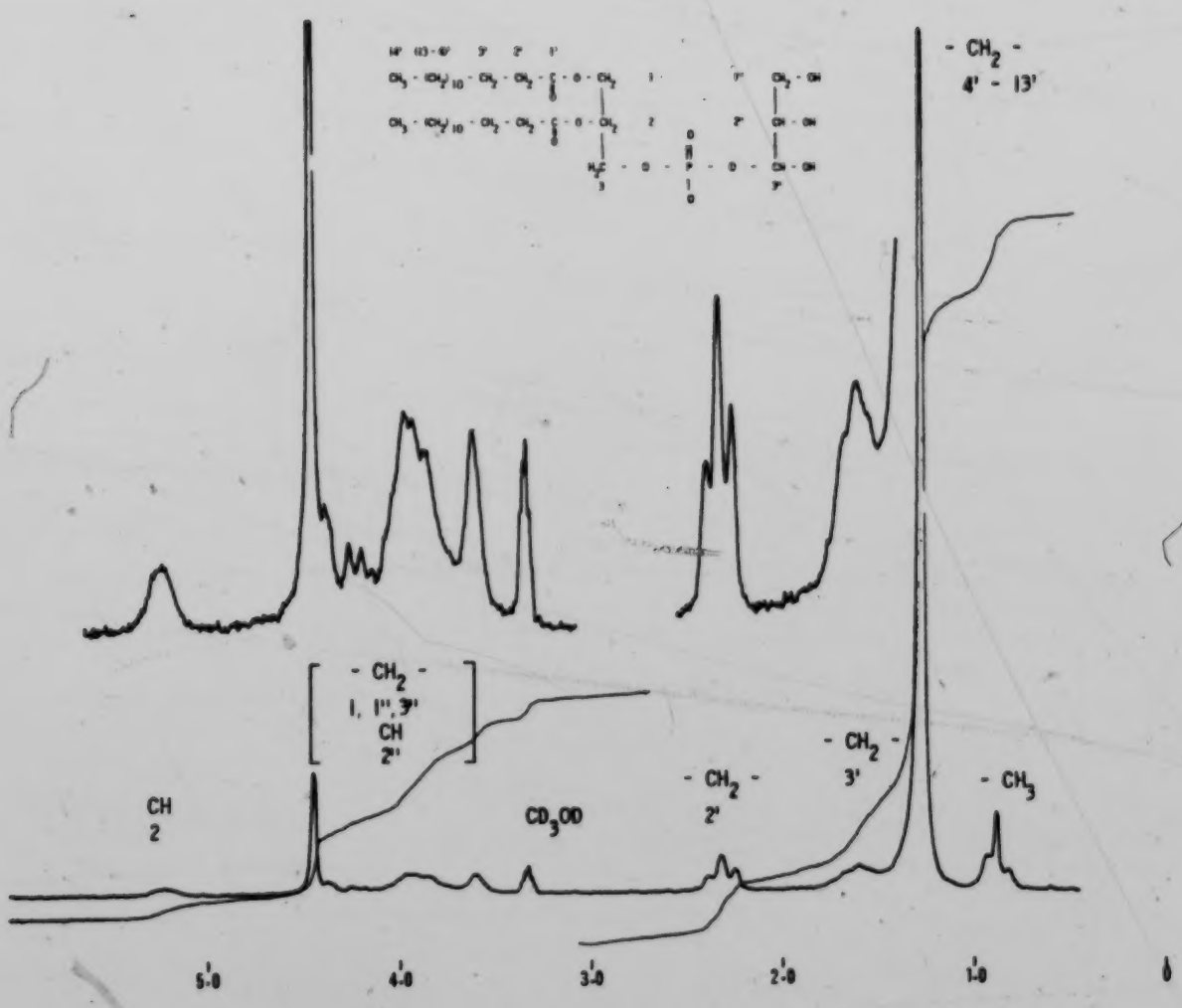

Figure 7. Proton magnetic resonance spectrum of DMPG. Frequency = 100 MHz. Sample size 55 mg. Solvent $CDCl_3$:CD_3OD (2:1 v/v) + TMS as internal reference. T = 31°C.

TABLE I

Chemical Shift Assignments

Proton Magnetic Resonance Spectrum of DMPG

Chemical shift d = ppm	Assignment	No. of Protons
0.88	Methyl protons of acyl chains.	6
1.27	Methylene protons of acyl chains C4' to C13'.	48
1.60	Methylene protons β to carbonyl functions of acyl chains. C3'.	
2.32	Methylene protons α to carbonyl functions of acyl chains. Position C2'.	4
3.63-4.44	Methylene protons from C1, C1'', C3''; Methyne proton from C2''.	9
5.22	Methyne proton. Position C2.	1

Spectrum obtained at 100.1 MHz. Solvent $CDCl_3$:CD_3OD (2/1v/v). Sample size 52 mg.

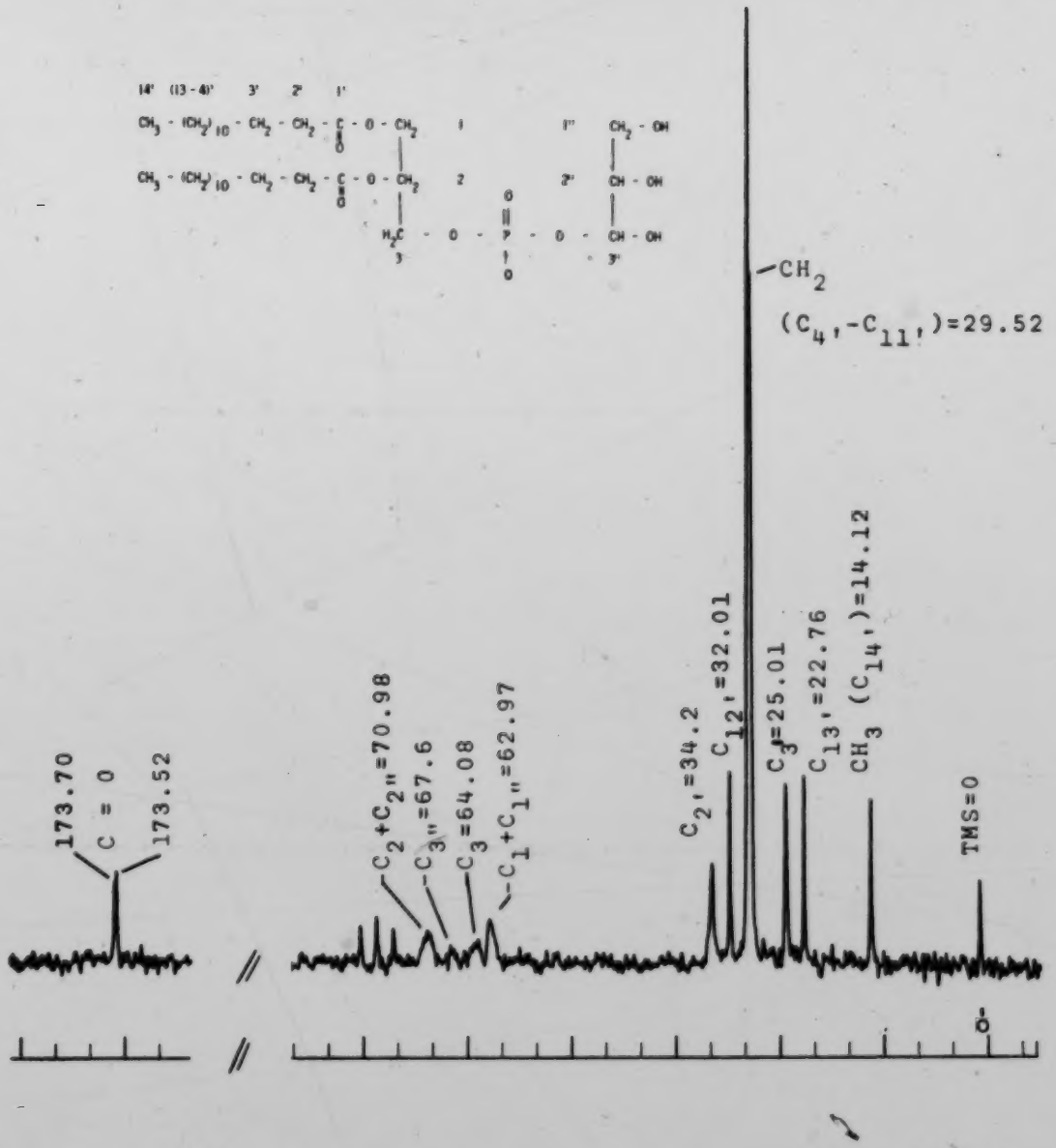

Figure 8. ^{13}C nuclear magnetic resonance spectrum of DMPG. Frequency = 15.08 MHz. Sample size 452 mg. Solvent $CDCl_3$ + TMS as internal reference.

TABLE II

^{13}C Chemical Shift Assignments for DMPG and some Related Compounds

Compound	$C^{=O}$	Glycerol			Methylene					Methyl
		C1-CH_2O	C2-CHO	C3-CH_2O	2'	3'	4'-11'	12'	13'	14'
DMPG	173.70	62.97	70.98	64.08	34.2	25.01	29.82 29.52	32.01	22.27	14.12
	173.52	C1''-CH_2O	C2''-CHO	C3''-CH_2O						
		62.97	70.98	67.6						
		C1-CH_2O	C2-CHO	C3-CH_2O	2'	3'	4'-13'	14'	15'	16'
DPPC (119)	174.2 173.8	63.9	71.5	64.4	35.2	25.9	30.7	32.9	23.7	15.0
sn-glycero-3-phosphocholine (in D_2O) (119)		63.2	71.7	67.6						
glycerol-3-phosphate (119)		63.4	72.0	67.2						

Chemical shifts were measured in δ-ppm down field from internal TMS. Chemical shifts reported relative to dioxane (119) were converted to the TMS reference scale by adding 67.4 ppm to δ values downfield from dioxane (122).

C. DIFFERENTIAL THERMAL ANALYSIS

Differential thermal analysis was used to investigate the thermal properties of the synthetic phospholipids. The method is non-perturbing at the molecular level and is sensitive enough to yield data with relatively small lipid samples (approximately 2 mg).

All the synthetic phospholipids used in this study were intramolecularly homogeneous with respect to acyl chain composition; therefore, reference to phospholipid species with 'identical' or 'non-identical' chains refers only to intermolecular acyl chain heterogeneity.

Unless otherwise specified, the transition temperatures (T_c) were recorded as the temperature(s) at which the inflection point(s) occurred within the thermographic peaks.

1. Differential thermal analysis of the sodium salts of synthetic phosphatidylglycerols

The thermograms of the phosphatidylglycerols (Na^+) were virtually identical to those obtained for the pure synthetic phosphatidylcholines (Fig. 9). The main endothermic peaks showed a high degree of co-operativity (sharp, narrow peak) and, with DMPG-Na^+ and DPPG-Na^+, a pre-transition was observed that was qualitatively similar to those observed with the pure saturated phosphatidylcholines. Pre-transitions were not observed with either of the dioleoyl phospholipids.

The main transitions for DMPG-Na^+, DPPG-Na^+ and DOPG-Na^+ occurred at temperatures (T_c) very close or identical

Figure 9. Differential thermal analysis thermograms for pure phosphatidylglycerols and pure phosphatidylcholines. The sodium salts of the phosphatidylglycerols were obtained as described in the Methods section. Dried lipid samples were hydrated using excess Tris-HCl (0.01M) in NaCl (0.15M) at pH 9.0. Heating rate approximately 10°C per minute. ΔT scale 0.1°C/in.

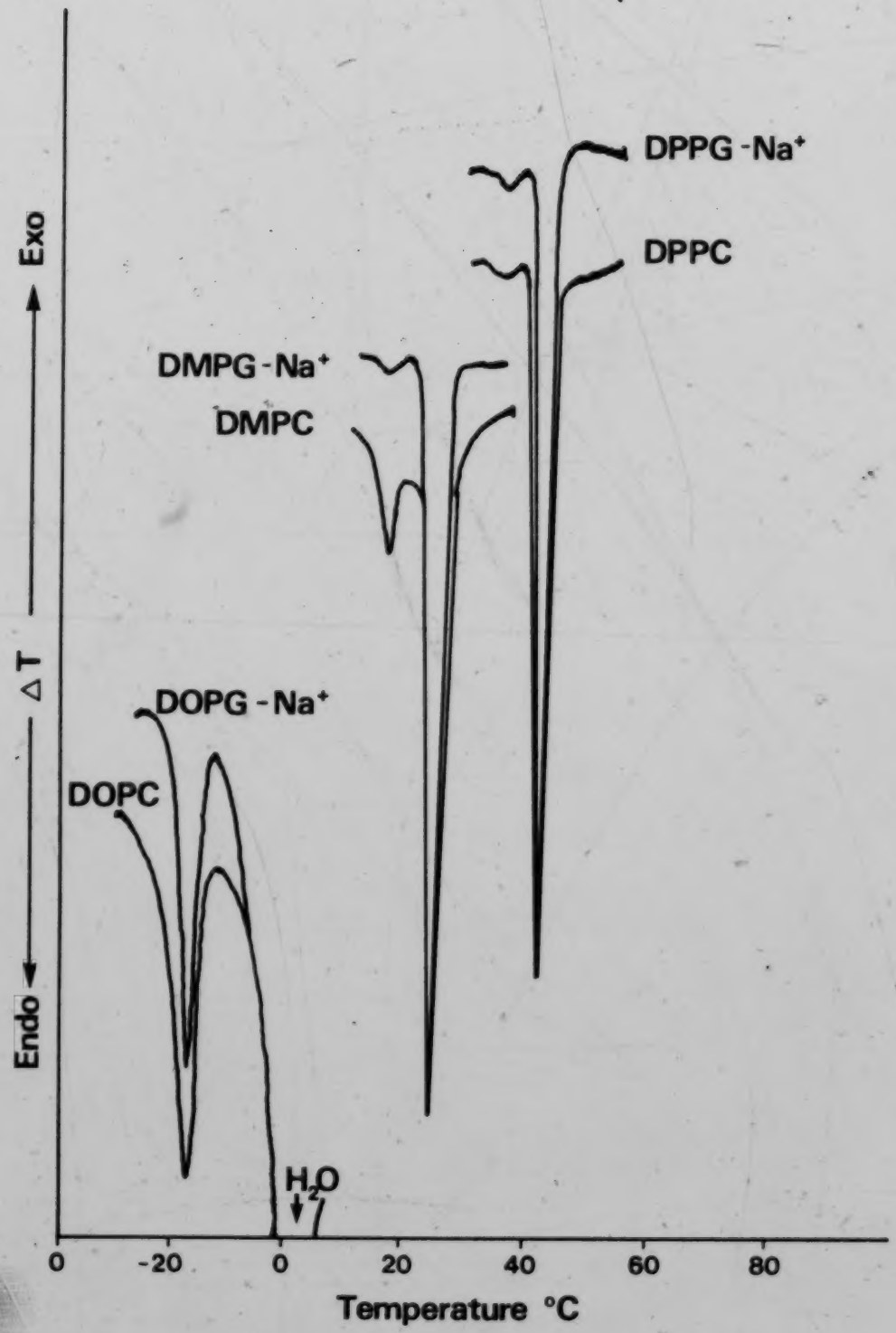
DPPG -Na+
DPPC
DMPG -Na+
DMPC
DOPG -Na+
DOPC
Exo
ΔT
Endo
H2O
0
-20
0
20
40
60
80
Temperature °C

to those observed for the corresponding phosphatidylcholines: DMPC, DPPC and DOPC, respectively (Table III).

2. Differential thermal analysis of mixtures of phosphatidylglycerol sodium salts and phosphatidylcholines with identical acyl chains

Lipid mixtures containing the sodium salt of a synthetic phosphatidylglycerol and the corresponding phosphatidylcholine (identical acyl chains) appeared to be completely miscible in all proportions. The mixtures underwent a highly co-operative gel to liquid-crystal phase transition at the temperature characteristic for the pure components (Figs. 10,11).

Pre-transitions similar to those observed with pure saturated phosphatidylcholines and phosphatidylglycerols were observed with samples which contained a wide range of phosphatidylcholine:phosphatidylglycerol molar ratios (Figs. 10,11).

3. Differential thermal analysis of mixtures of phosphatidylglycerol sodium salts and phosphatidylcholines with non-identical acyl chains

Mixtures of phosphatidylglycerols with acyl chain composition di-C_n and phosphatidylcholines with acyl chain composition di-$C_{n\pm2}$ showed a single gel-liquid crystal endotherm that was slightly less co-operative than the endotherms observed for mixtures with identical acyl chains. (Fig. 12: DMPG:DLPC; DMPG:DPPC. Fig. 13: DPPG:DMPC; DPPG:DSPC).

The transition temperature observed with this type of

TABLE III

Transition Temperature of Various Phospholipids in Multilamellar Suspension

Phospholipid	Pre-transition		Main Transition	
	T_{exper}	$T_{literature}$	T_{exper}	$T_{literature}$
DOPC	-	-	-18° to -20°	-22° (123) -16° (124)
DOPG	-	-	-18°	-18° (100)
DMPC	18°	14.2° (78)	24°	23.9° (78)
DMPG	18°	-	24°	23° (79)
DPPC	37°	37° (80)	42°	42.4° (80)
DPPG	36.5°	35° (80)	42°	41° (80)

Fig. 10. Differential thermal analysis thermogram of DMPG-Na^+:DMPC mixtures. The required molar ratios of lipid were mixed in $CHCl_3$. The $CHCl_3$ was removed under a stream of N_2 and subsequently in vacuo at room temperature. Hydration and heating conditions as for Fig. 9.

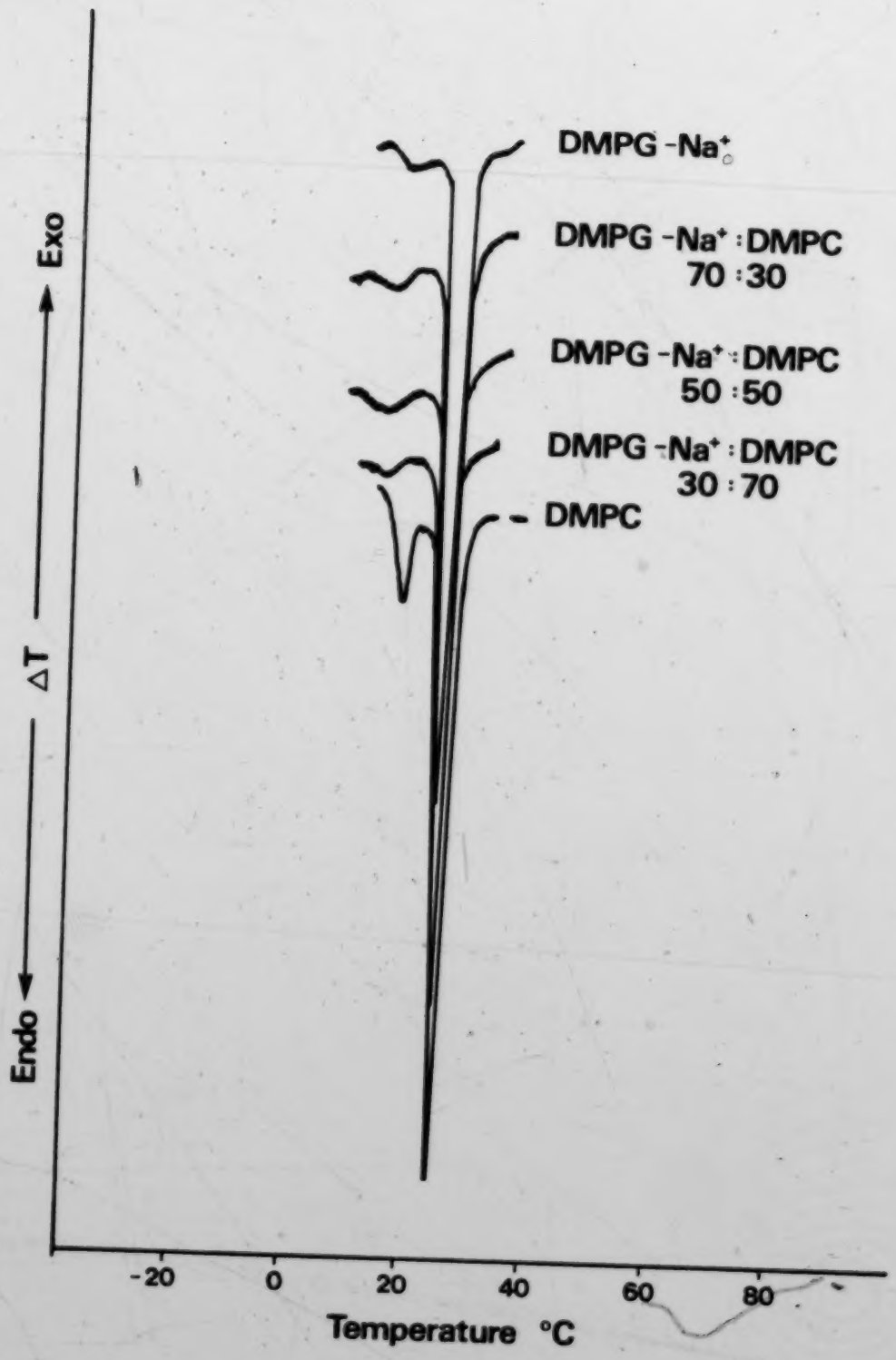
DMPG -Na+
DMPG -Na+ : DMPC
70 : 30
DMPG -Na+ : DMPC
50 : 50
DMPG -Na+ : DMPC
30 : 70
DMPC
Exo
ΔT
Endo
-20
0
20
40
60
80
Temperature °C

Figure 11. Differential thermal analysis thermograms of DOPG-Na^+:DOPC and DPPG-Na^+:DPPC mixtures. Experimental details as for Fig. 9.

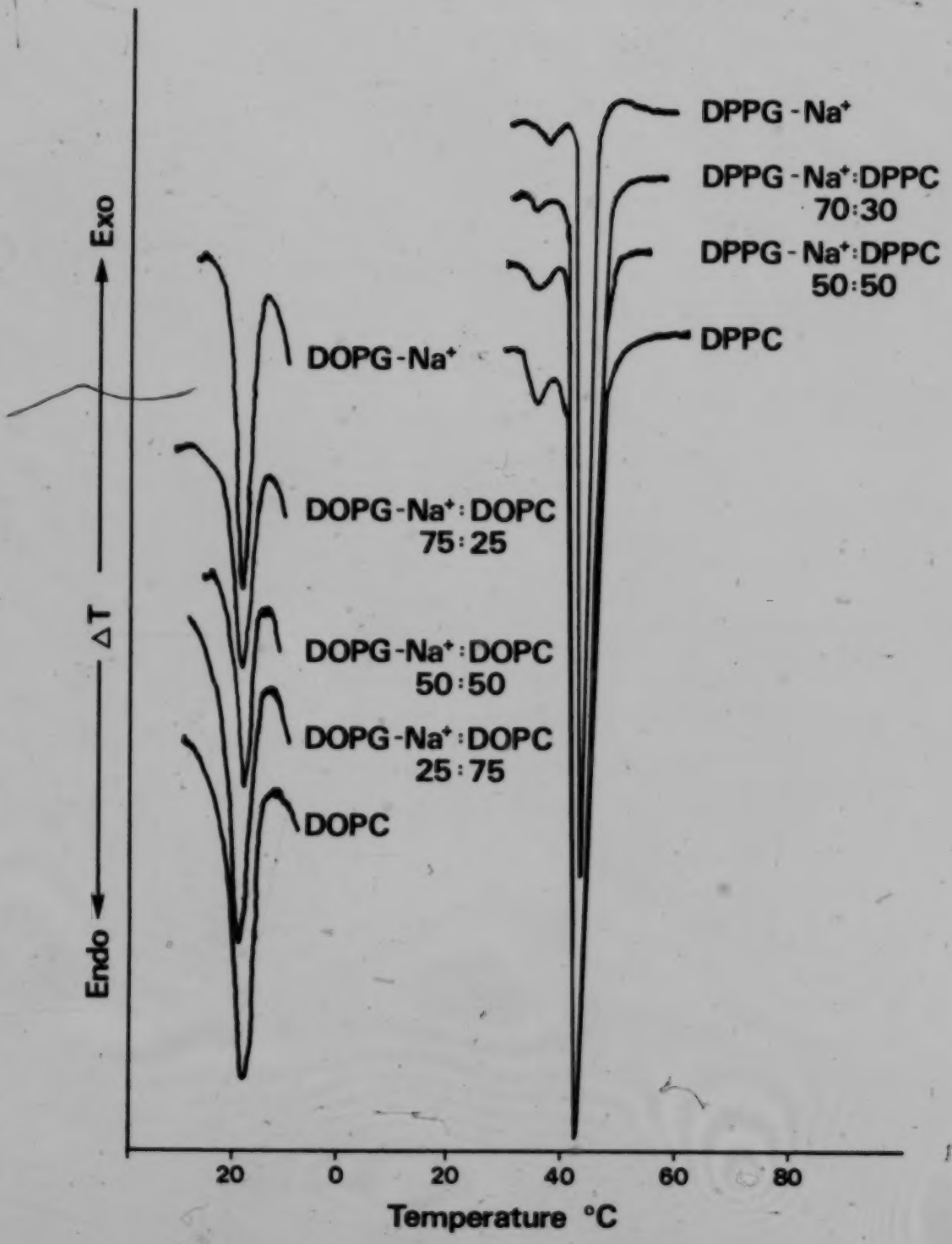
DPPG - Na+
DPPG - Na+:DPPC
70:30
DPPG - Na+:DPPC
50:50
DPPC
DOPG - Na+
DOPG - Na+:DOPC
75:25
DOPG - Na+:DOPC
50:50
DOPG - Na+:DOPC
25:75
DOPC
Exo
ΔT
Endo
20
0
20
40
60
80
Temperature °C

Figure 12. Differential thermal analysis thermograms of equimolar mixtures of DMPG-Na^+ and phosphatidylcholines. Experimental details as for Fig. 9.

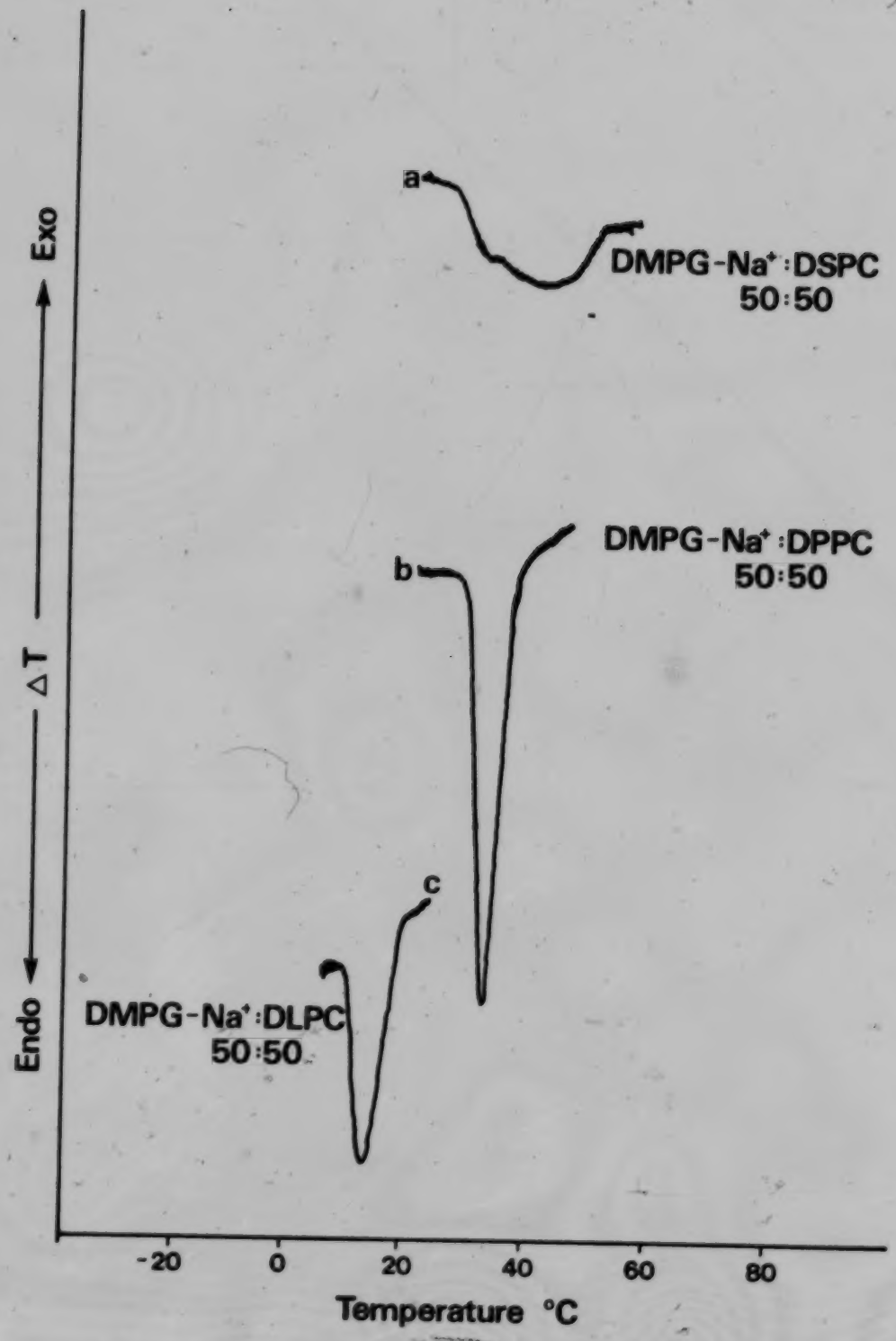
a
DMPG-Na⁺:DSPC
50:50
b
DMPG-Na⁺:DPPC
50:50
c
DMPG-Na⁺:DLPC
50:50
Exo
ΔT
Endo
-20
0
20
40
60
80
Temperature °C

Fig. 13. Differential thermal analysis thermograms of equimolar mixtures of DPPG-Na^+ and phosphatidylcholines. Experimental details as for Fig. 9.

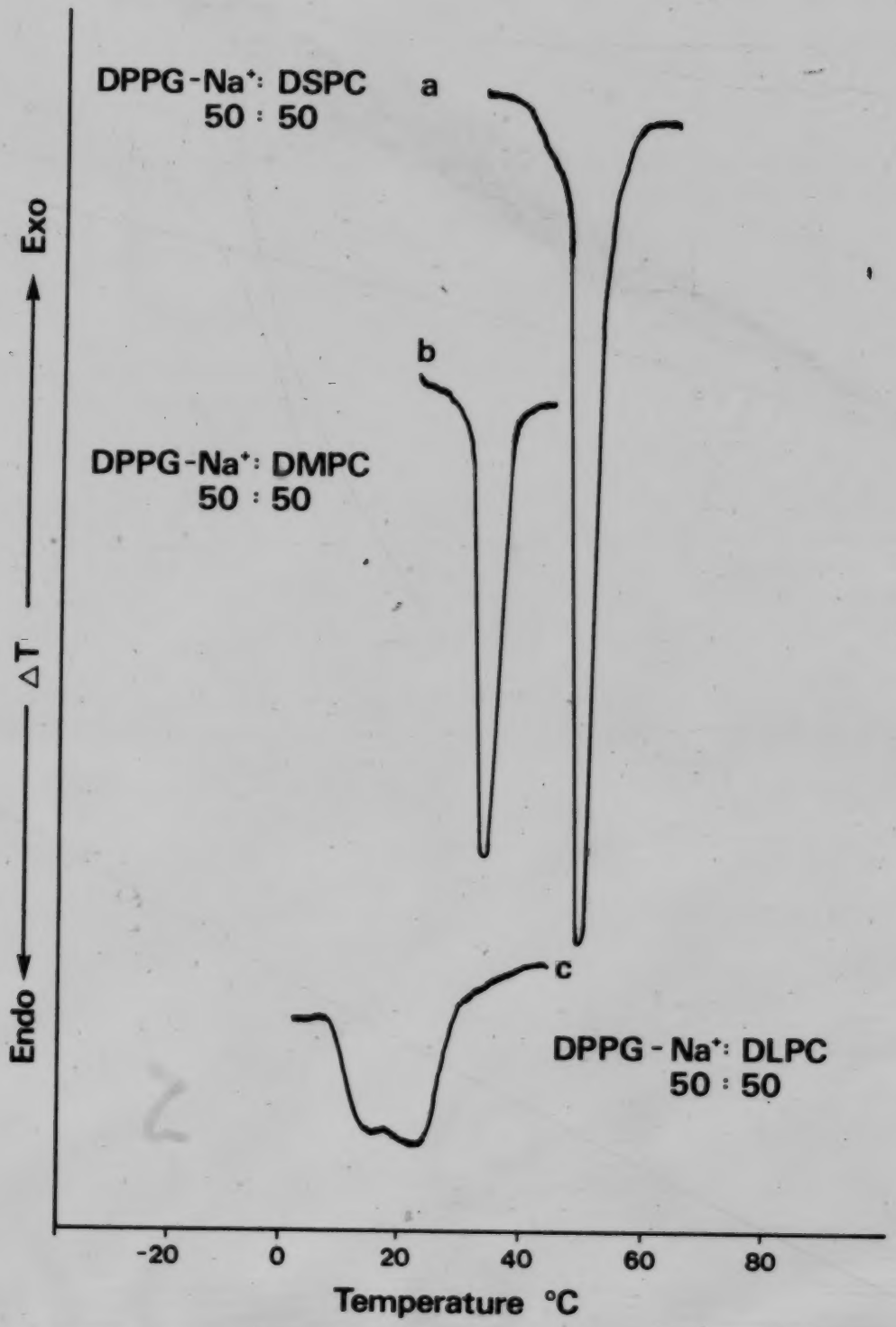
DPPG-Na⁺: DSPC
50 : 50
a
b
DPPG-Na⁺: DMPC
50 : 50
c
DPPG - Na⁺: DLPC
50 : 50
Exo
ΔT
Endo
-20
0
20
40
60
80
Temperature °C

mixture appears to be essentially a linear function related to the transition temperatures (T_c) of the pure components and the mole fraction (X_n) such that:

$$X_1T_{c_1} + X_2T_{c_2} = T_{c_{mixture}}$$

Mixtures of di-C_n phosphatidylglycerols with di-$C_{n\pm4}$ phosphatidylcholines resulted in thermograms with broad non-cooperative endothermic peaks with two inflection points. These inflection points were at temperatures between the T_cs observed for the pure components and varied with the composition of the particular mixture. (Fig. 12: DMPG:DSPC; Fig. 13: DPPG:DLPC).

4. Differential thermal analysis of mixtures of phosphatidylglycerol calcium salts and phosphatidylcholines

Cooperative melting behaviour was observed in mixtures in which the acyl chains of the phosphatidylcholines were equivalent to (di-C_n) or two carbons longer than (di-C_{n+2}) the acyl chains of the phosphatidylglycerol-Ca^{++}. This is illustrated in Fig. 14 for DPPG-Ca^{++}:DPPC and DPPG-Ca^{++}:DSPC mixtures.

Mixtures in which the acyl chains of the phosphatidylcholine were shorter than the acyl chains of the DPPG-Ca^{++} exhibited non-cooperative melting behaviour. The thermpgrams of DPPG-Ca^{++}:DMPC and DPPG-Ca^{++}:DLPC showed broad transitions with two inflection points (minima) - indicative of heterogeneous lipid domains (Fig. 15).

Fig. 14. Differential thermal analysis thermograms of equimolar mixtures of DPPG:DPPC and DPPG:DSPC in the presence of Ca^{++}. Dried lipid samples were hydrated with 10 µl of 1.0M $CaCl_2$. Other experimental details as for Fig. 9.

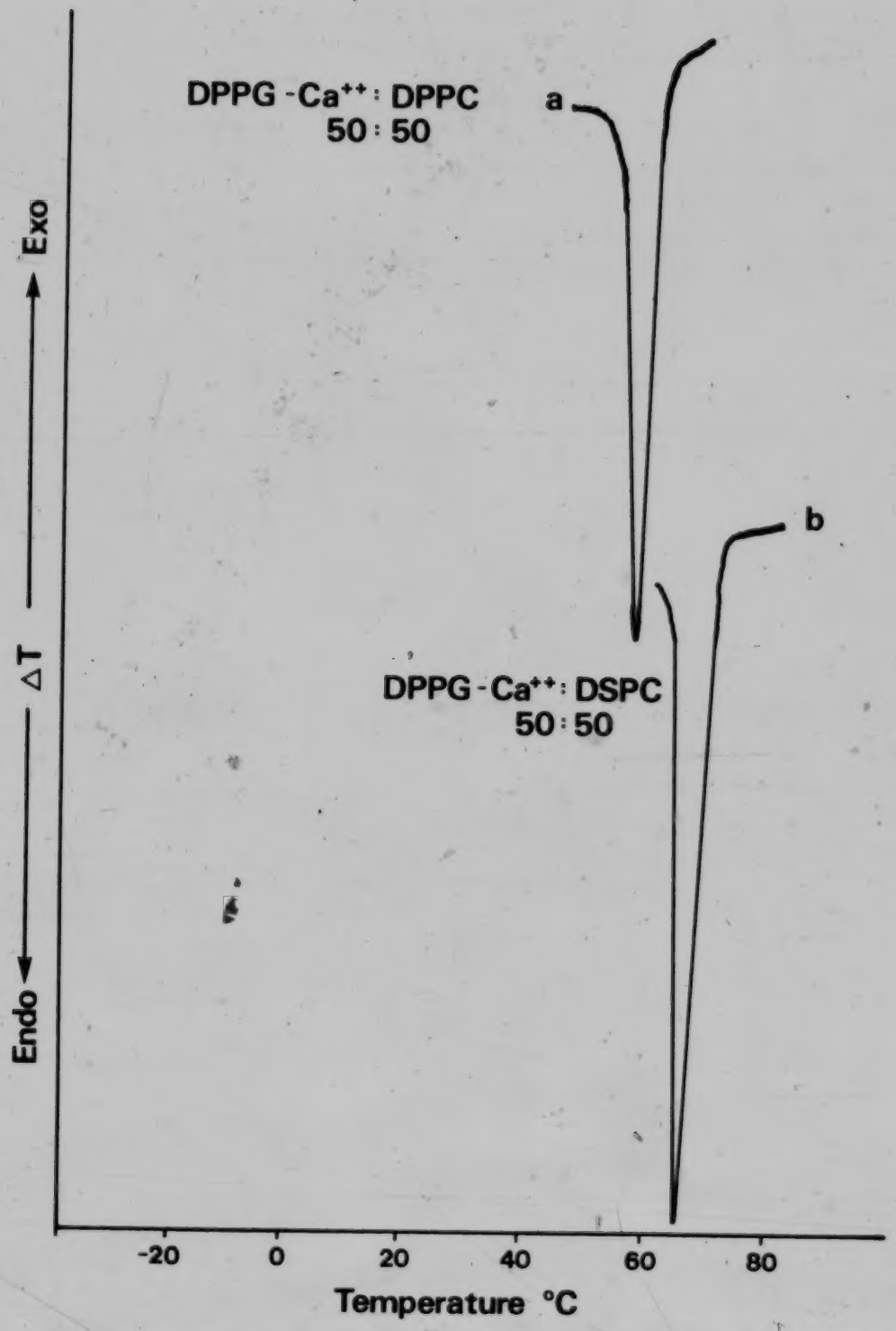
DPPG - Ca++ : DPPC
50 : 50
a
b
DPPG - Ca++ : DSPC
50 : 50
Exo
ΔT
Endo
-20
0
20
40
60
80
Temperature °C

Figure 15. Differential thermal analysis thermograms of equimolar mixtures of DPPG:DMPC, DPPG:DLPC and DPPG:DOPC in the presence of Ca^{++}. Experimental details as for Fig. 14.

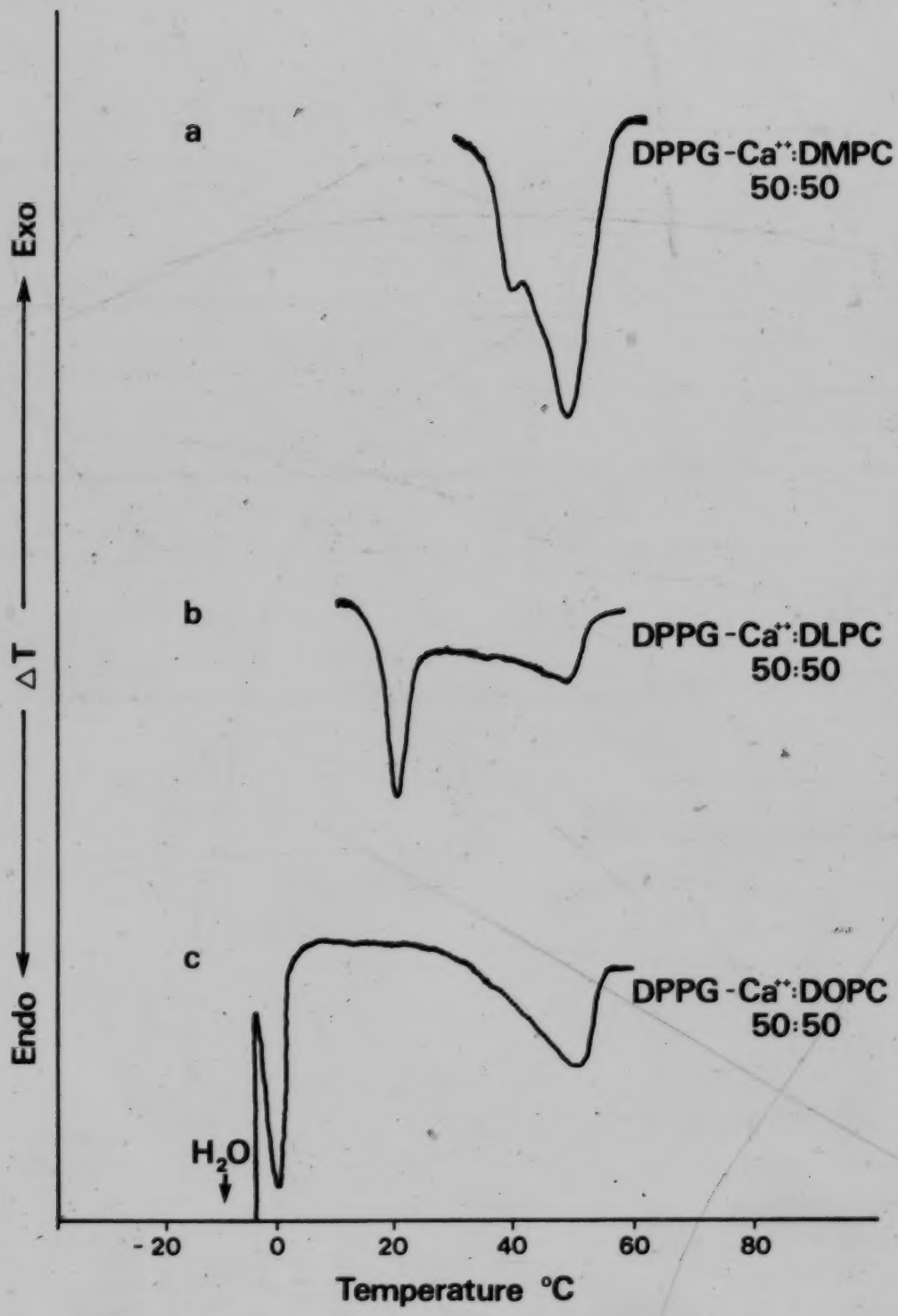
a
DPPG-Ca++:DMPC
50:50
b
DPPG-Ca++:DLPC
50:50
c
DPPG-Ca++:DOPC
50:50
Exo
ΔT
Endo
H2O
-20
0
20
40
60
80
Temperature °C

Mixtures of DOPC and DPPG-Ca^{++} also exhibited non-cooperative melting behaviour. Two distinct endotherms were visible, one at -3°C, the other at 48°C (Fig. 15).

The behaviour of DMPG-Ca^{++}:phosphatidylcholine mixtures was analogous to that observed with DPPG-Ca^{++}: phosphatidylcholine mixtures. Fig. 16 illustrates the cooperative thermal behaviour of the DMPC and DPPC with DMPG-Ca^{++} and the non-cooperative behaviour of the DLPC: DMPG-Ca^{++} mixtures.

Mixtures of DOPG:DOPC and DOPG:DSPC in the presence of Ca^{++} showed thermal properties which were at least partially predictable from examination of the thermograms of the DMPG-Ca^{++} and DPPG-Ca^{++} mixtures with phosphatidylcholines. The DOPG-Ca^{++}:DOPC mixtures melted cooperatively (sharp, narrow endotherm), as expected for a phosphatidylglycerol and the corresponding phosphatidylcholine. However, the effect of calcium on the transition temperature of these mixtures was less profound than the effect on lipid mixtures with saturated acyl chains. The thermograms of the DOPG-Ca^{++}:DSPC mixtures showed two widely separated endotherms (-10°, + 45°). The non-cooperativity shown by these mixtures (Fig. 17) was anticipated on the basis of the widely different transition temperature of the two components. (Tc DOPG-Ca^{++} = -12°C; Tc DSPC = +55°C).

Fig. 16. Differential thermal analysis data for mixtures of DMPG and phosphatidylcholines in the presence of Ca^{++}. Experimental details as for Fig. 14. The solid circles represent minima in the thermograms while the bars represent the range of temperature over which ΔT deviation from baseline is observed.

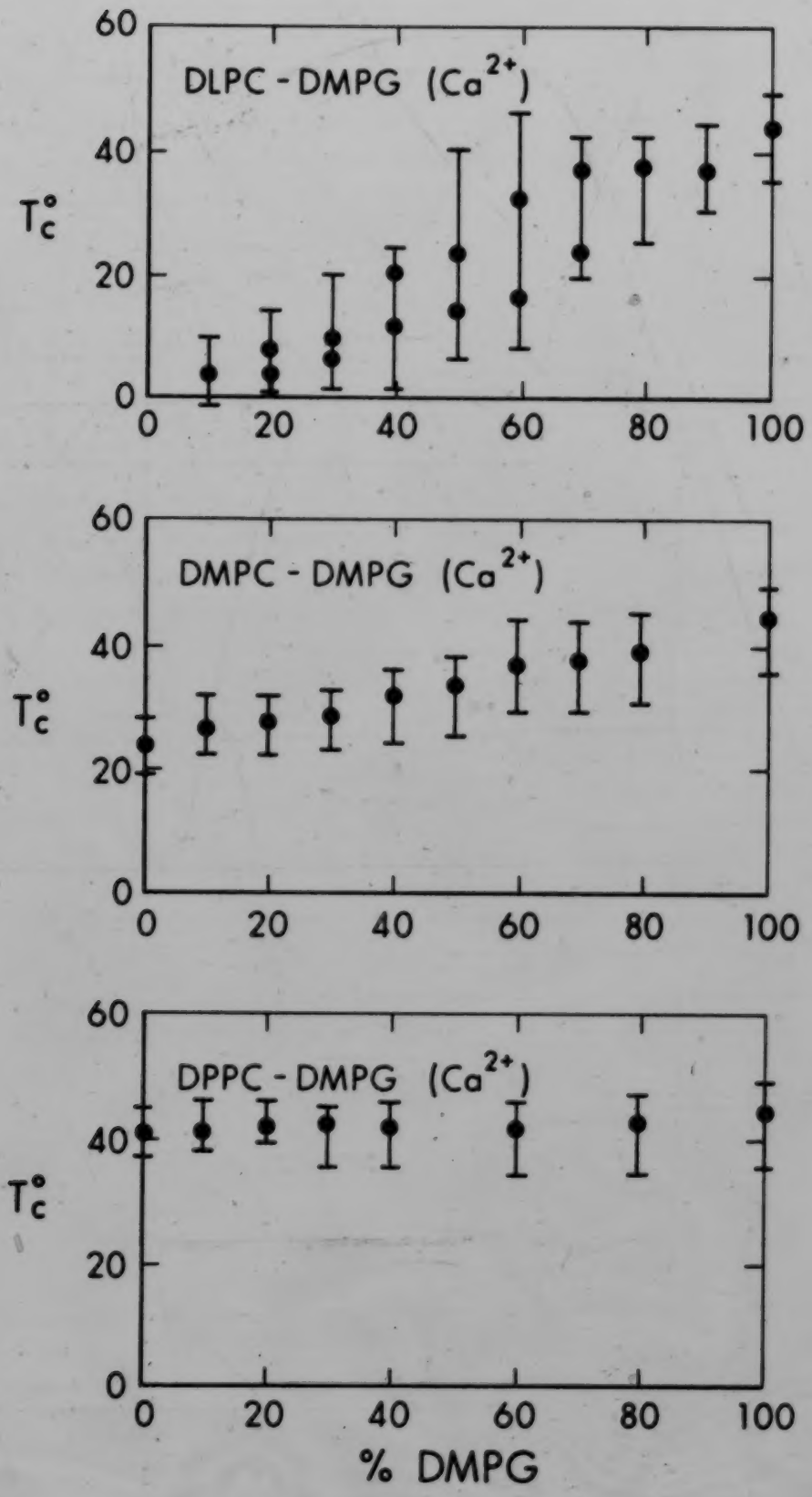
DLPC - DMPG (Ca^{2+})
DMPC - DMPG (Ca^{2+})
DPPC - DMPG (Ca^{2+})
T_c°
0
20
40
60
80
100
% DMPG

Fig. 17. Differential thermal analysis thermograms of mixtures of DOPG with phosphatidylcholines in the presence of Ca^{++}. Experimental details as for Fig. 14. Sample a had 4 µl of ethylene glycol added to eliminate the ice-water transition in the 0 to -20°C range.

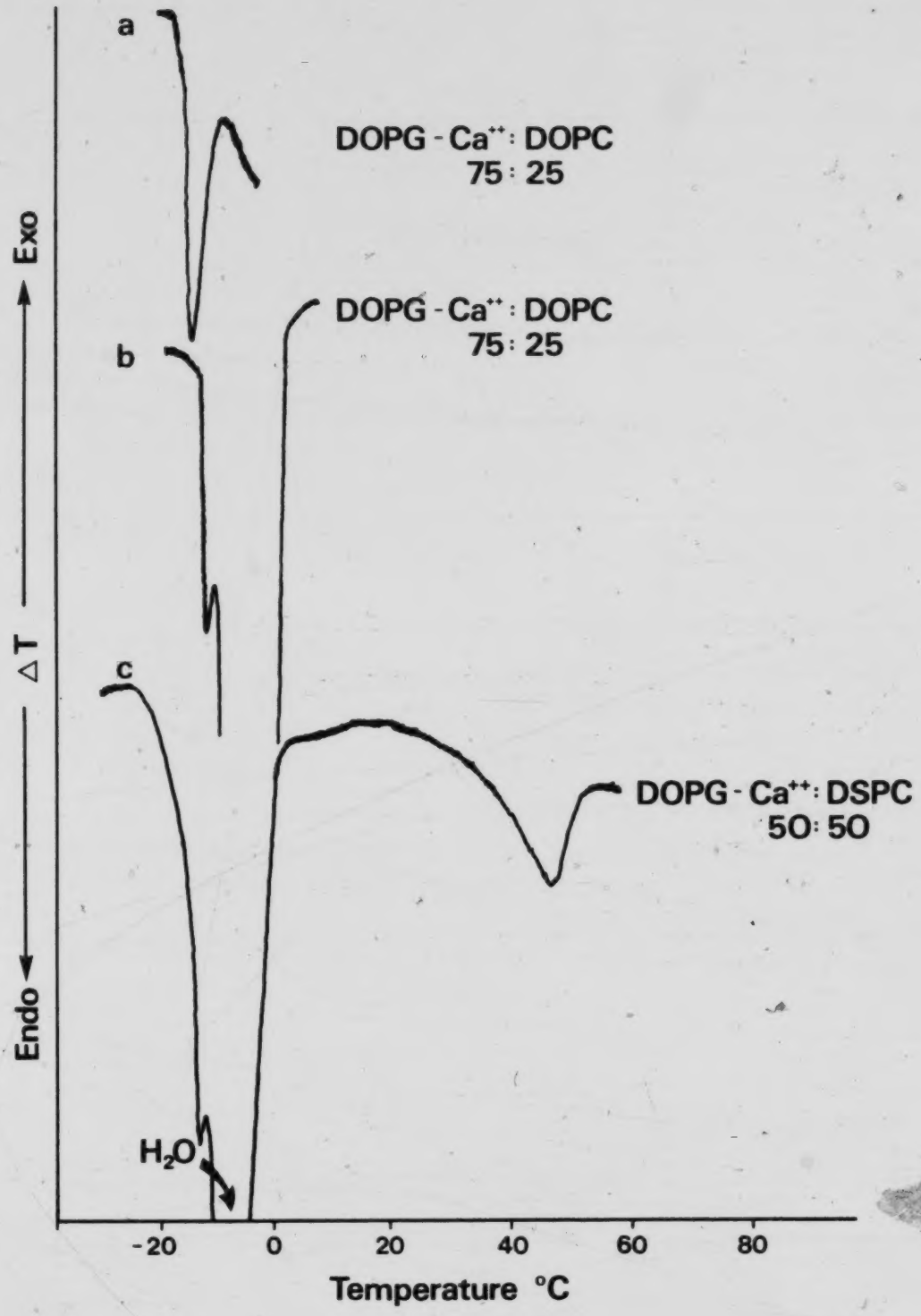
a
DOPG - Ca++ : DOPC
75 : 25
b
DOPG - Ca++ : DOPC
75 : 25
c
DOPG - Ca++ : DSPC
50 : 50
Exo
ΔT
Endo
H2O
-20
0
20
40
60
80
Temperature °C

5. Differential thermal analysis of DPPG-Ca^{++}

Samples of DPPG which were allowed to equilibrate several hours in 1.0M $CaCl_2$ prior to a heating run gave a single, relatively non-cooperative endotherm centered at 89°C (Fig. 18a). The non-linearity of the base line between 60°C and 80°C was suggestive of some minimal thermal activity but analysis of the nature of the activity was not possible.

The cooling curve consisted of a single, sharp exothermic peak centered at approximately 58°C (Fig. 18b).

Samples of DPPG-Ca^{++} which were subjected to consecutive heating runs without time to equilibrate between runs gave the complex but reproducible thermogram illustrated in Figure 18c. This thermogram consisted of: (1) an endotherm centered at 59°C, (2) a broad exotherm at 68°C, (3) an endotherm at 77°C, (4) an exotherm at 81°C, and finally (5) an endotherm centered at 89°C.

The cooling curve, following a heating curve of this type was identical to Fig. 18b.

Due primarily to the simplicity of the cooling curves, it was felt that the complexity of the 'non-equilibrated' heating curves was a result of progressive interconversion of the lipid to a series of metastable forms rather than a number of different thermally stable forms. This was demonstrated to be the case by the following series of experiments.

A 'non-equilibrated' sample of DPPG-Ca^{++} was heated

Fig. 18. Differential thermal analysis thermograms of DPPG-Ca^{++}. DPPG was hydrated with 10 µl of 1.0M $CaCl_2$.

(a) Heating curve of sample allowed to equilibrate prior to thermal analysis.

(b) Cooling curve subsequent to (a).

(c) Heating curve of sample subjected to consecutive heating runs without time to equilibrate.

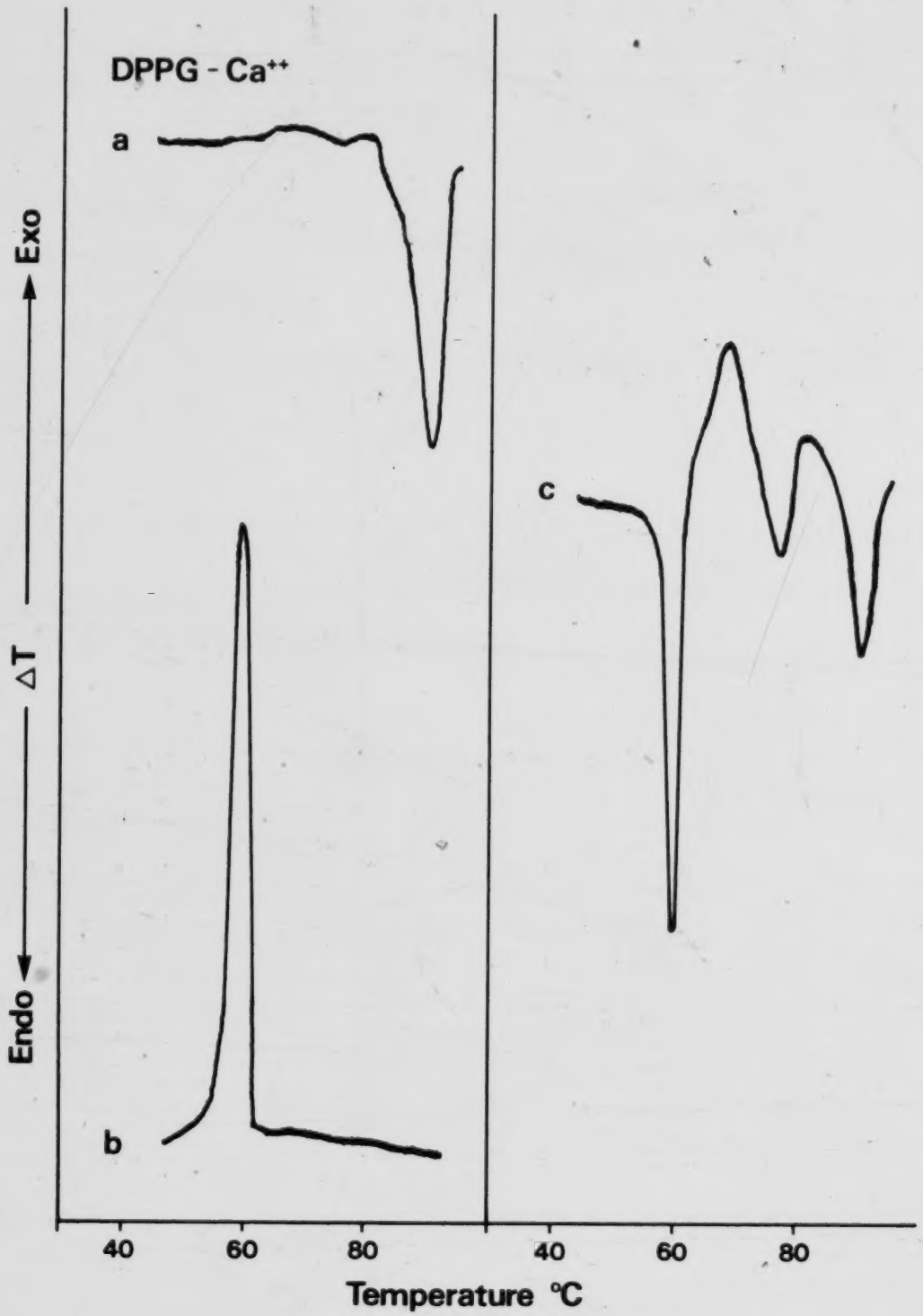
DPPG - Ca++
a
b
c
Exo
ΔT
Endo
40
60
80
40
60
80
Temperature °C

to 70°C (Fig. 19c), then cooled (Fig. 19d) to below 40°C. Only a trace of an exotherm at 58°C was visible in the cooling curve. The subsequent heating curve showed just a trace endotherm at 59°C and no exotherm at 68°C (Fig. 19e). The thermogram from 70°C through 90°C was essentially identical to the same region of the 'non-equilibrated' sample heating curve (Fig. 19a). The cooling curve, following heating to 90°C, is illustrated in Fig. 19b.

A similar series of analyses demonstrated that heating a sample to 80°C (Fig. 20a) converted the lipid to a form that, on subsequent cooling and heating, was thermally stable to above 80°C. The cooling curve (Fig. 20b) showed no exotherm at 58°C and the subsequent heating curve (Fig. 20c) consisted of a single endotherm centered at 89°C, essentially the same as an 'equilibrated' sample.

A sample previously heated to 95°C could be cooled to 60°C (Fig. 20d) with no transition evident. Reheating to 95°C showed the endotherm at 89°C had been almost completely eliminated (Fig. 20e). A complete cooling curve of this mixture consisted of a single sharp endotherm centered at 58°C (Fig. 20f).

6. Differential thermal analysis of DMPG-Ca^{++}

Thermograms of equilibrated samples of DMPG-Ca^{++} showed a single relatively cooperative endotherm centered at 87°C (Fig. 21b). 'Non-equilibrated' samples (less than 30 minutes between runs) showed an exotherm at 44°C, a

Figure 19. Differential thermal analysis thermograms of DPPG-Ca^{++}.

(a) 'Non-equilibrated' sample-conditions as for Fig. 18c.

(b) Cooling curve following heating to 90°C.

(c) Heating curve of 'non-equilibrated' sample to 70°C.

(d) Cooling curve of c.

(e) Complete heating curve subsequent to c and d.

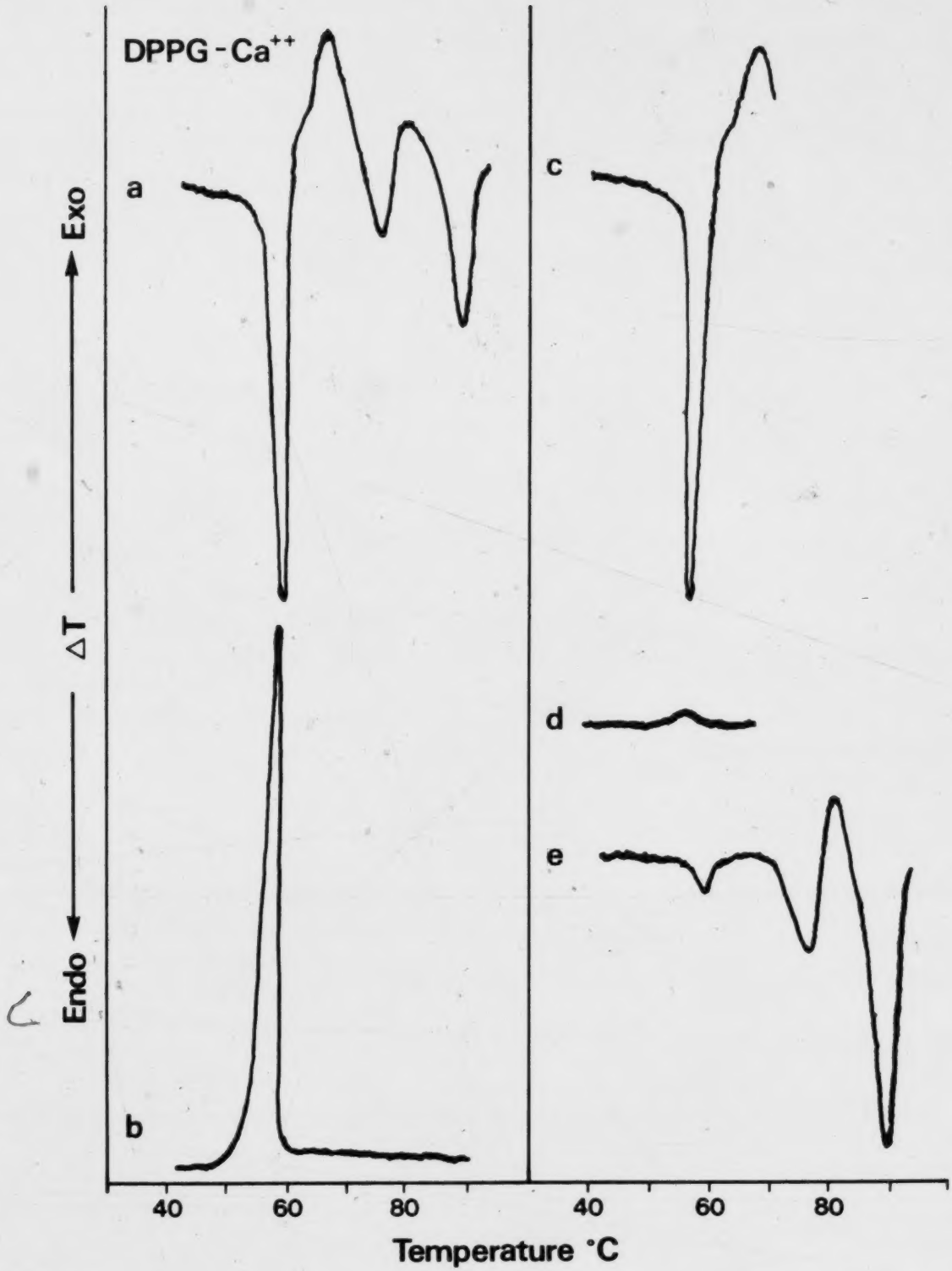
DPPG - Ca++
a
b
c
d
e
Exo
ΔT
Endo
40
60
80
40
60
80
Temperature °C

Figure 20. Differential thermal analysis thermograms of DPPG-Ca^{++}.

(a) 'Non-equilibrated' sample heated to 80°C.

(b) Cooling curve subsequent to a.

(c) Heating curve subsequent to a and b.

(d) Cooling curve of c to 60°C.

(e) Heating curve from 60°C to 90°C.

(f) Cooling curve following e.

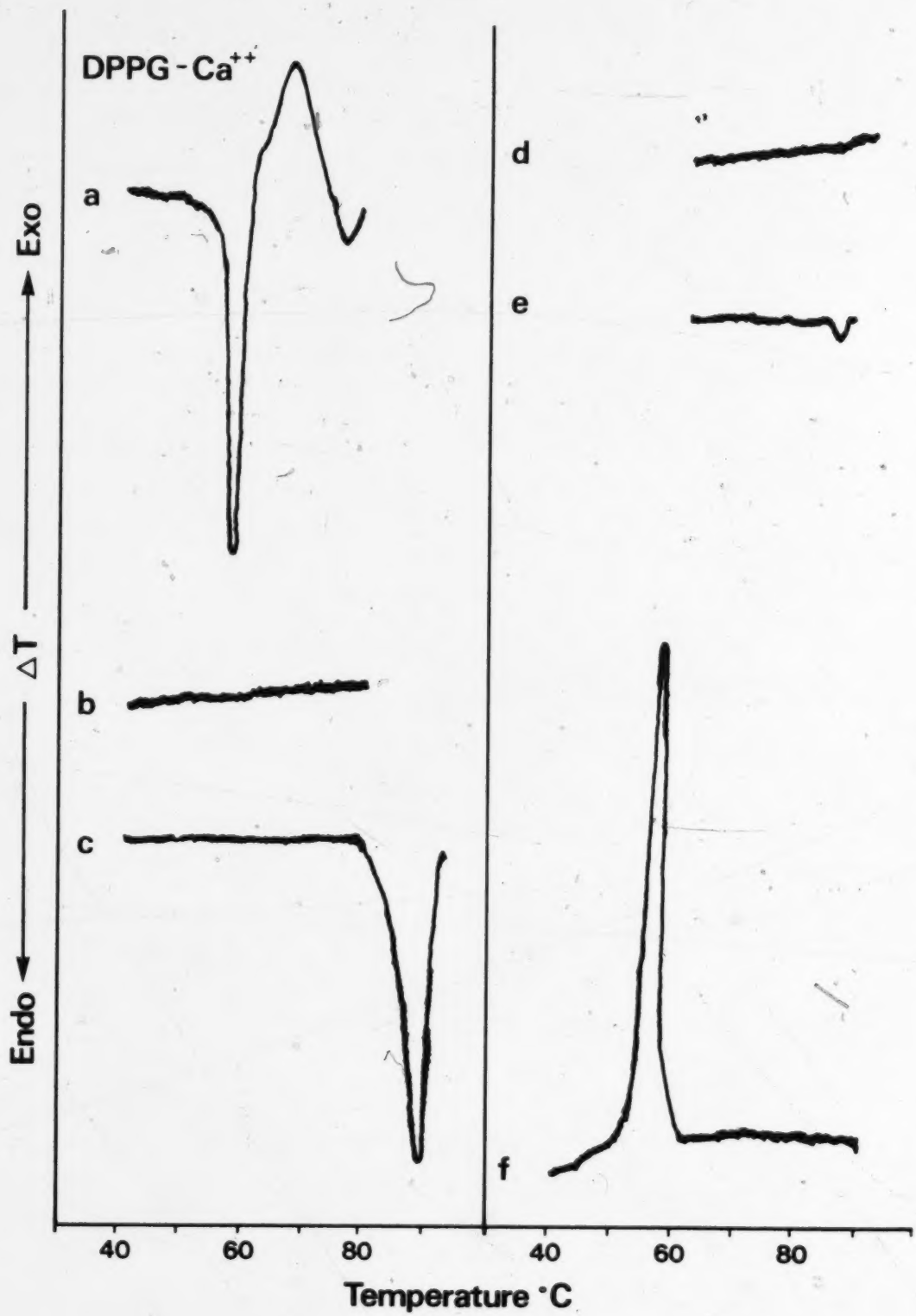
DPPG - Ca++
a
b
c
d
e
f
Exo
ΔT
Endo
40
60
80
40
60
80
Temperature °C

Fig. 21. Differential thermal analysis thermogram of DMPG-Ca^{++}. Samples were hydrated with 10 µl 1.0M $CaCl_2$. The term 'non-equilibrated' indicates heating runs were less than 30 min. apart.

(a) Heating curve for 'non-equilibrated' sample.

(b) Heating curve for equilibrated sample.

(c) Cooling curve obtained following either a or b.

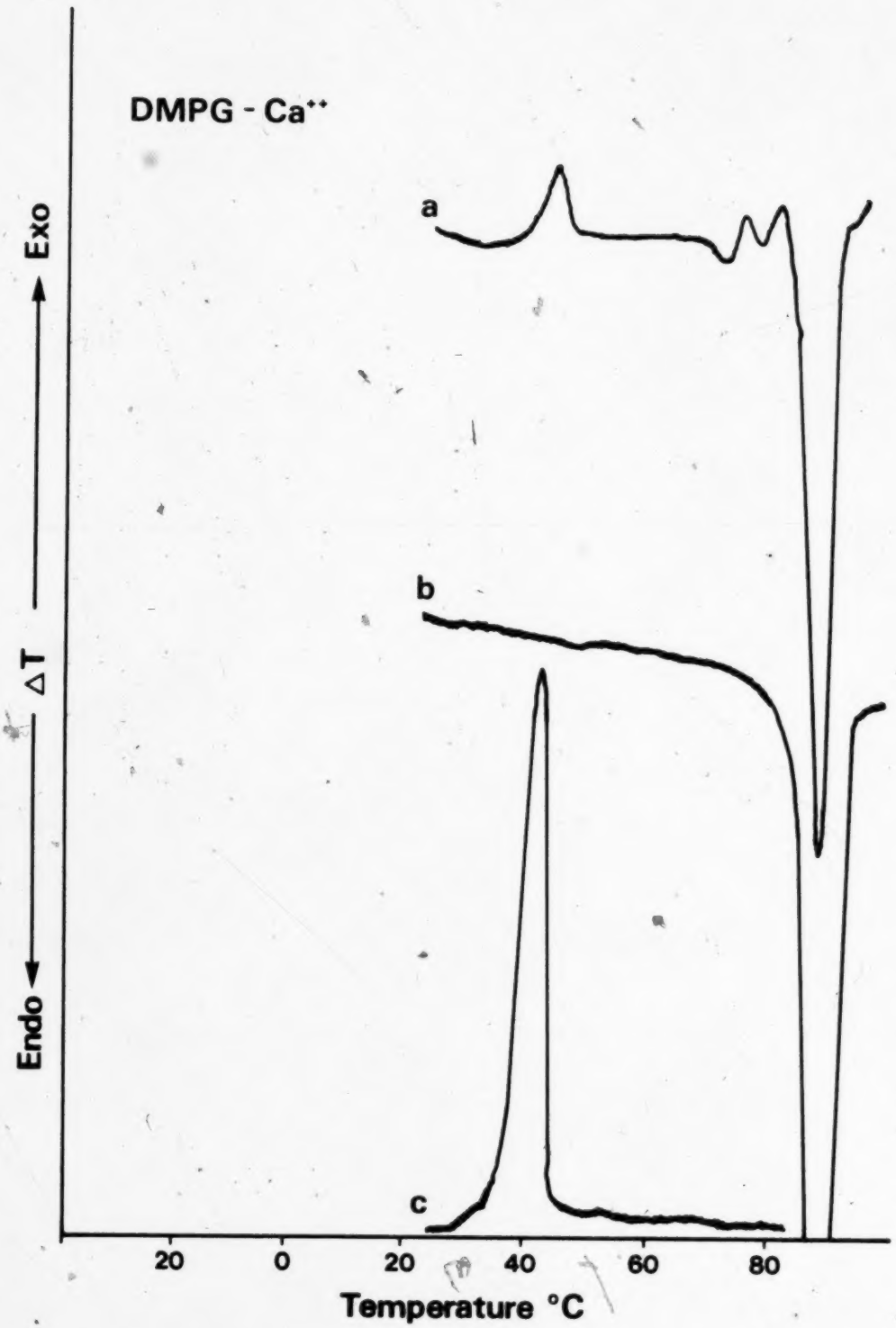
DMPG - Ca++
Exo
ΔT
Endo
a
b
c
20
0
20
40
60
80
Temperature °C

complex series of low energy endotherms and exotherms between 68°C and 82°C, followed by a large cooperative endotherm at 87°C (Fig. 21a).

The cooling curve for both 'equilibrated' and 'non-equilibrated' samples, previously heated to 90°C, consisted to a single sharp exotherm at 40°C (Fig. 21c). Metastable behaviour analogous to that seen with the DPPG-Ca^{++} could be demonstrated.

7. Differential thermal analysis of DPPG-Mg^{++}

The heating curve for DPPG-Mg^{++} consisted of a single, cooperative endotherm, centered at 59°C (Fig. 22a). A sample which had been allowed to equilibrate for approximately three days in 1.0M $MgCl_2$ at room temperature gave a more complex thermogram consisting of two small endotherms at 59°C and 65°C, a small exotherm at approximately 69°C and a large endotherm centered at 76°C (Fig. 22b). After the first heating run, the thermal behaviour of this sample reverted to the single 59°C endotherm seen in Fig. 22a.

The conversion of the DPPG-Mg^{++} to the high-melting (76°C) form appeared to be slow (>3 days) and the small complex detail seen in Fig. 22b probably results from incomplete conversion of the DPPG-Mg^{++} to the high-melting form.

8. Differential thermal analysis of DMPG-Mg^{++}

The thermal behaviour observed for DMPG-Mg^{++} (Fig. 23) was more complex than that observed for DPPG-Mg^{++}. The

Figure 22I. Differential thermal analysis of DPPG.

(a) DPPG-Na^+.- heating scan. Experimental details as for Fig. 9.

(b) DPPG-H^+ - heating scan. Experimental details as for Fig. 29e.

Figure 22II. Differential thermal analyses of DPPG-Mg^{++}.

(a) Heating curve for DPPG-Na^+ hydrated with 7 µl 1.0M $MgCl_2$.

(b) Heating curve for DPPG-Na hydrated with 10 µl of 1.0M $MgCl_2$.

Sample was allowed to equilibrate 3 days at room temperature prior to heating. After the first heating run the sample reverted to a thermogram identical to a.

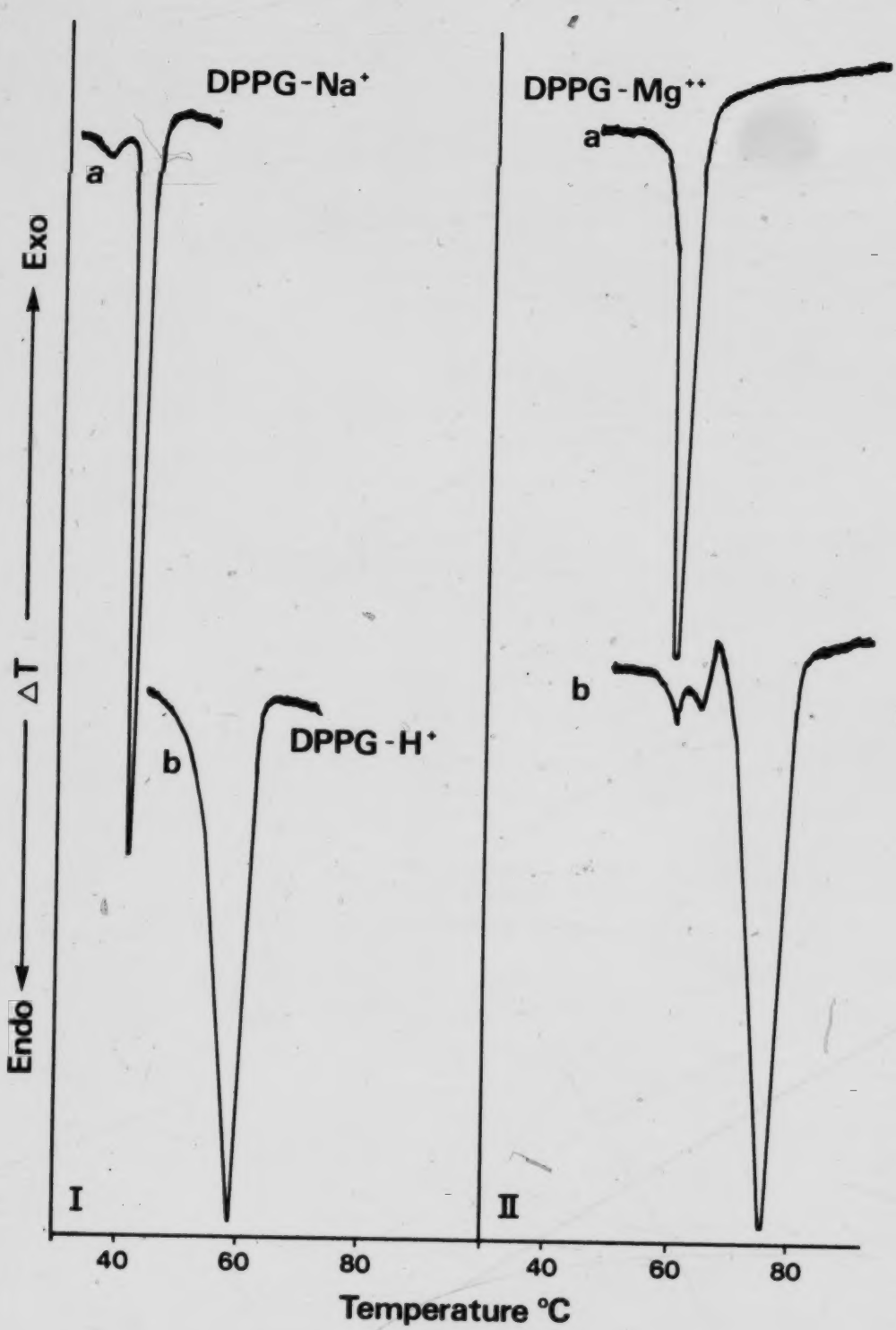
DPPG-Na⁺
DPPG-Mg⁺⁺
DPPG-H⁺
a
b
Exo
ΔT
Endo
I
II
40
60
80
Temperature °C

Fig. 23. Differential thermal analysis of DMPG-Mg^{++}. Samples were hydrated with 7 µl of 1.0M $MgCl_2$.

(a) Complete heating curve.

(b) Complete cooling curve.

(c) Heating to 55°C.

(d) Cooling curve subsequent to c.

(e) Heating curve following c and d.

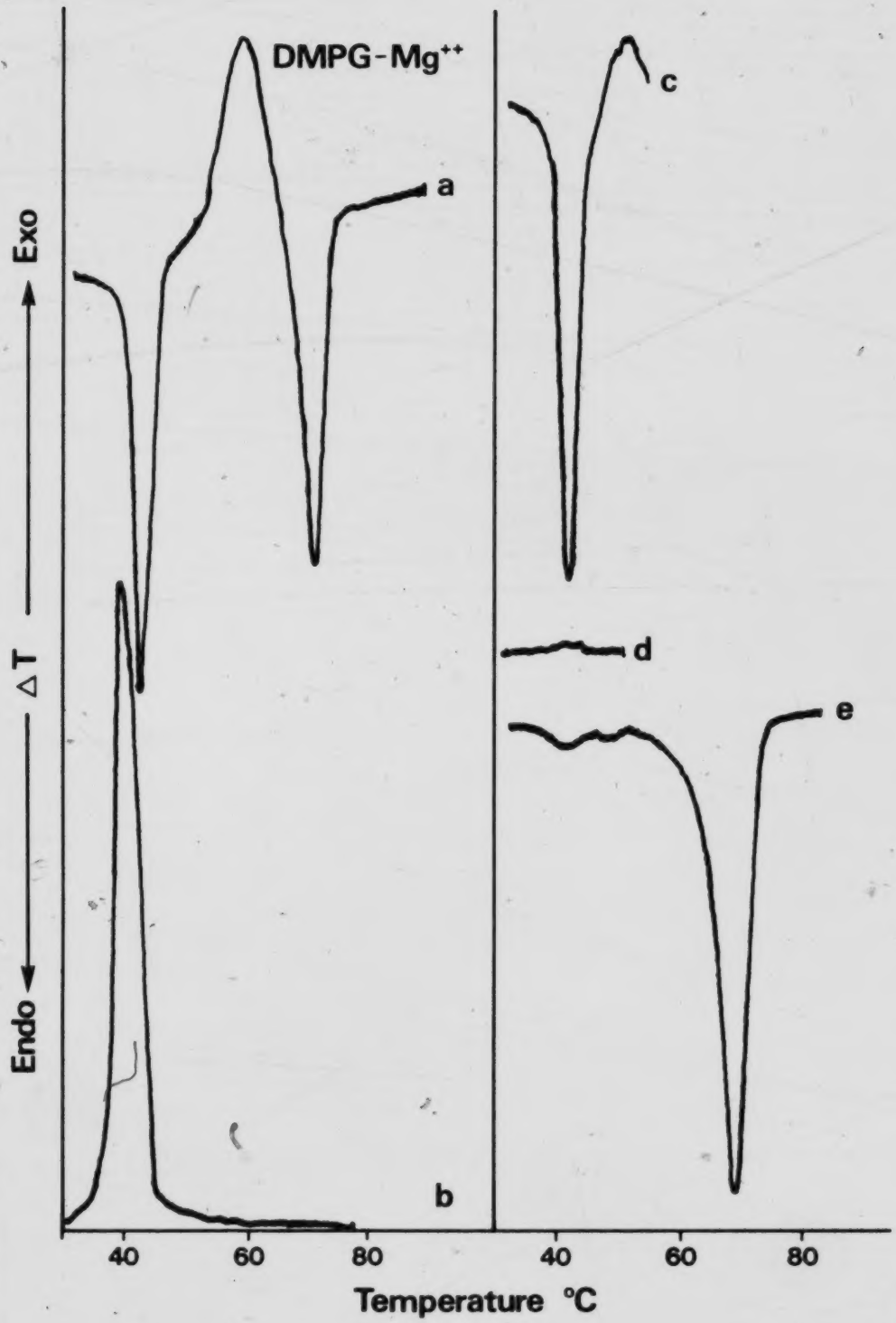
DMPG-Mg++
a
b
c
d
e
Exo
ΔT
Endo
40
60
80
40
60
80
Temperature °C

DMPG-Mg^{++} thermogram had features which bore more resemblance to the DPPG-Ca^{++} heating curve than to the DPPG-Mg^{++} curve.

The DMPG-Mg^{++} thermogram consisted of a sharp endotherm at 44°C followed by a broad exotherm centered between 50°C and 60°C, then a cooperative endotherm at 68°C (Fig. 23a).

The cooling curve consisted of a single sharp exotherm at 40°C (Fig. 23b).

Heating a sample to approximately 55°C (Fig. 23c) resulted in elimination of the 40°C exotherm on cooling (Fig. 23d) and converted the DMPG-Mg^{++} to a more stable form which on subsequent heating gave a single endotherm at 68°C (Fig. 23e).

The DMPG-Mg^{++} spontaneously converted, at room temperature, to the higher melting form (68°C) if allowed to equilibrate overnight. This was in contrast with DPPG-Mg^{++} which required in excess of three days for a similar conversion.

9. Effect of cholesterol on the thermal behaviour of phosphatidylglycerols

Mixtures of DPPG-Na^{+} or DMPG-Na^{+} with cholesterol in a 3:1 molar ratio resulted in a pronounced decrease in the cooperativity of the phase transitions (Fig. 24a: DMPG; Fig. 25d: DPPG). At a 2:1 molar ratio of phosphatidylglycerol to cholesterol the phase transitions of both the DMPG-Na^{+} and DPPG-Na^{+} were abolished throughout the temperature range scanned (-50°C to +95°C).

Fig. 24. Differential thermal analysis of DMPG: cholesterol (3:1).

(a) Heating curve for sample hydrated with 7 µl Tris-HCl (0.01M) in NaCl (0.15M) at pH 9.0.

(b) Heating curve for sample in 7.0 µl 1.0M $CaCl_2$.

(c) 'Non-equilibrated' sample (less than 30 min. between heating runs) in presence of 1.0M $CaCl_2$.

(d) Cooling curve subsequent to either b or c.

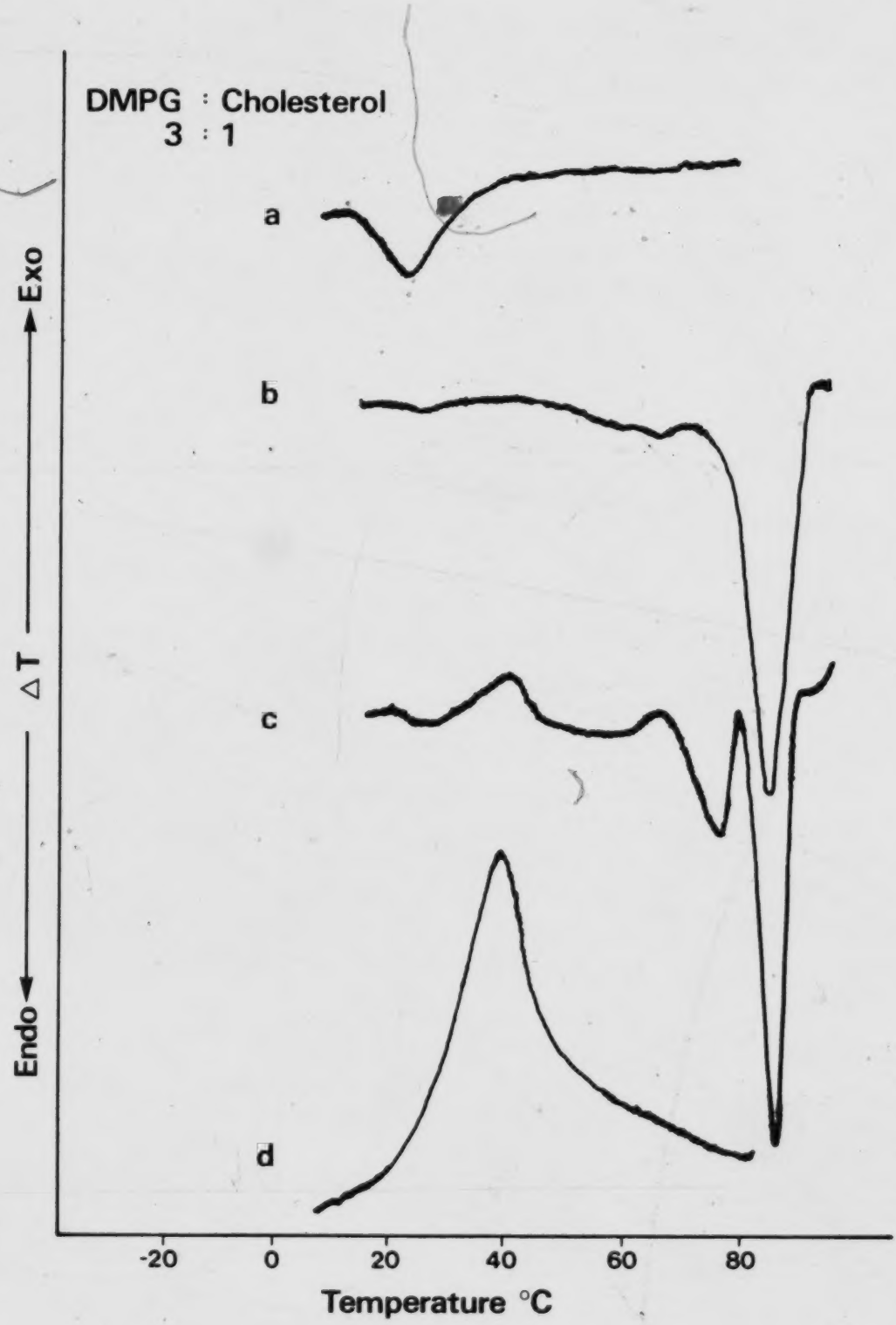
DMPG : Cholesterol
3 : 1
a
b
c
d
Exo
ΔT
Endo
-20
0
20
40
60
80
Temperature °C

Fig. 25. Differential thermal analysis of DPPG: cholesterol (3:1)

(a) Heating curve of sample hydrated with 7.0 µl of 1.0M $CaCl_2$.

(b) Heating curve of 'non'equilibrated' (less than 30 min. between runs) sample in the presence of 1.0M $CaCl_2$.

(c) Cooling curve following either a or b.

(d) Heating curve for sample hydrated with 7.0 µl of Tris-HCl (0.01M) in NaCl (0.15M) at pH 9.0.

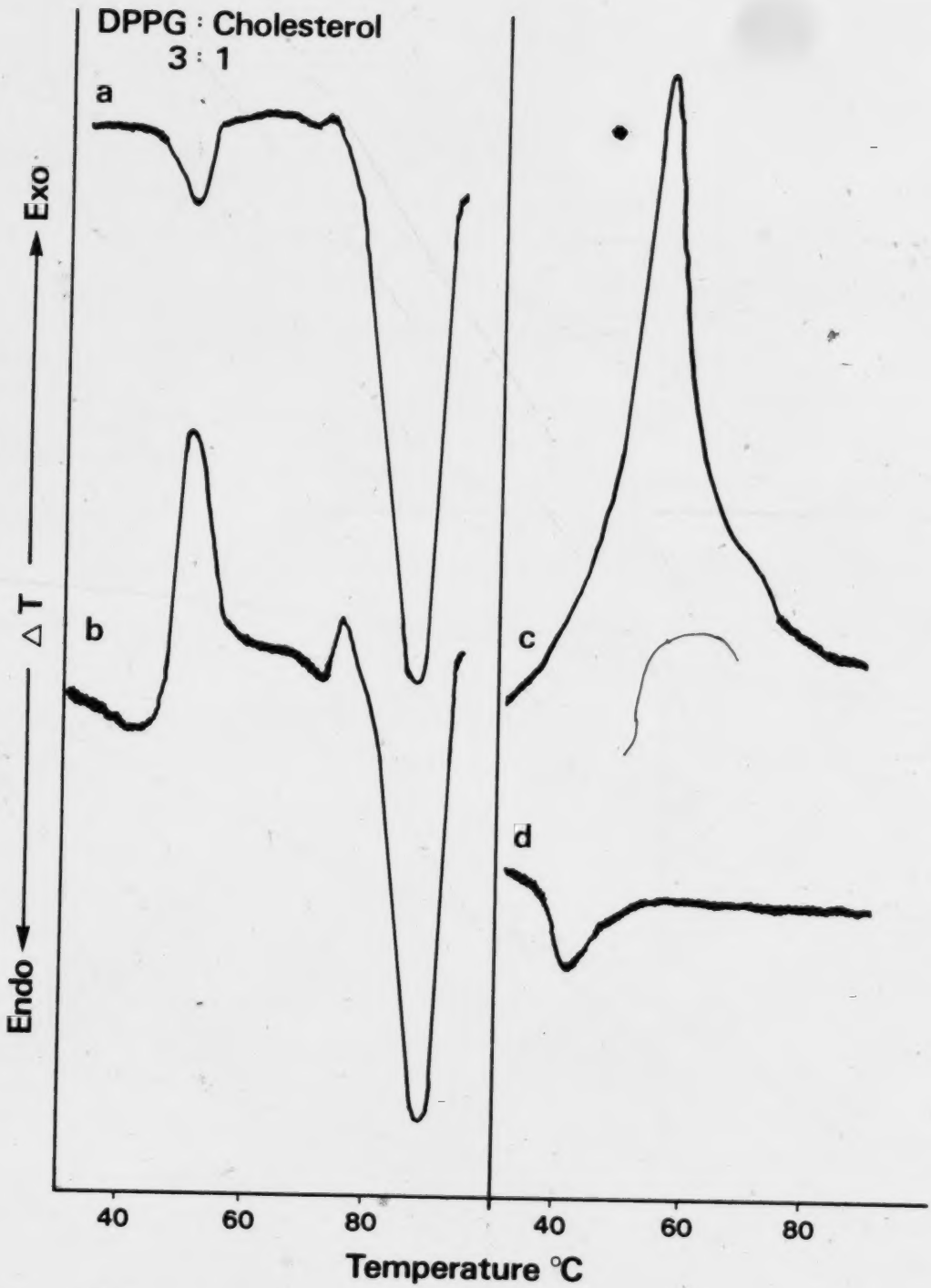
DPPG : Cholesterol
3 : 1
a
b
c
d
Exo
ΔT
Endo
40
60
80
40
60
80
Temperature °C

The presence of Ca^{++} opposed the effects of cholesterol on the DPPG and DMPG. For example, at 3:1 molar ratio of PG-Ca^{++} to cholesterol many of the complex features of the pure PG-Ca^{++} thermograms were still evident. Thermograms of equilibrated samples of DMPG-Ca^{++}:cholesterol (3:1) consisted of a single broad endotherm centered at 86°C (Fig. 24b). Similarly, the major feature of the DPPG-Ca^{++}:cholesterol (3:1) thermogram consisted of a large endotherm at approximately 88°C (Fig. 25a). A small endotherm at 50°C was also present with the DPPG-Ca^{++} samples. This was not observed with DMPG-Ca^{++} samples.

Thermograms of 'non-equilibrated' samples of DMPG-Ca^{++}:cholesterol (3:1) were similar to the DMPG-Ca^{++} thermograms in the absence of cholesterol (Fig. 24c). The exotherm at 40°C was present and complex behaviour was observed between 50°C and 80°C. Although the thermograms of DMPG-Ca^{++} (Fig. 21a) and DMPG-Ca^{++}:cholesterol (3:1) showed some differences between 60°C and 80°C the patterns of individual samples also exhibited some variation in this temperature range due to hysteretic effects. Thus it was not possible to definitely attribute the differences to the effect of cholesterol on the melting behaviour.

The cooling curve for DMPG-Ca^{++}:cholesterol (3:1) consisted of a single very broad endotherm centered at approximately 40°C (Fig. 24d).

Thermograms of 'non-equilibrated' DPPG-Ca^{++}:cholesterol (3:1) showed two major differences from the DPPG-Ca^{++}

thermograms (Fig. 25b). The endotherm seen at 59°C was eliminated in the presence of cholesterol and the exotherm at 66°C in the absence of cholesterol was shifted to approximately 50°C.

The cooling curve of DPPG-Ca^{++}:cholesterol (3:1) consisted of a single broad endotherm (Fig. 25c), centered at approximately 56°C, similar in form to the DMPG-Ca^{++}:cholesterol (3:1) cooling curve.

Mixtures of DMPG-Ca^{++} or DPPG-Ca^{++} with cholesterol in molar ratio 2:1 exhibited heating curves qualitatively similar to those seen with mixtures having molar ratio 3:1 (Fig. 26: DMPG; Fig. 27: DPPG). However, a major difference induced by the higher cholesterol concentration was evident in the cooling curves. At PG-Ca^{++}:cholesterol ratios of 2:1, each cooling curve consisted of a single exotherm centered at 80°-85°C (Fig. 26c: DMPG; Fig. 27b: DPPG). In contrast with the 3:1 mixtures of PG-Ca^{++}:cholesterol, no super-cooling of the high melting form was observed with the 2:1 PG-Ca^{++}:cholesterol samples.

At a 1:1 DPPG-Ca^{++}:cholesterol molar ratio, the appearance of the thermogram was quantitatively altered (Fig. 27d). The alteration appeared to involve a decrease in the cooperativity and size of the thermographic peaks rather than complete elimination of any of the thermographic detail.

Fig. 26. Differential thermal analysis of DMPG: cholesterol (2:1). Samples were hydrated with 7 µl of 1.0M $CaCl_2$.

(a) Complete heating curve.

(b) Heating curve for 'non-equilibrated' sample.

(c) Cooling curve subsequent to either a or b.

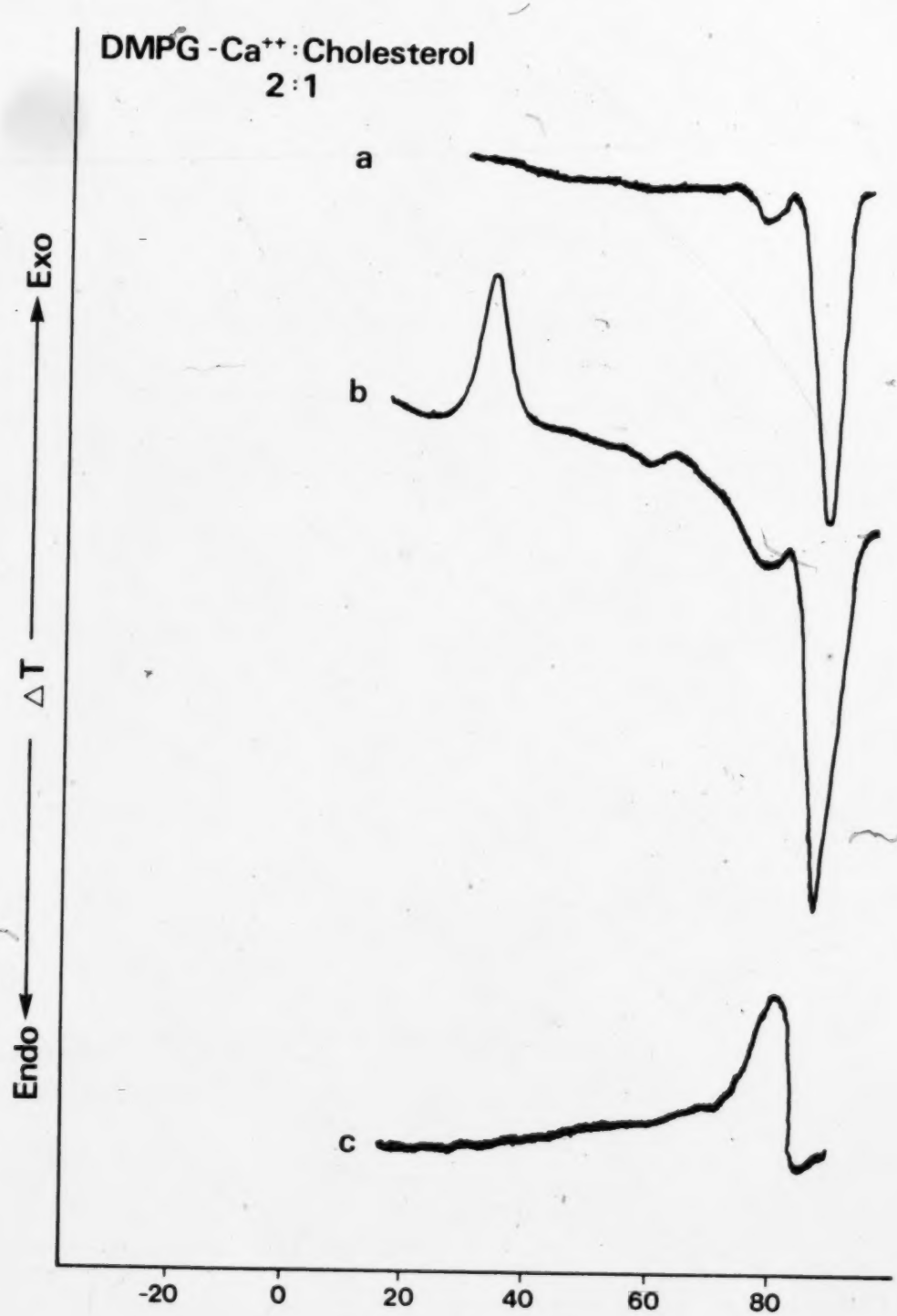
DMPG - Ca++ : Cholesterol
2 : 1
a
b
c
Exo
ΔT
Endo
-20
0
20
40
60
80
Temperature °C

Fig. 27. Differential thermal analysis of DPPG: cholesterol mixtures.

(a) Heating curve for DPPG:cholesterol (2:1) in the presence of 1.0M $CaCl_2$.

(b) Cooling curve subsequent to a or c.

(c) Heating curve of 'non-equilibrated' DPPG:cholesterol (2:1) in the presence of 1.0M $CaCl_2$.

(d) Heating curve for DPPG:cholesterol (1:1) in 1.0M $CaCl_2$.

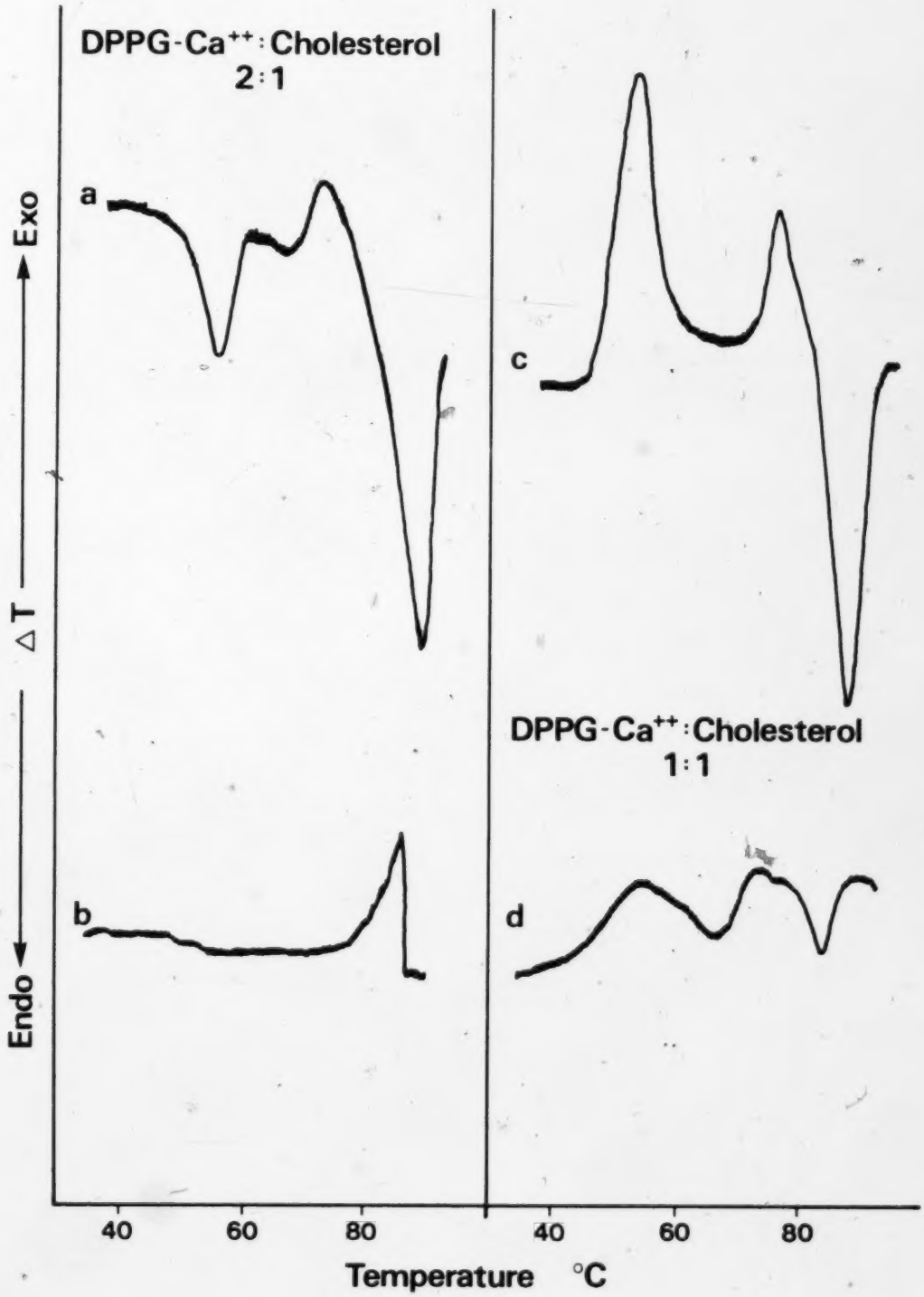
DPPG-Ca++:Cholesterol
2:1
DPPG-Ca++:Cholesterol
1:1
a
b
c
d
Exo
Endo
ΔT
40
60
80
40
60
80
Temperature °C

10. Differential thermal analysis of phosphatidylcholine:phosphatidylglycerol-Ca^{++} mixtures in the presence of cholesterol

Fig. 28 illustrates the effects of increasing cholesterol concentrations in mixtures containing equimolar amounts of DPPG-Ca^{++} and DLPC. At a molar ratio of 8:1 total phospholipid:cholesterol the thermogram is changed to a broad non-cooperative endotherm centered at approximately 30°C (Fig. 28b). At a 4:1 phospholipid:cholesterol ratio, the 30°C endotherm had decreased slightly in size but the shape remained the same (Fig. 28c). At a 2:1 phospholipid to cholesterol ratio the lipid transition was completely abolished (Fig. 28d).

Behaviour analogous to the DPPG-Ca^{++}:DLPC:cholesterol case was observed with DMPG-Ca^{++}:DLPC:cholesterol mixtures.

11. Thermal behaviour of mixtures of phosphatidylglycerol-Na^{+} and phosphatidylglycerol-H^{+}

The extraction procedures and sample preparation indicated in the legends of Fig. 29 (DPPG) and Fig. 30 (DMPG) resulted in samples with transition temperatures which varied through a range of approximately 18°C. Samples extracted and prepared under progressively more acidic conditions had progressively higher melting points approaching a limiting value for the protonated form (Fig. 29a-e). With the DPPG samples only one endotherm was observed in each case. With DMPG, although the same progressive increase in transition temperature could be observed with increasing PG-H^{+}:PG-Na^{+}

Fig. 28. Effect of cholesterol on the thermal behaviour of DPPG-Ca^{++}:DLPC mixtures.

(a) Heating curve of DPPG-Ca^{++}:DLPC (1:1) in 1.0M $CaCl_2$.

(b) Heating curve of DPPG-Ca^{++}:DLPC: cholesterol (1:1:0.25) in 1.0M $CaCl_2$.

(c) Heating curve of DPPG-Ca^{++}:DLPC: cholesterol (1:1:0.5) in 1.0M $CaCl_2$.

(d) Heating curve of DPPG-Ca^{++}:DLPC: cholesterol (1:1:1) in 1.0M $CaCl_2$.

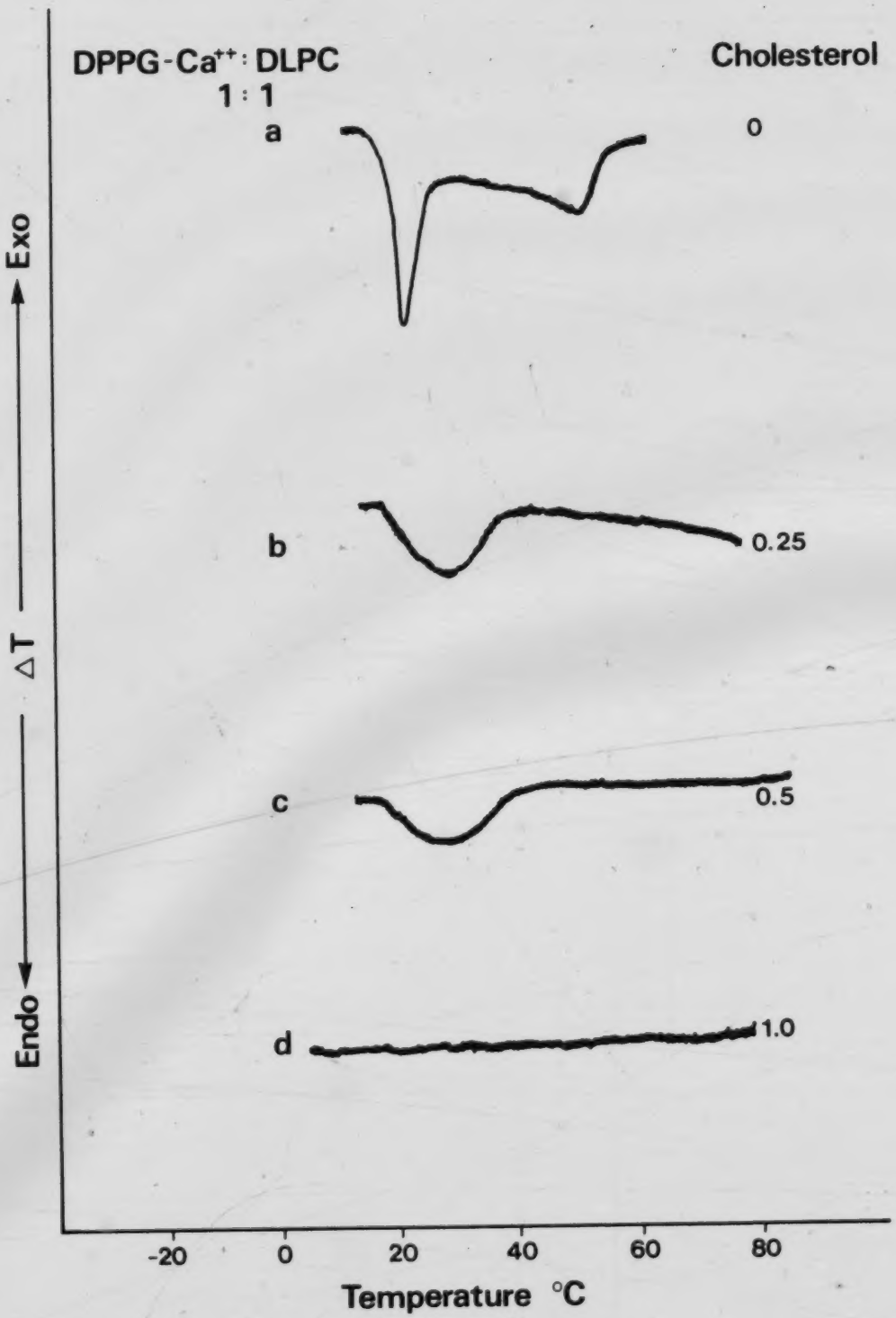
DPPG-Ca++ : DLPC
1 : 1
Cholesterol
a
0
b
0.25
c
0.5
d
1.0
Exo
ΔT
Endo
-20
0
20
40
60
80
Temperature °C

Fig. 29. Differential thermal analysis of mixtures of DPPG-Na^+ and DPPG-H^+.

(a) Sample extracted from a monophasic Bligh and Dyer mixture of 0.1M NaCl; 0.01M Na_2 EDTA at pH 9.0. Hydrated with Tris-HCl (0.01M) at pH 9.0.

(b) Extracted from 0.05M NaCl; saturated EGTA at pH 7.5. Hydrated with Tris-HCl (0.01M) at pH 9.0

(c) Extracted from 0.1M NaCl; 0.01M Na_2 EDTA at pH 4.5. Hydrated with distilled H_2O.

(d) Extracted from 0.05M NaCl; saturated EGTA at pH 4.0. Hydrated with distilled H_2O.

(e) Extracted from 0.05M NaCl; saturated EGTA at pH 3.0. Hydrated with distilled H_2O.

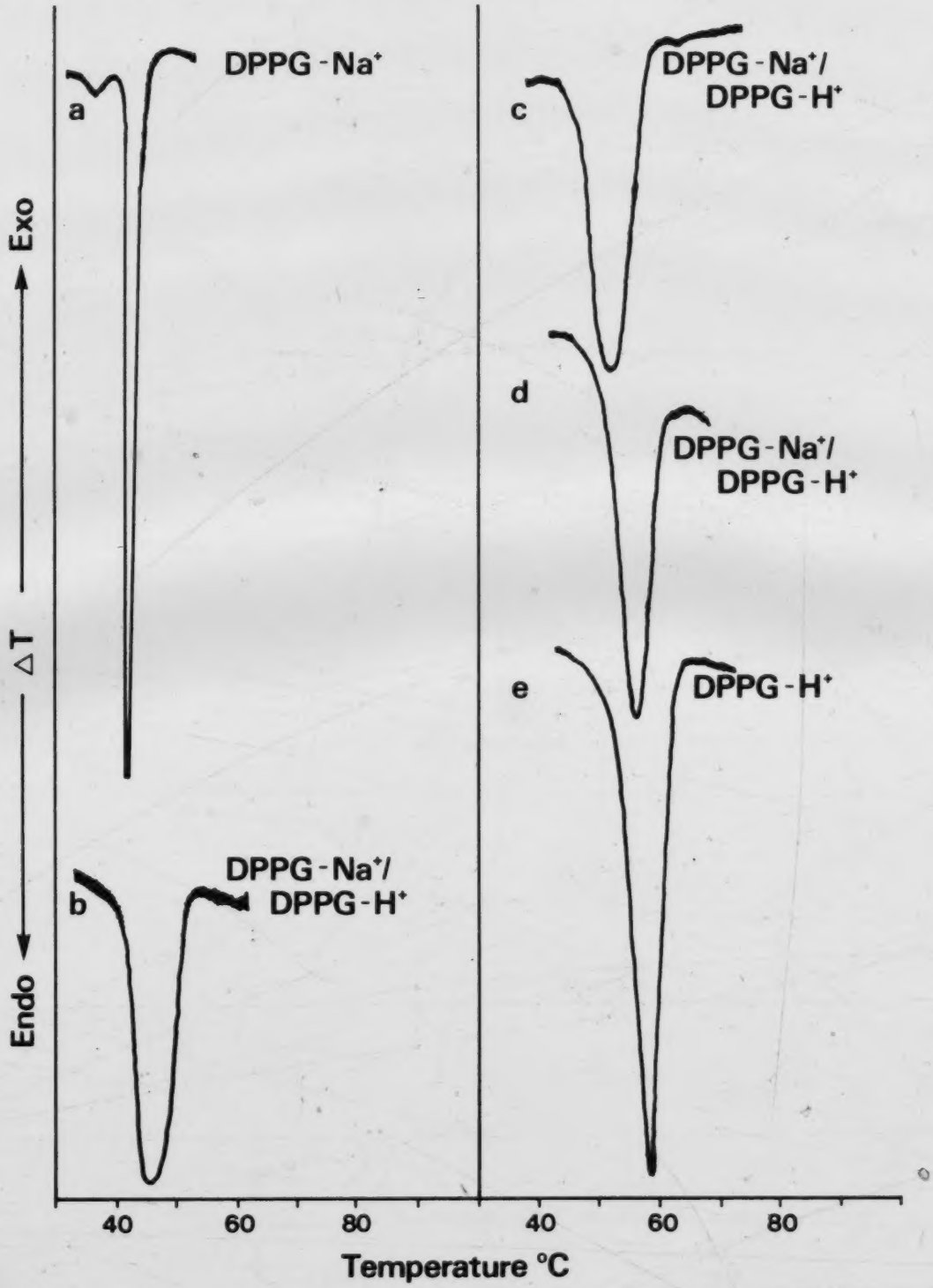
DPPG - Na+
a
DPPG - Na+/
DPPG - H+
c
d
DPPG - Na+/
DPPG - H+
e
DPPG - H+
b
DPPG - Na+/
DPPG - H+
Exo
ΔT
Endo
40
60
80
40
60
80
Temperature °C

Fig. 30. Differential thermal analysis of mixtures of DMPG-Na^+ and DMPG-H^+.

(a) Extracted from a monophasic Bligh and Dyer mixture (see Methods) containing 0.05M NaCl, 0.01M EGTA at pH 8.5. Hydrated with NaOH at pH 9.

(b) Extracted from 1.0M NaCl; 0.1M Na_2 EDTA at pH 4.5. Hydrated with distilled H_2O.

(c) Extracted from 1.0M NaCl; 0.1M Na_2 EDTA at pH 4.5. Hydrated with Michaelis buffer at pH 3.0.

(d) Extracted from 0.05M NaCl; saturated EGTA at pH 4.0. Hydrated with Michaelis buffer at pH 2.5.

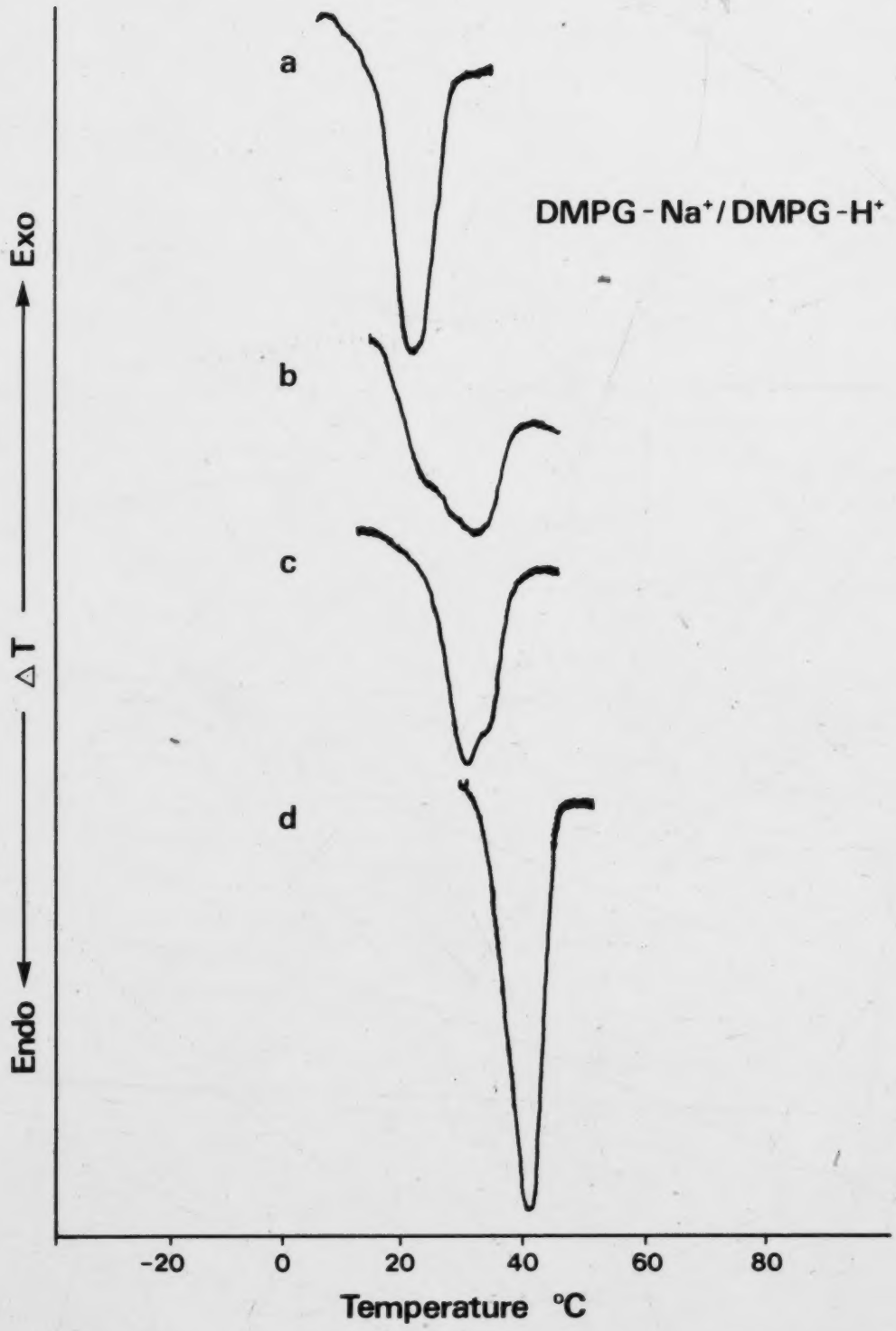
a
b
c
d
DMPG - Na⁺ / DMPG - H⁺
Exo
ΔT
Endo
-20
0
20
40
60
80
Temperature °C

ratio, the transitions of the mixtures were much broader and exhibited two minima, indicating less ideal mixing of the DMPG-Na^+:DMPG-H^+ forms (Fig. 30b,c). This non-ideality is further illustrated in Fig. 31 where the higher-melting component was seen as a shoulder on the heating curve (Fig. 31a) but was more clearly evident on the cooling curve as a distinct peak at approximately 29°C. The lower-melting main component in Fig. 31 had a transition temperature of 24°C, suggesting a relatively pure DMPG-Na^+ component, but the higher transition temperature of 29°C was approximately 15°C less than expected for pure DMPG-H^+.

D. TITRATIONS OF DMPG IN AQUEOUS DISPERSION

As attempts to obtain homogeneous samples of DMPG-Na^+ or DMPG-H^+ from aqueous suspensions by manipulating the pH of the bulk aqueous phase had been unsuccessful, these titration experiments were designed to examine the accessibility of the DMPG polar head groups to the aqueous medium.

Titrations of sonicated dispersions of PS (82), PA (125) and PI (126) had been done by Abramson _et al_. who reported all the functional groups were readily available for titration. Barton and Jevons, however, had reported that the multilamellar structures present in coarse aqueous dispersions of PA interfered with titrations by limiting the accessibility of the polar head groups to the titrant solution (83).

Fig. 31. Differential thermal analysis of a mixture of DMPG-Na and DMPG-H^+.

(a) Heating curve of DMPG extracted from 0.1M NaCl; 0.01M EGTA at pH 8.5. Hydrated with distilled H_2O.

(b) Cooling curve subsequent to a.

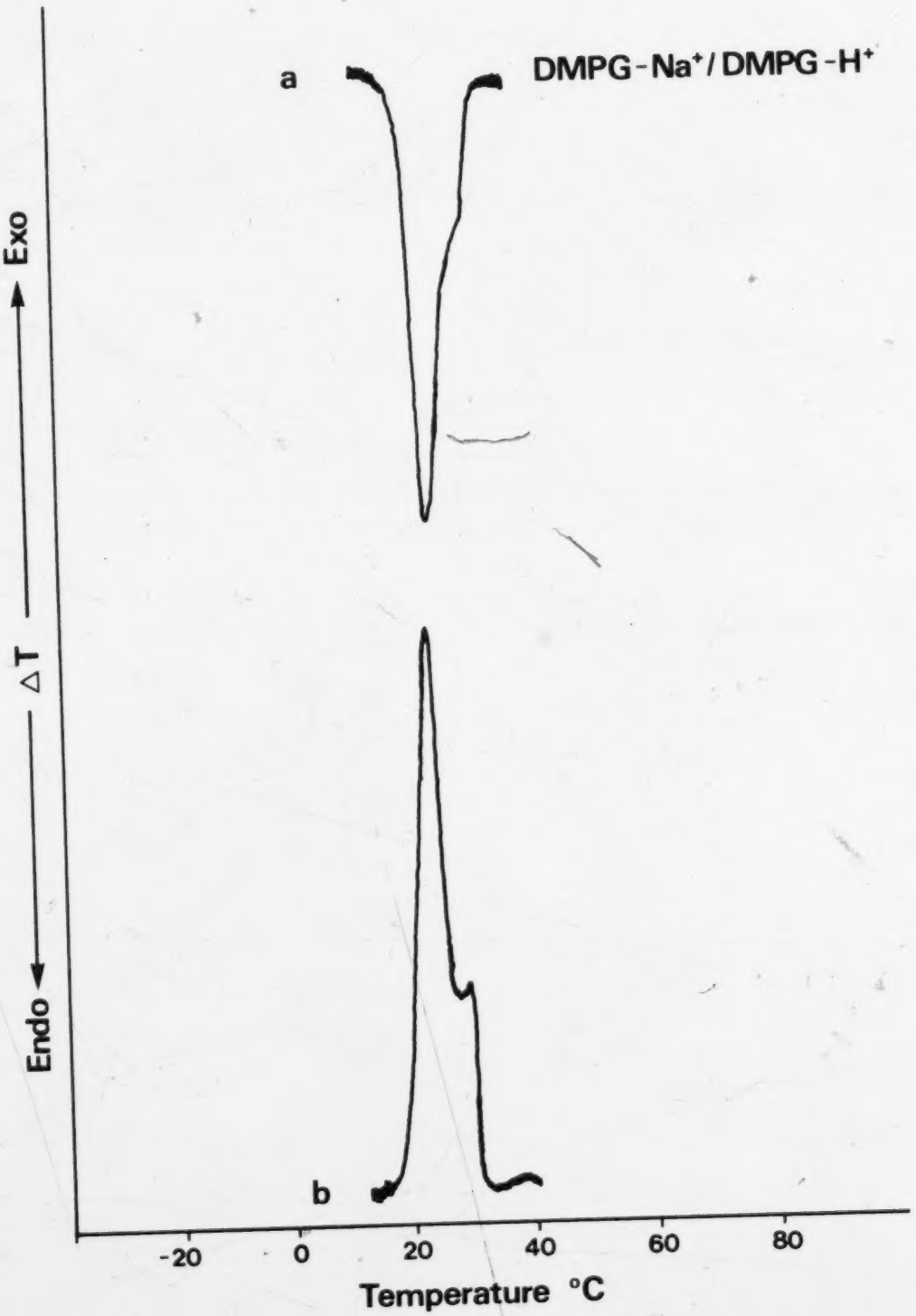
a
DMPG-Na+/DMPG-H+
Exo
ΔT
Endo
b
-20
0
20
40
60
80
Temperature °C

The titration experiment outlined in Fig. 32 indicated that the titration (Fig. 32a) and back titration curves (Fig. 32b) were not superimposable. Extensive equilibration was allowed between addition of aliquots of NaOH titrant on the back titration (total time for back titration was ≈ 30 hrs.) so the hysteresis observed was probably not due simply to diffusion kinetics. The experiments illustrated in Fig. 33 were done to determine if the hysteresis resulted from structural limitations on the availability of the DMPG functional groups.

Sonication of the titration mixture between titrant additions should result in disruption of any liposomal or vesicular lipid structures (127) and consequently remove any structural restraints on access of titrant to the DMPG head groups. The differences between Fig. 33b (sonicated) and Fig. 33c (unsonicated) have been rationalized as follows. During titration of samples from the initial pH ∿ 7.9 to pH 2.75, a change, possibly structural, occurred in the DMPG sample which resulted in proton entrapment and rendered the polar head groups inaccessible to titrant. During back titration without sonication (Fig. 33c), the rapid rise in pH between pH 3 and pH 7 indicated a decrease in H^+ availability for titration compared to the sonicated mixture (Fig. 33b). At higher pH, protons are gradually released from the unsonicated dispersions resulting in a low pH relative to the sonicated titration mixtures.

In a study on proton binding by PI, Wills et al. (128)

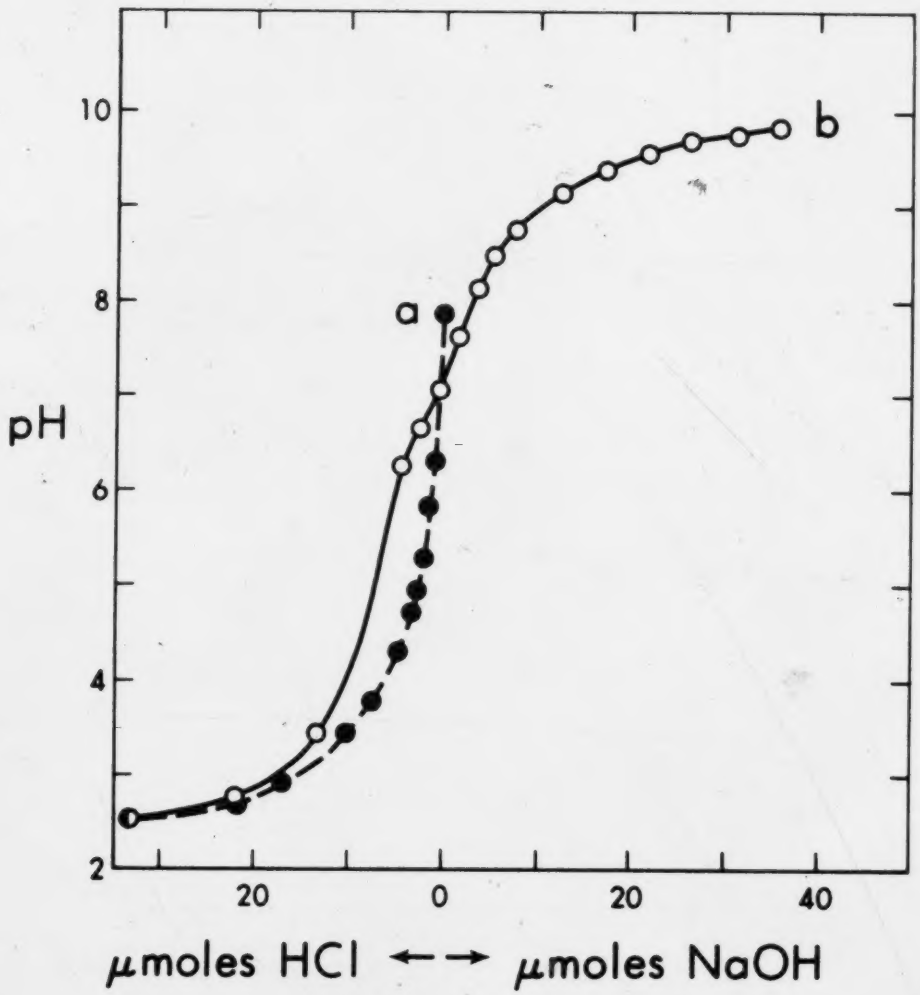

Figure 32. Hysteretic effect during titration of DMPG. Titration of 33 μmoles of DMPG in 5.0 ml 0.145M NaCl. Curve a: Sample at initial pH = 7.9 titrated with 34 μmoles of HCl (.0970M). Curve b: Back titration of curve a with NaOH (.0967M). Sample was sonicated for 2 minutes prior to titration and stirred mechanically throughout the titrations.

Figure 33. Titration curves of DMPG-Na^+. Titration at T = 25°C of 29.9 µmoles DMPG in 5.0 mls 0.145M NaCl. Titrants, 0.0970M HCl and 0.0967M NaOH were added by microliter syringe. Samples, initially at pH 7.9, were titrated to approximately pH 2.5 with HCl then back titrated with NaOH. Curve a: blank titration of 5.0 ml 0.145M NaCl with 30 µmoles HCl followed by back titration with NaOH. Curve b: titration of DMPG, pH adjusted to 2.75 with HCl, back titrated with NaOH. Sample was sonicated at room temperature for 2 minutes after addition of each aliquot of titrant. Curve c: conditions as for curve b but without sonication. After addition of each aliquot of titrant, the samples were mechanically stirred until pH remained constant.

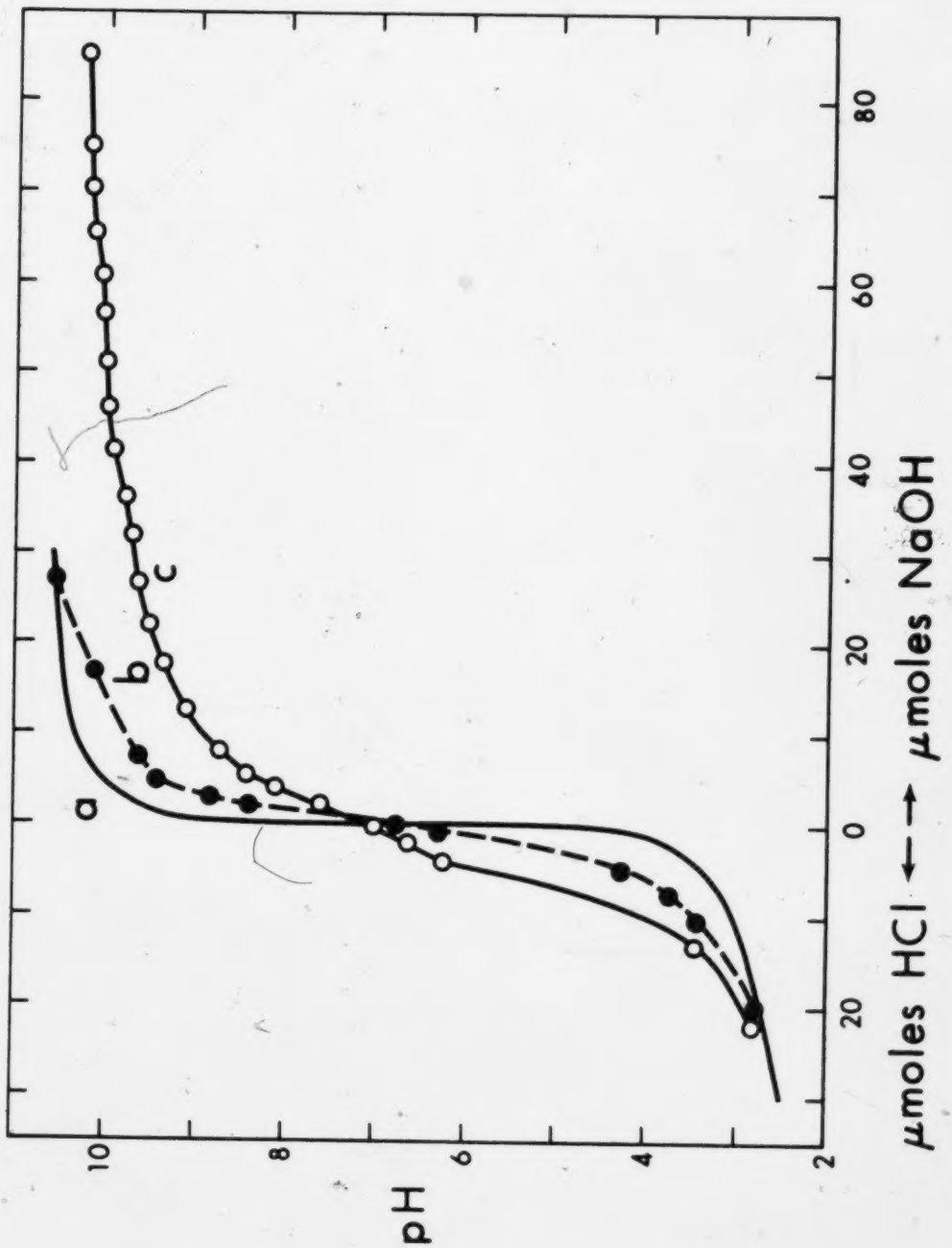
pH
10
8
6
4
2
20
0
20
40
60
80
μmoles HCl ← → μmoles NaOH
a
b
c

reported that at acidic pH (3-4) unilamellar vesicles of PI underwent a conformational change to form "onion-like" multilamellar structures. Protons bound during this conformational change became inaccessible to titrant but were gradually released when the titration mixture was made basic (pH 8-11). It is possible that a similar mechanism causes the hysteretic effects observed during DMPG titrations.

Although these titration data are strictly qualitative, the evidence that all the polar head groups of DMPG are not readily accessible to the bulk aqueous environment helps to explain the inability to obtain completely protonated or completely Na^+-salt forms of DMPG by manipulation of the pH conditions of aqueous DMPG suspensions. They may also provide an explanation for the reported minimal change in the thermal behaviour of DMPG when the pH of the buffered medium was lowered from 7 to 3 (79).

Our experimental data for DMPG (Fig. 30) and DPPG (Fig. 29) and theoretical treatment of electrostatic effects on lipid phase transitions by Trauble *et al*. (129,130) and Jahnig (131) indicate that, for medium chain length phospholipids, elimination of one negative charge per polar head group should result in an increase in transition temperature of approximately 17°C. The smaller changes in transition temperatures reported for DMPG (79) and DLPG (76) when the pH was changed from 7 to 3 may reflect failure to obtain a completely protonated sample by reducing the bulk pH of the aqueous dispersion.

E. THERMAL BEHAVIOUR OF SYNTHETIC PHOSPHOLIPIDS EXAMINED BY LIGHT SCATTERING

Light scattering properties of phospholipids in aqueous dispersions were used as an alternate way of examining the thermal behaviour of various phospholipids to corroborate the differential thermal analysis data. Of particular interest was the degree of transition cooperativity in mixtures of PG(diC_n) with the corresponding PC(diC_n), and the concentration dependence of the transition temperature.

The transition widths determined by the light scattering experiments are reported as $^{1}_{s}T^{10}_{90}$ values. These values were calculated graphically and represent the transition width (°C) for 10% to 90% of the detectable intensity ($I_{90°}$) change.

1. Temperature dependence of light scattering properties of phosphatidylcholines

Yi and MacDonald have shown that changes in the refractive properties of lipid bilayers in aqueous dispersion during the gel to liquid-crystalline transition resulted in a corresponding change in the amount of light scattered by the dispersion (132). Representative scans of light intensity at 90° to the incident light as a function of temperature are illustrated for DMPC (Fig. 34) and DPPC (Fig. 35). Heating and cooling curves obtained for the same sample were superimposable. The transition widths were 1.2°C and 1.1°C for DMPC and DPPC respectively. The approximately 50-fold difference in the concentration of the two samples (DMPC -

Fig. 34. Temperature dependence of intensity of light scattered at 90°C (I_{90}) from DMPC aqueous dispersion. Incident wavelength = 450 nm. Cooling rate 0.37°C/min. Sample DMPC (9.5 mg/ml) in distilled H_2O. The sample was sonicated briefly to disperse.

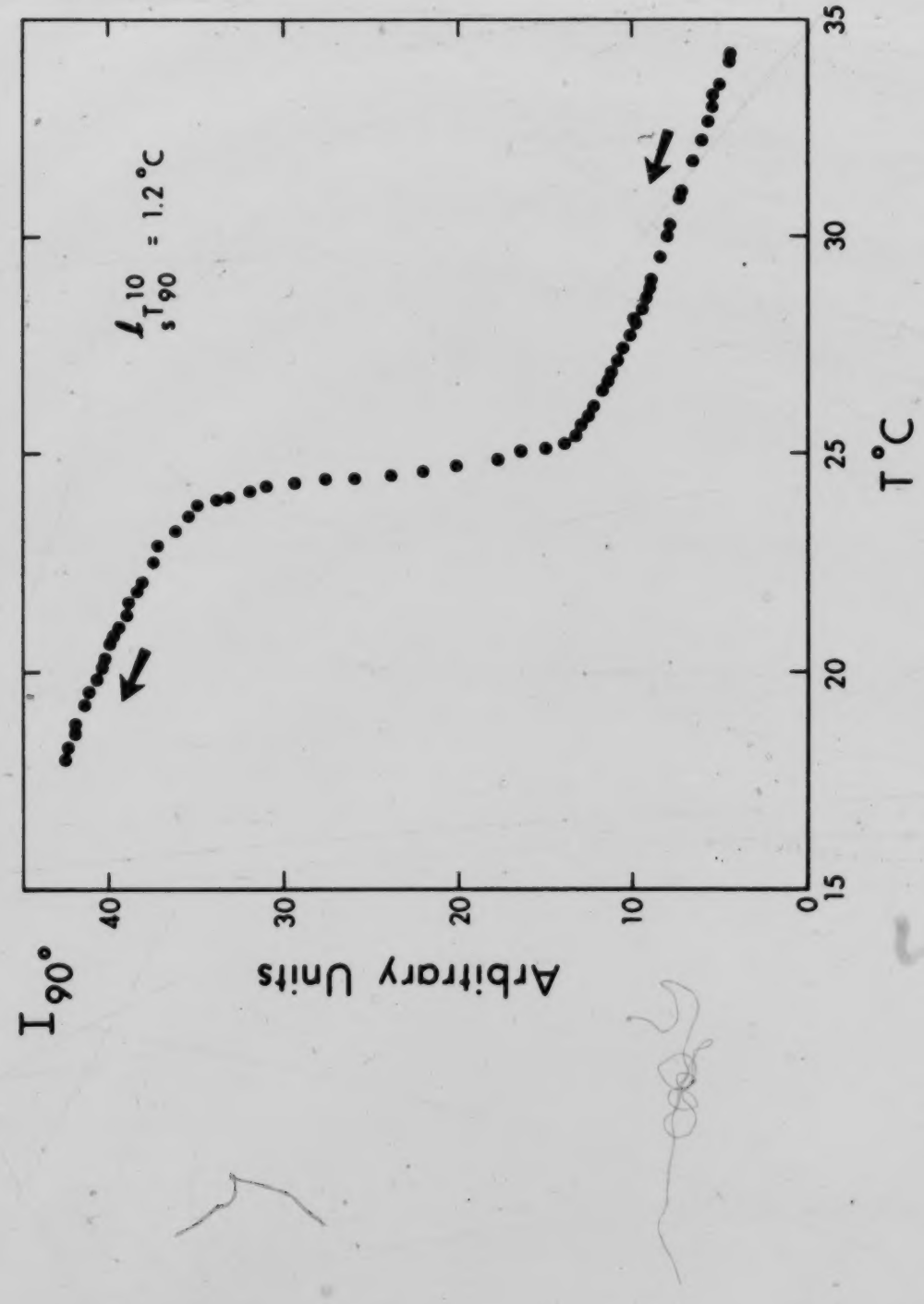
$I_{90°}$
Arbitrary Units
0
10
20
30
40
15
20
25
30
35
T°C
ΔT_{90}^{10} = 1.2°C

Fig. 35. Temperature dependence of intensity of light scattered at 90° from a DPPC aqueous dispersion. Incident wavelength = 450 nm. Cooling rate = 0.58°C/min. Sample: DPPC (0.164 mg/ml) in distilled H_2O. Sample was sonicated briefly to disperse prior to scanning.

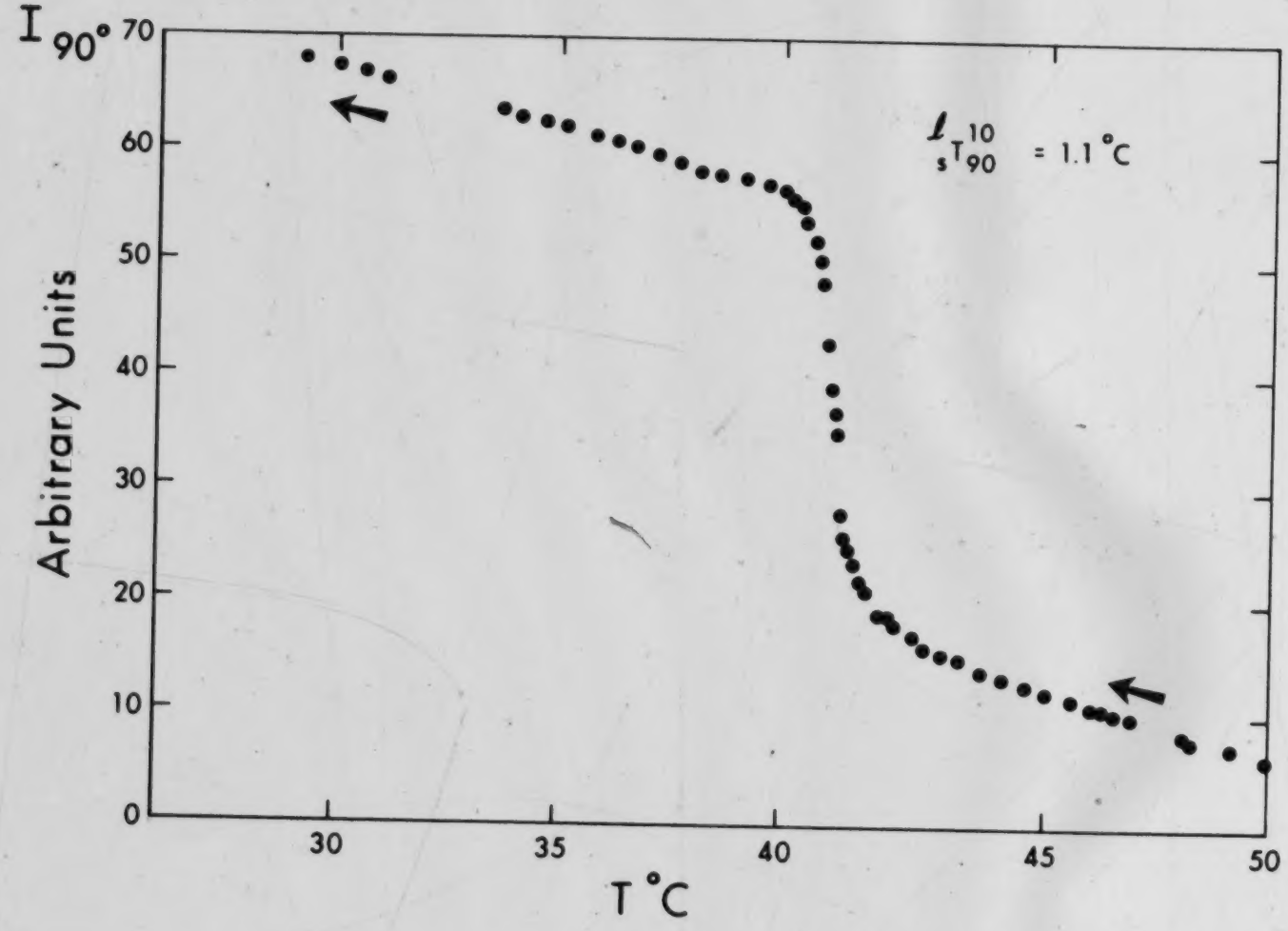
$I_{90°}$
70
60
50
40
30
20
10
0
Arbitrary Units
30
35
40
45
50
T °C
$\ell_{s}T_{90}^{10}$ = 1.1 °C

9.5 mg/ml; DPPC - 0.164 mg/ml) did not appreciably alter the transition widths ($^{1}_{s}T^{10}_{90}$).

2. Temperature dependence of the light scattering properties of PG:PC mixtures

The phase transitions of DMPG:DMPC (Fig. 36) and DPPG:DPPC (Fig. 37) mixtures as detected by light scattering were cooperative and were not appreciably different from the phosphatidylcholine transitions. However, a slight broadening (decrease in cooperativity) could not be excluded on the basis of our data.

Mixtures of DMPG:DLPC in distilled water gave the anomalous results illustrated in Fig. 38. On heating (Fig. 38a), a decrease in $I_{90°}$ was observed, starting at approximately 4°C, which corresponded roughly with the onset of the transition observed for this mixture with differential thermal analysis. However, beginning at 16°C, the scattered light intensity increased sharply to $I_{90°} \simeq 50$ ($T \simeq 20°C$) then continued a much slower rise as the temperature was increased to 40°C. Fig. 38b illustrates the cooling scan done immediately following Fig. 38a. In the region between 40°C and 20°C the scattered light intensity continued to rise slowly to approximately 20°C when a rapid drop in $I_{90°}$ began. The remainder of the cooling scan (20°C to 8°C) was essentially the reverse of Fig. 38a. The hysteretic behaviour observed between 20°C and 40°C was reproducible throughout a number of scans. When the aqueous DMPG:DLPC mixture was made 0.1M

Fig. 36. Temperature dependence of intensity of light scattered at 90° from a DMPG:DMPC aqueous dispersion. . Incident wavelength = 450 nm. Cooling rate 0.23°C/min. Sample DMPG:DMPC (24:76) at 9.35 mg/ml in distilled H_2O. Sample was sonicated briefly to disperse prior to scanning.

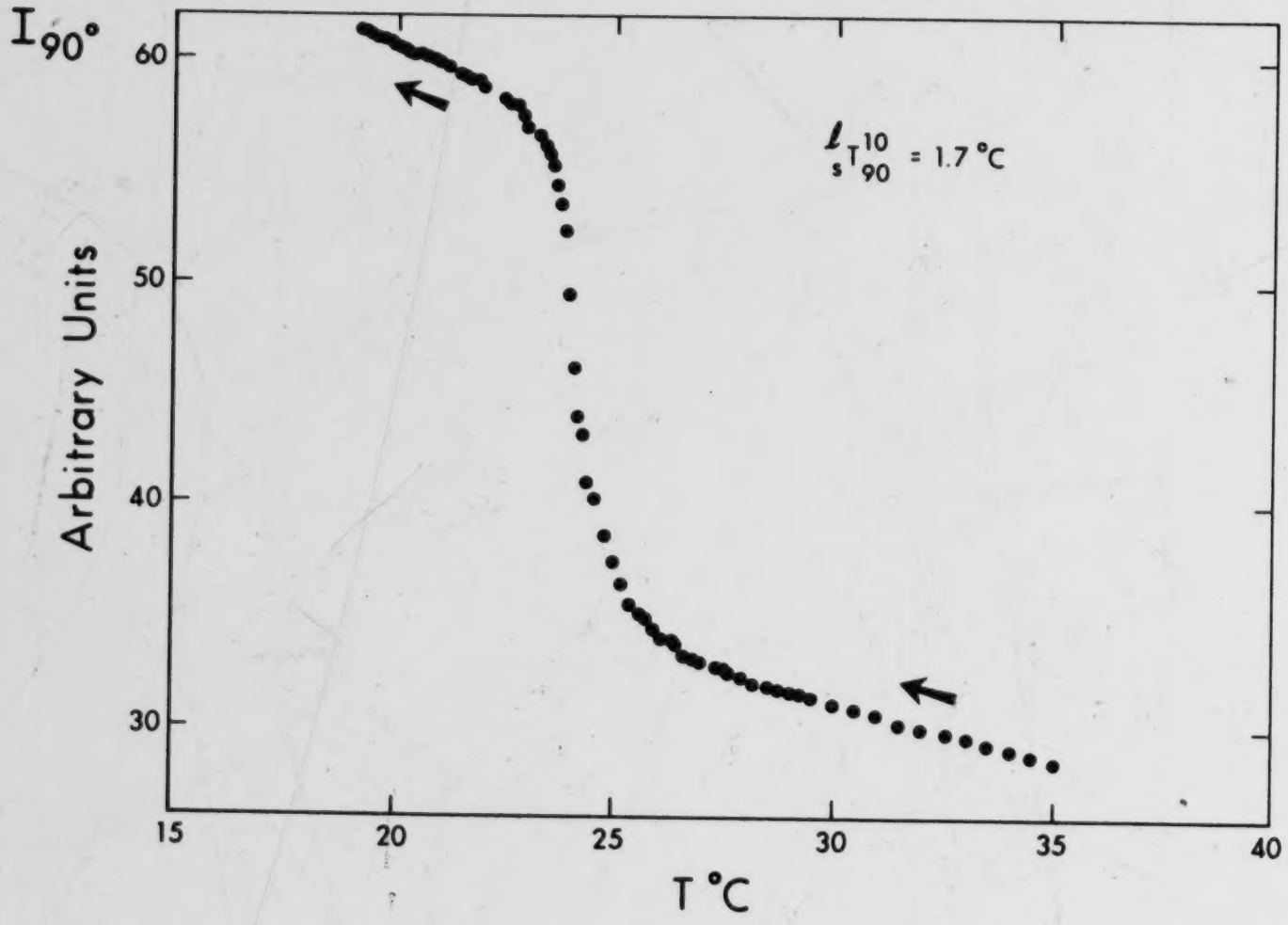
$I_{90°}$
60
50
40
30
Arbitrary Units
$\ell_s T_{90}^{10}$ = 1.7 °C
15
20
25
30
35
40
T °C

Fig. 37. Temperature dependence of intensity of light scattered at 90° from a DPPG:DPPC aqueous dispersion. Incident wavelength = 450 nm. Heating rate = 0.5°C/min. Sample: DPPG:DPPC (48:52) at 4.62 mg/ml in distilled H_2O. Sample was sonicated briefly to disperse prior to scanning.

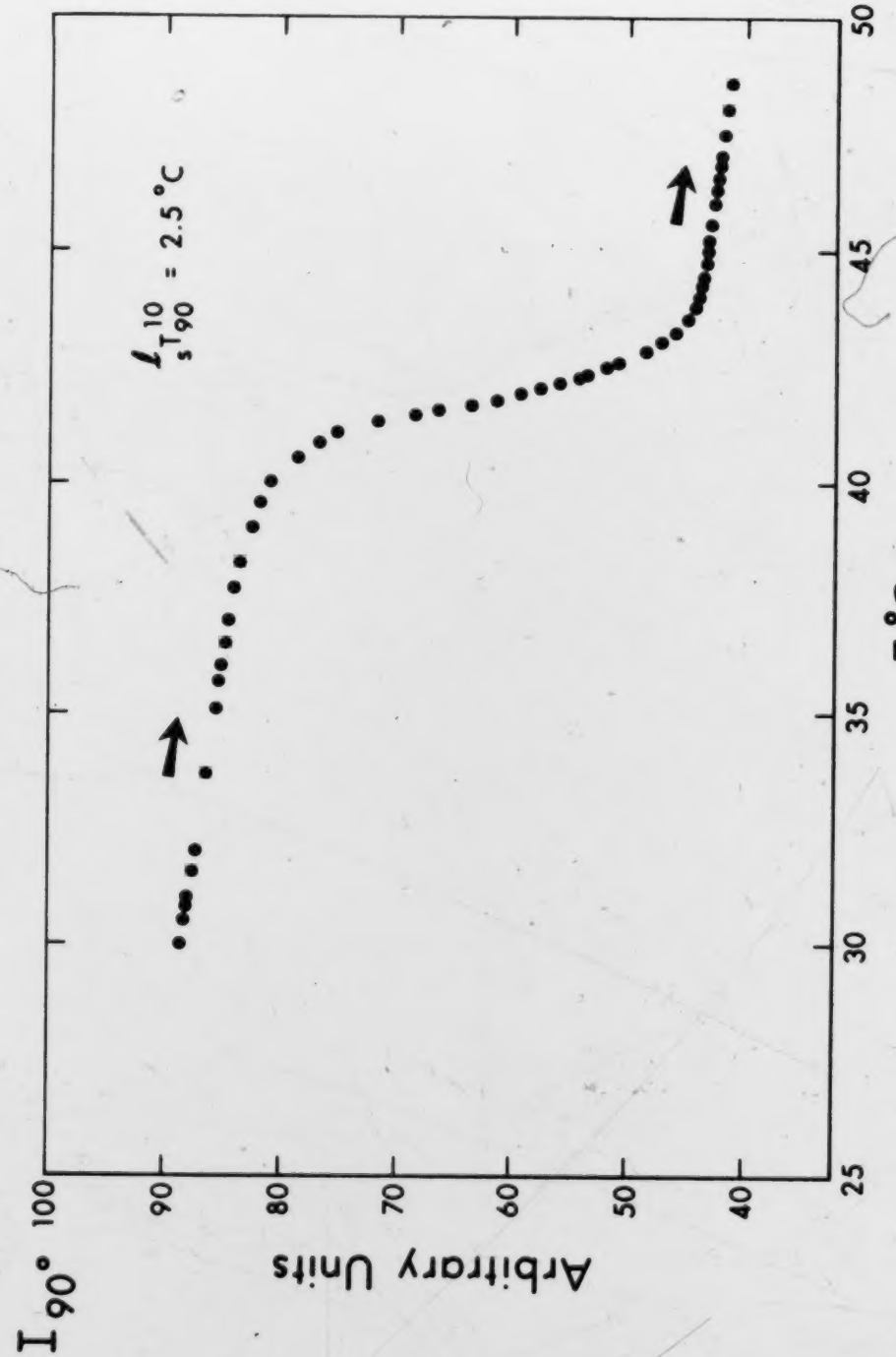
$I_{90°}$
Arbitrary Units
100
90
80
70
60
50
40
25
30
35
40
45
50
T °C
$\ell_{s}T_{90}^{10}$ = 2.5 °C

Fig. 38. Temperature dependence of intensity of light scattered at 90° from a DMPG:DLPC aqueous dispersion. Incident wavelength = 450 nm. Sample: DMPG:DLPC (50:50) at 4.0 mg/ml in distilled H_2O. Sonicated briefly to disperse prior to scanning.

(a) Heating scan at 0.21°C/min.

(b) Cooling scan subsequent to a at 0.39°C/min.

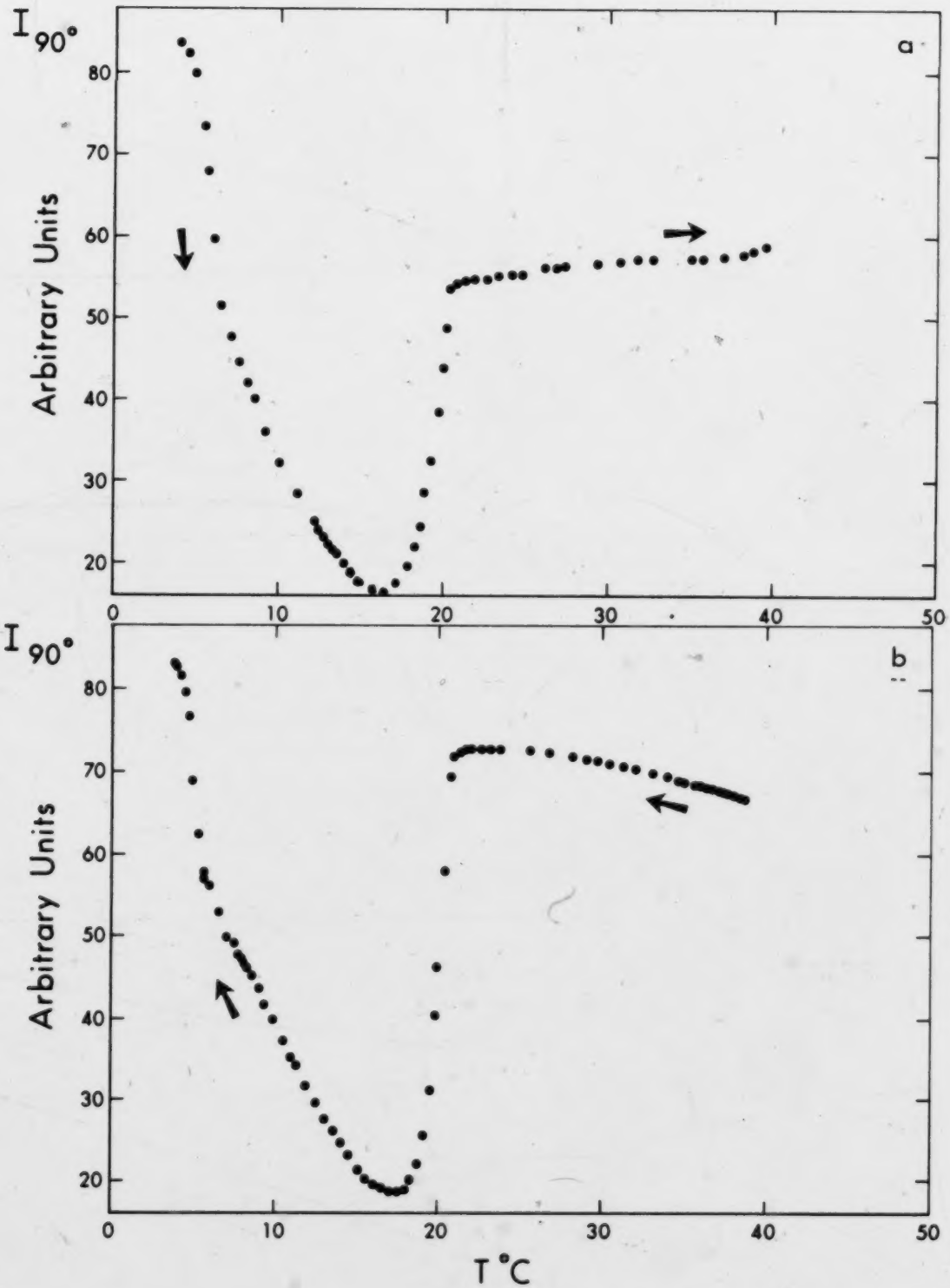
$I_{90°}$
a
Arbitrary Units
80
70
60
50
40
30
20
0
10
20
30
40
50
$I_{90°}$
b
Arbitrary Units
80
70
60
50
40
30
20
0
10
20
30
40
50
T °C

in NaCl, the hysteretic behaviour and the rapid $I_{90°}$ change at approximately 20°C were eliminated and a broad but completely reversible scan was observed (Fig. 39). Analogous behaviour was observed for DPPG:DLPC mixtures (Fig. 40).

The concentration dependence of the transition temperature and transition width as determined by light scattering is illustrated in Fig. 41. No detectable changes in either transition temperatures or widths were apparent within the concentration range studied (0.164 to 9.5 mg/ml). The heating and cooling scans yielded essentially identical data.

The close agreement in transition temperatures determined by DTA (Table III) and light scattering (Table IV) confirm that this thermal property of hydrated phospholipids is not concentration dependent. The light scattering data do not resolve the problem of the cooperativity of DMPG:DMPC and DPPG:DPPC mixtures. Both light scattering and DTA indicate the cooperativity (transition width) is essentially the same for mixtures and single phospholipids. Either the mixtures are nearly ideally miscible or the two techniques used are not sensitive enough to detect the deviation from ideality. Accurate transition enthalpy determinations for the single components and for mixtures could resolve this problem.

The source of the anomalous light scattering behaviour of the DMPG:DLPC and DPPG:DLPC mixtures in distilled H_2O is not known. Yi and MacDonald (132) observed

Fig. 39. Temperature dependence of intensity of light scattered at 90° from a DMPG:DLPC aqueous dispersion. Incident wavelength = 450 nm. Sample: DMPG:DLPC (50:50) at 4.0 mg/ml in 0.1M NaCl. Cooling rate 0.48°C/min.

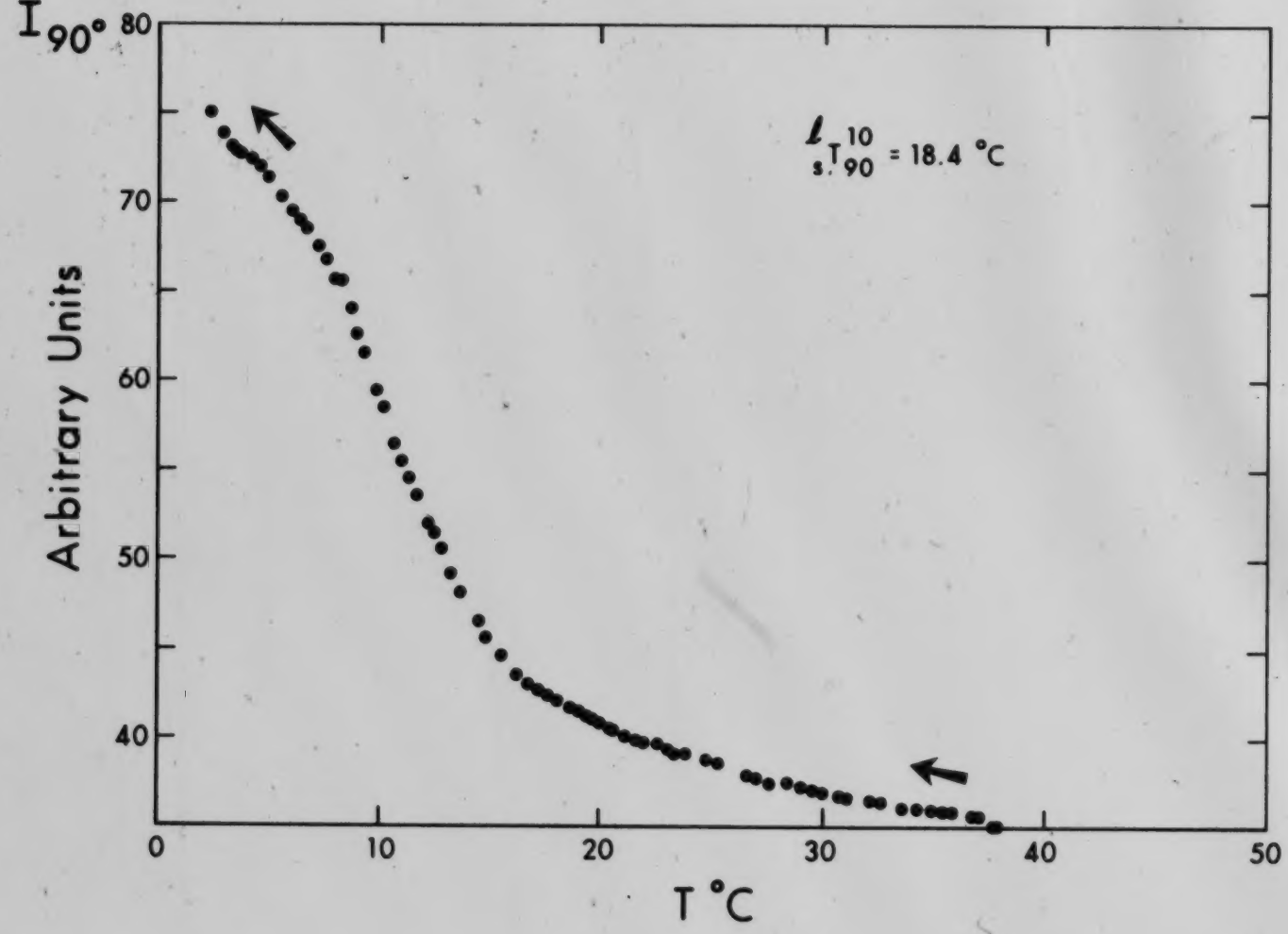
$I_{90°}$
80
70
60
50
40
Arbitrary Units
$\ell_{s.T_{90}}^{10}$ = 18.4 °C
0
10
20
30
40
50
T °C

Fig. 40. Temperature dependence of intensity of light scattered at 90° from a DPPG:DLPC aqueous dispersion. Incident wavelength = 450 nm. Sample: DPPG:DLPC (50:50) at 4.0 mg/ml.

(a) Sample in distilled H_2O. Heating rate 0.53°C/min.

(b) Sample in 0.1M NaCl. Cooling rate 0.31°C/min.

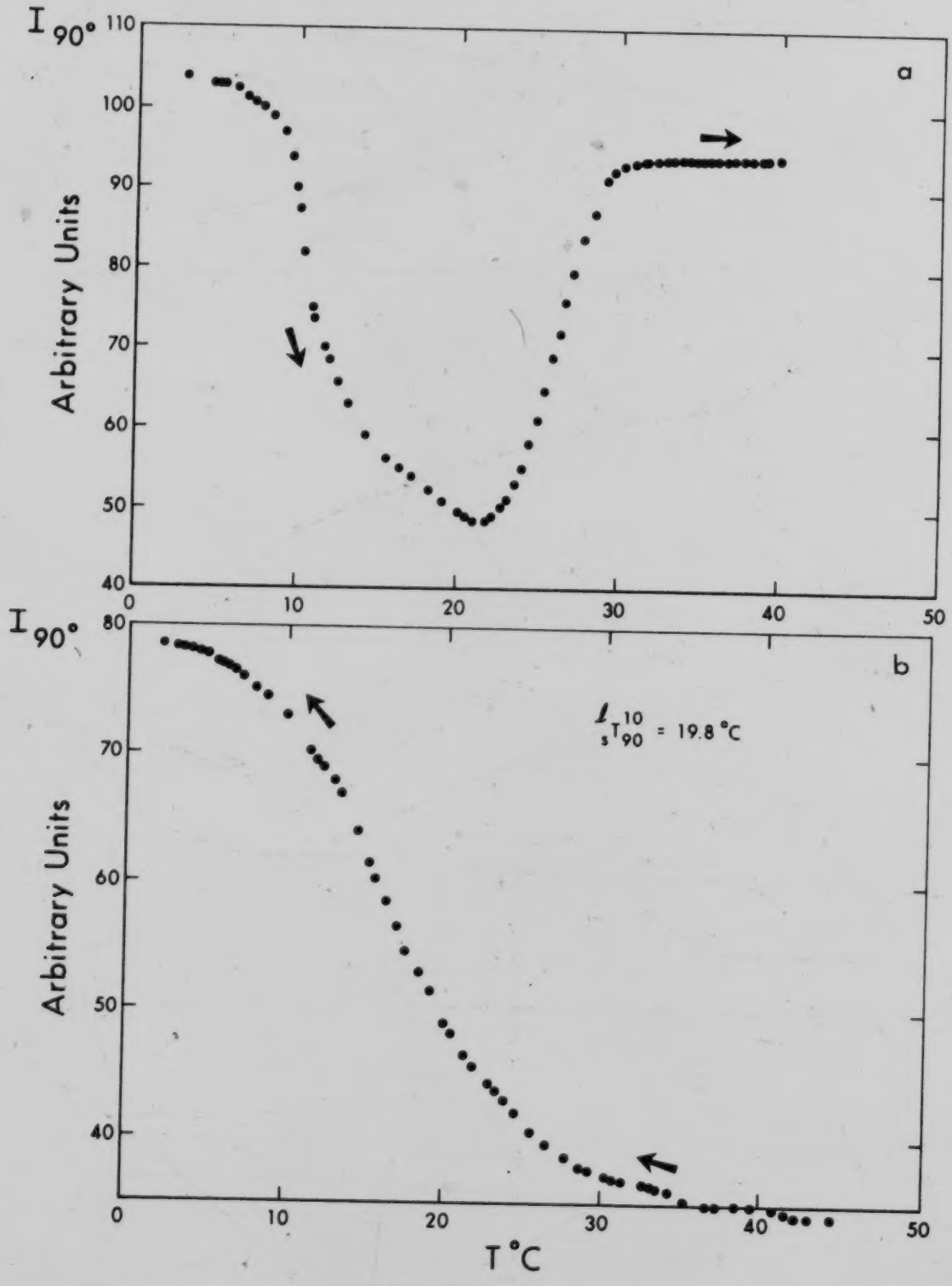
$I_{90°}$
Arbitrary Units
a
b
$\ell_s T_{90}^{10}$ = 19.8 °C
T °C

Fig. 41. Effect of phospholipid concentration on the gel-liquid-crystalline transition temperature. Data obtained from light scattering experiments. Heating and cooling rates were 0.2°C to 0.5°C/min. Open circles indicate transition temperatures of pure phosphatidylcholines. Closed circles indicate transition temperatures of lipid mixtures as labelled. The bars represent $_{s}^{1}T_{90}^{10}$ values.

(a) Results from heating scans.

(b) Results from cooling scans.

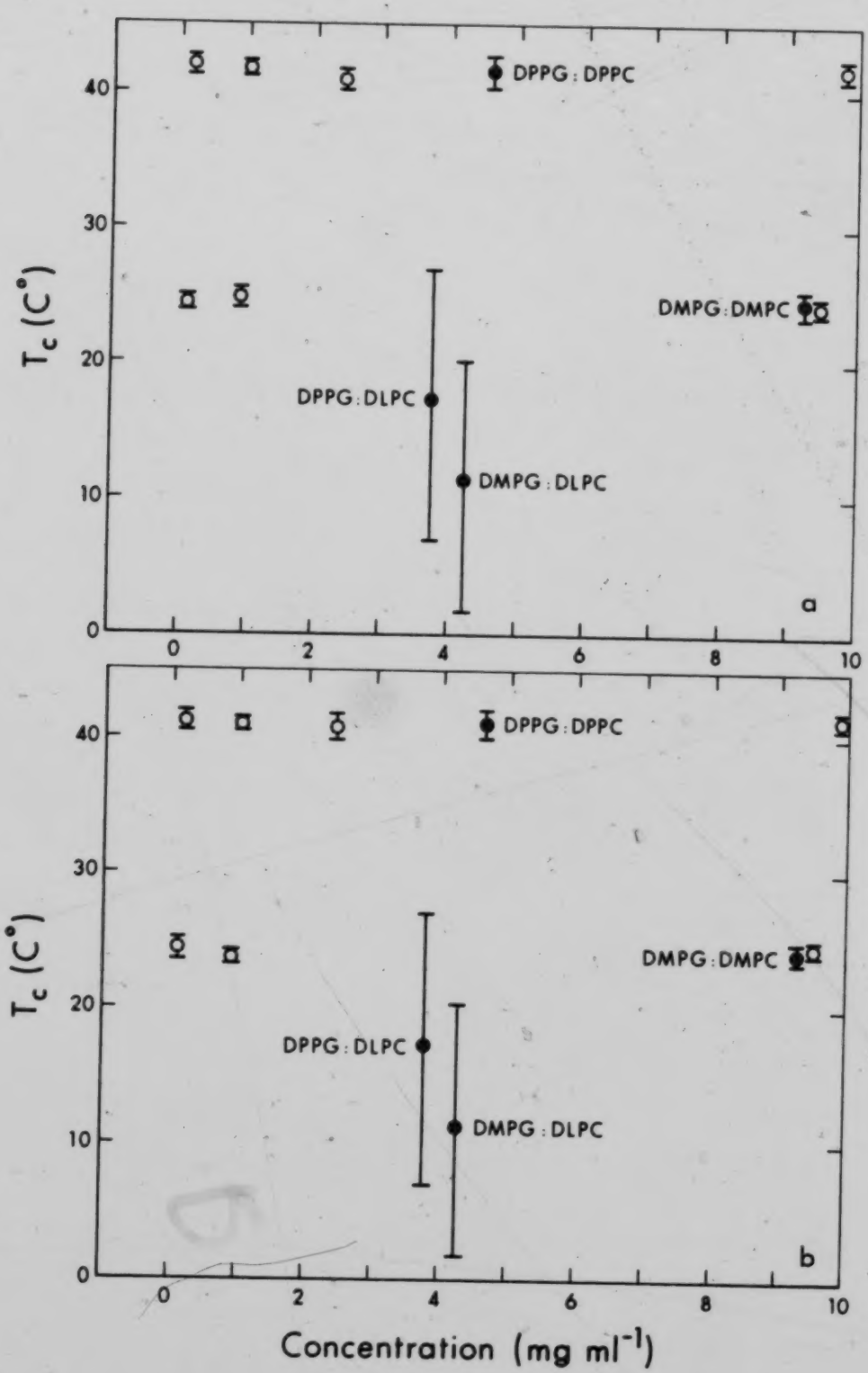
DPPG:DPPC
DMPG:DMPC
DPPG:DLPC
DMPG:DLPC
a
b
T_c (C°)
Concentration (mg ml^{-1})
0
10
20
30
40
0
2
4
6
8
10

TABLE IV

Thermal Transitions in Synthetic Phosphatidylglycerols and Phosphatidyl Cholines as Detected by Light Scattering

Phospholipid Composition	Tc °C	$^{1}_{s}T_{90}^{10}$ °C	No. of Determinations
DMPC	24.48	1.23	6
DPPC	41.65	1.41	8
Ave for PCs	-	1.32	14
DMPG:DMPC 24:76	24.31	1.75	2
DPPG:DPPC 48:52	41.35	2.25	2
DMPG:DLPC 50:50		18.4	2
DPPG:DLPC 50:50		19.8	2

hysteretic behaviour and anomalous changes in the optical density of sonicated DPPC dispersions and attributed these to an aggregation-disaggregation phenomenon. A temperature-dependent structural morphology change may also be involved in the anomalous light scattering behaviour of the DMPG:DLPC and DPPG:DLPC mixtures although this is strictly speculation.

As the transition data obtained by DTA at extremely high lipid concentrations was used to evaluate the lipid physical state-function relationship in prothrombin activation (lipid concentration $\sim$ 0.2 mg/ml) it was necessary to evaluate the concentration effect on the thermal behaviour. This was made possible by correlation of the light scattering and DTA results.

F. DISCUSSION OF THE PHYSICOCHEMICAL STUDIES

1. Phosphatidylglycerol-Na^+ salts

Within the limits of the techniques used, the thermal behaviour of the phosphatidylglycerol-Na^+ salts (diC_n) was identical to the behaviour of the corresponding phosphatidylcholines (diC_n). The transition temperatures of the PG's and corresponding PC's were the same (Table III). The sharp, narrow peaks of the DTA thermograms were indicative of highly cooperative transitions and the pre-transition which has been reported for pure saturated phosphatidylcholines (78,80) was observed with the phosphatidylglycerols.

The nature of the thermal pre-transition has not been unambiguously resolved. A conformational rearrangement

in the polar head group has been reported (133,134) and denied (135). The orientation of the acyl chains has been reported to change from tilted to perpendicular with respect to the plane of the bilayer at the pre-transition temperature (136). Janiak *et al.* (137) have concluded that the acyl chains had a 30° tilt relative to the bilayer phase which was maintained until after the main gel to liquid-crystalline transition.

A structured H_2O matrix or intact hydration shell of the polar head groups is apparently associated with the events of the pre-transition as reduction of the water content of a phosphatidylcholine sample to below 20% w/w (137), presence of ethylene-glycol (1:1 v/v) in an aqueous phosphatidylcholine suspension (138), or presence of Zn^{++}, Sn^{++} or Ca^{++} in the aqueous medium (139), all eliminate the pre-transition. Perturbation of either the acyl chain region or the polar head groups of the bilayers results in elimination of the pre-transition. It appears, therefore, that the events involved in the pre-transition are dependent on a balance of interaction between hydrophobic and hydrophilic regions of the bilayer. There is no indication *a priori* that DMPG-Na^+ and DPPG-Na^+ should have a pre-transition. Until further detail at the molecular level is available to aid interpretation of the nature of the pre-transition, the high degree of similarity in the thermal behaviour of the PC's and PG's can only be considered coincidental. Nevertheless, the occurrence of a pre-transition in mixtures of

PG-Na^+ (diC_n) and PC (diC_n) implies the interclass and intra-class molecular interactions must be very similar and supports the conclusion that the miscibility of the two classes approaches the ideal.

2. <u>The effect of Ca^{++} on the thermal behaviour of DMPG and DPPG</u>

In the presence of Ca^{++}, DMPG was readily converted to a thermally stable (T_c = 87°C) form. An equilibration time of approximately 30 minutes between DTA heating scans was sufficient for the conversion to the thermodynamically stable species (Fig. 21b). Metastable behaviour was observed if differential thermal analyses were repeated at time intervals shorter than approximately 30 minutes. The conversion of DPPG to a single stable form (T_c = 89°C) was not as readily achieved as several hours equilibration were required to abolish the metastable behaviour demonstrated in Figs. 19 and 20. The low temperature endotherm (T_c = 59°C) of the non-equilibrated DPPG-Ca^{++} samples (Fig. 18c), the endotherm observed with DPPG-Mg^{++} (Fig. 22IIa), and the endotherm of DPPG-H^+ (Fig. 22Ib) all occurred at the same temperature and appeared to result from the gel to liquid-crystalline transition of samples from which the electrostatic repulsion between the polar head groups had been eliminated. Similar behaviour is observed with DMPG-Mg^{++} (Fig. 23a) and DMPG-H^+ (Fig. 30d).

The exotherm immediately following the low temperature endotherm in DMPG-Mg^{++} has been attributed to a

structural rearrangement resulting in formation of more highly ordered 'crystal' structures from liposomes (79). If this interpretation is applicable to the thermal behaviour of DMPG-Ca^{++} and DPPG-Ca^{++}, it is evident that the influence of Ca^{++} is greater on the shorter chain DMPG (Fig. 21a) as it is able to induce the structural rearrangement without prior melting of the acyl chains.

3. Summary of Ca^{++} effects on thermal behaviour of DLPG, DMPG and DPPG

(a) DLPG: Information obtained from references 75 and 76 included for comparison purposes. Rapid equilibration to the stable, high transition form (T_c = 75°C) was attained. No metastable behaviour was reported.

(b) DMPG: Equilibration to the stable high transition form (T_c = 87°C) required approximately 30 minutes. The exotherm at 44°C (possibly related to structural rearrangement) was not preceded by an endotherm. Metastable behaviour was observed if there was less than 30 minutes separating heating scans.

(c) DPPG: Equilibration to the stable high transition (T_c = 89°C) form required two to three hours between DTA heating scans.

4. The effect of Mg^{++} on the thermal behaviour of DMPG and DPPG

DMPG-Mg^{++} exhibited metastable behaviour (Fig. 23a) unless allowed to equilibrate for approximately 12 hours

between DTA heating scans. Thermograms of the stable, high transition DMPG-Mg^{++} consisted of a single endotherm at 68°C. Partial conversion of DPPG to a Mg^{++}- complexed, stable form (T_c = 76°C) required in excess of three days. Under normal experimental conditions the effect of Mg^{++} on DPPG appeared limited to charge neutralization which resulted in the simple thermogram illustrated in Fig. 22a.

The effects of divalent cations on anionic phospholipids have been reported to involve changes in hydrocarbon chain packing (88,94) and/or structural rearrangements (76, 79,94). The facility with which alterations involving the hydrocarbon chain region of a bilayer can be made should be inversely proportional to the strength of the intermolecular hydrophobic interactions. The differential thermal analysis data supported this observation. With DLPG, Mg^{++} and Ca^{++} both formed stable, higher transition (T_c = 75°C) complexes (76,77). The DLPG-Ca^{++} complex forms rapidly - no metastable behaviour has been reported (76). Ca^{++} converted DMPG to a stable form (T_c = 87°C) in approximately 30 minutes whereas Mg^{++} required approximately 12 hours to produce a less stable (T_c = 76°C) DMPG-Mg^{++} complex. Conversion of DPPG by Ca^{++} to the stable high-transition form (T_c = 89°C) required approximately 3 hours while Mg^{++} required three days to produce any alterations in excess of those expected due to charge neutralization of the polar head groups. In addition to differences in the kinetics of formation of PG-divalent cation complexes due to changes in acyl chain lengths, the

absolute change in the thermal behaviour also varied. Formation of the stable, high transition PG-Ca^{++} complex resulted in an increase in transition temperature (relative to PG-Na^{+}) of 77°C (76), 63°C and 48°C for DLPG, DMPG and DPPG respectively.

This inverse linear relationship between the maximal effect of Ca^{++} on the thermal behaviour of the PG's and the length of the PG acyl chains, as well as the differences observed with Mg^{++} and Ca^{++}, support the hypothesis that the thermal behaviour of the PG-divalent cation complexes reflects alterations in the acyl chain region of the bilayer which become progressively more difficult to accomplish as the hydrophobic interactions increase.

5. Postulated mechanism for Ca^{++}-PG interactions

As previously discussed, the stable high transition temperature forms of PS-Ca^{++} and PA-Ca^{++} appear to involve a 1:1 phospholipid to Ca^{++} ratio which requires two negative charges per polar head group. The PS-Ca^{++} complex reportedly forms essentially anhydrous 'crystals' (94). The morphological similarities as detected by freeze-fracture electron microscopy of the PS-Ca^{++} (99) and DMPG-Ca^{++} (79) complexes and the high thermal stability of both complexes implies a similar type of complex for PS-Ca^{++} and DMPG-Ca^{++}. As the PG polar head group has a single negative charge, any postulated 1:1 PG to Ca^{++} complex would involve a prohibitively large electrostatic term. As the effects of Ca^{++} on the

thermal behaviour of the PGs have been demonstrated to be much more profound than that expected from elimination of the charge repulsion between polar head groups the possibility of polymeric lattice structure must be considered.

X-ray diffraction studies of lactose-$CaBr_2$ complexes (140) have demonstrated chelation of Ca^{++} by the O(3), O(4) and O(2'), O(3') vicinal hydroxyl groups of the galactose and glucose moieties, respectively. The chelation is accompanied by displacement of H_2O from the hydration shell of the Ca^{++}. Analogous structures have been determined for hydrated Ca^{++}-galactose chelates (141). Mixed Ca^{++}- chelate complexes have been reported for several acid sugars involving Ca^{++}-carboxyl group and Ca^{++}-vicinal hydroxyl group chelate formation (141,142). It appears probable that the high thermal stability of the PG-Ca^{++} complexes and the structural similarity with PS-Ca^{++} (99) complexes results from Ca^{++} chelation involving the anionic phosphate groups and the vicinal hydroxyl groups of the PG. Chelate formation would result in a complex entropy change due to the increased order of the PG-Ca^{++} complex and the simultaneous release of H_2O from both the hydrated Ca^{++} and the hydration shell of the PG polar head group.

It is postulated that the dehydration during chelate formation, combined with structural rearrangement, as previously reported for DLPG-Ca^{++} (76), DLPG-Mg^{++} (76) and DMPG-Ca^{++} (79), accounts for the complex metastable behaviour observed during formation of the thermodynamically stable

forms of DMPG-Mg^{++} (Fig. 23), DMPG-Ca^{++} (Fig. 21a) and DPPG-Ca^{++} (Fig. 18c). However, on the basis of available data it is impossible to assign a specific cause-effect relationship to the complex thermograms.

It has been reported that above the transition temperature of the stable form of the DMPG-Ca^{++} (79) and DLPG-Mg^{++} (76) complexes the closely packed 'crystal' structures were disrupted with concomitant melting of the acyl chains. This liquid-crystalline form of the PG-Ca^{++} complexes exhibited substantial supercooling. The exotherm which occurred on the cooling scan DTA thermograms was at the same temperature (within experimental limits) as the endotherm obtained on heating a PG sample with the polar head group charge repulsions eliminated. Freeze fracture electron microscopy studies of DMPG-Mg^{++} (79) have indicated liposomal structures exist, both below the low temperature DTA endotherm and above the cooling curve exotherm, subsequent to melting the stable 'crystal' structures. It appears, therefore, that thermal disruption of the 'crystal' structures resulted in formation of liquid-crystalline liposomes which underwent a liquid-crystalline to gel transition at a T_c characteristic for 'charge neutralized' liposomes. The transition of the thermodynamically stable PG-Ca^{++} form at high temperature apparently facilitated rehydration of the PG polar head groups. This hydrated PG form was above its T_c and so could be cooled substantially before the liquid-crystalline to gel transition occurred. Experimental evidence for this is

illustrated in Fig. 42. A sample of DPPG-Ca^{++}, from which excess H_2O had been removed with a microliter syringe and by brief drying (30 min.) in vacuo at room temperature, had a heating thermogram (Fig. 42a) similar to that observed with 'equilibrated' samples in excess H_2O. This 'dehydrated' sample did not demonstrate the complex, metastable behaviour usually observed with hydrated samples (Fig. 18c). The cooling curve of this 'dehydrated' sample (Fig. 42b) consisted of an exotherm at approximately 90°C. No exotherm was visible at 58°C as was usual for hydrated samples (Fig. 18b). Addition of H_2O to the sample and subsequent equilibration resulted in the heating thermogram observed in Fig. 42c. The cooling curve consisted of a single exotherm at 58°C (Fig. 42d).

6. Summary of the postulated mechanism for the effects of Ca^{++} on the thermal behaviour of DMPG and DPPG

1. Charge neutralization of DMPG or DPPG polar head groups by H^+ or divalent cations results in an increase in transition temperature of approximately 17°C.

2. At a 1:2 ratio of Ca^{++}:PG both DMPG and DPPG undergo a dehydration process, accompanied by chelation of Ca^{++} by the vicinal hydroxyl groups of the PG, and a conformational rearrangement which results in a stable 'crystal' structure.

3. Melting of the stable 'crystal' structure at T = 87-89°C facilitates rehydration of the polar head groups.

Figure 42. Effect of dehydration on thermal behaviour of DPPG-Ca^{++}.

DPPG sample previously hydrated with 10 µl of 1.0M $CaCl_2$ was partially dehydrated by removing excess H_2O with a µl syringe and by drying *in vacuo* for approximately 30 min. at room temperature.

(a) Heating curve.

(b) Cooling curve subsequent to a. Due to rapid cooling required to prevent the sample from boiling at T > 90°C only the low temperature side of the cooling curve exotherm could be recorded.

(c) Heating curve after the sample had been rehydrated with 10 µl of distilled H_2O and re-equilibrated.

(d) Cooling curve subsequent to c.

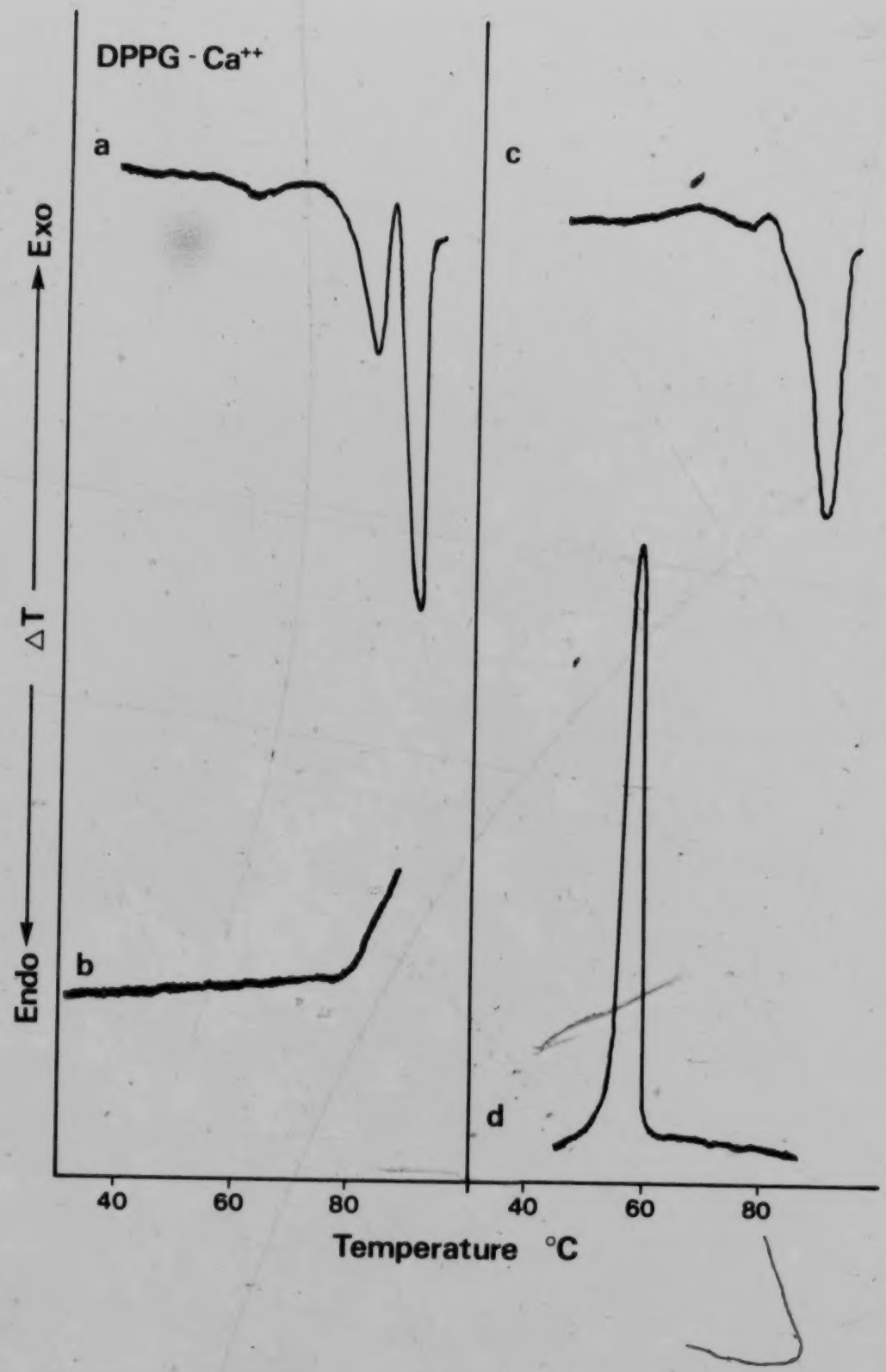
DPPG - Ca++
a
b
c
d
Exo
ΔT
Endo
40
60
80
40
60
80
Temperature °C

4. The rehydrated form is thermally equivalent to a hydrated 'charge-neutralized' sample and is metastable.

7. The effects of Ca^{++} on the thermal behaviour of PG:PC mixtures

Relatively small amounts of PC in PG samples inhibited the formation of the high transition (T_c = 87-89°C), PG-Ca^{++} 'crystal' structures. This is illustrated in Fig. 43a for a mixture of DMPG-Ca^{++}:DMPC (90:10). At a DMPG-Ca^{++}: DMPC ratio of 95:5 some thermal activity was observed between 45°C and 80°C. The exotherm following the low temperature endotherm indicated some of the structural and/or hydration changes usually observed with pure DMPG-Ca^{++} complexes may have occurred, but the remainder of the thermogram was not typical of the stable 'crystal' form of DMPG-Ca^{++}.

Tocanne et al. (75) have reported that 5% (mole/mole) lysylphosphatidylglycerol (1,2-didodecanoyl-sn-glycero-3-phospho-1'-(3'-O-lysyl)-sn-glycerol) in DLPG-Ca^{++} inhibited formation of the cochleate cylinders normally observed in freeze-fracture electron micrographs of DLPC-Ca^{++}.

It appears, therefore, that relatively small amounts of a lipid with a polar head group different than the main component PG can interfere with formation of the stable 'crystal' PG-Ca^{++}, possibly by preventing formation of a chelated PG-Ca^{++} lattice.

In mixtures with PC, the behaviour manifested by PG-Ca^{++} corresponded to that of a hydrated charge neutralized PG sample. The maximum increase in transition temperature

Figure 43. Differential thermal analysis of DMPG-Ca^{++}:DMPC.

(a) DMPG-Ca^{++}:DMPC (90:10). Hydrated with excess 1.0M $CaCl_2$.

(b) DMPG-Ca^{++}:DMPC (95:5) in excess 1.0M $CaCl_2$.

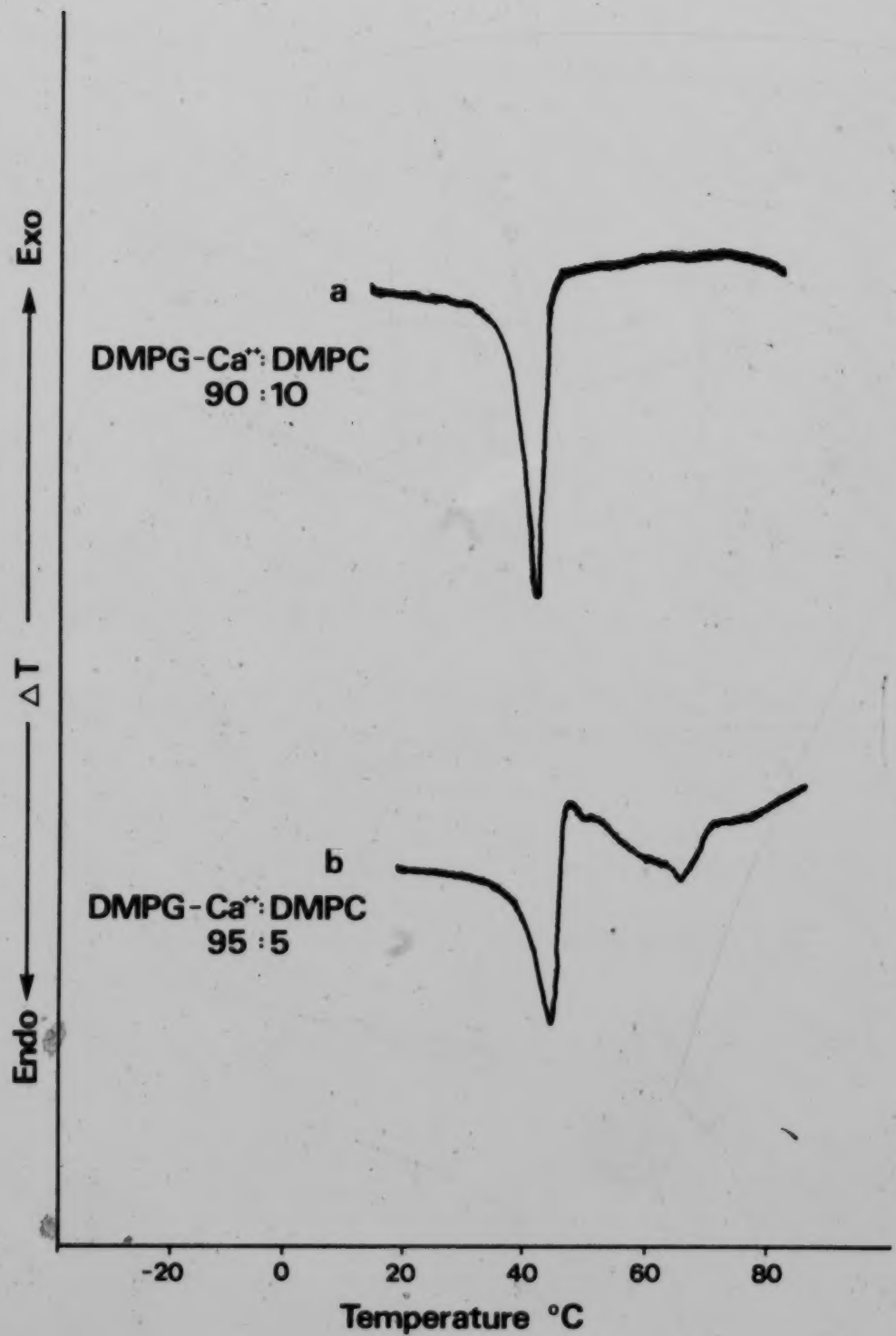
Exo
ΔT
Endo
a
DMPG-Ca++: DMPC
90 : 10
b
DMPG-Ca++: DMPC
95 : 5
-20
0
20
40
60
80
Temperature °C

was approximately 18°C and no metastable behaviour was observed.

The non-cooperative thermal behaviour of mixtures such as DMPG-Ca:DLPC (Fig. 16), DPPG-Ca^{++}-DLPC and DPPG-Ca^{++}:DMPG (Fig. 15) was interpreted as indicating the existence, within the boundaries of the phase transition, of domains of different composition enriched in either the high- or low-melting component of the mixture. The transition minima for these mixtures were different from the T_cs of either of the components, so although the miscibility of the components was far from ideal, there was no segregation into single component domains.

The only PG:Ca^{++} sample in which evidence of complete gel phase immiscibility occurred was DOPG-Ca^{++}:DSPC (50:50) (Fig. 17); in this case, the low temperature transition occurred at -12°C, the same as the T_c for pure DOPG-Ca^{++}.

Fig. 44 is a schematic illustration of the sequence of thermal events occurring during heating of a non-cooperatively melting DPPG-Ca^{++}:DOPC (50:50) mixture. During heating, DOPC enriched domains are the first to become liquid-crystalline. As a result of miscibility of DPPG-Ca^{++} in the DOPC domains, the transition is centered at approximately 0°C, about 18°C above the T_c for pure DOPC. The T_c of the higher-melting DPPG-Ca^{++}-enriched phase is lowered due to miscibility of DOPC with the gel phase DPPG-Ca^{++} and to the presence of the liquid-crystalline DOPC-enriched component. At the point on the thermogram illustrated by Fig. 44c, the

Figure 44. Schematic illustration of thermal transition events during heating of DPPG-Ca^{++}:DOPC.

(a) Below low temperature endotherm microdomains enriched in DPPG or DOPC occur.

(b) Low temperature transition results in formation of liquid crystalline regions enriched in DOPC.

(c) DOPC enriched component is liquid crystalline, DPPG enriched component gel.

(d) Gel-liquid-crystalline transition of DPPG enriched component.

(e) Completion of transition. Mixture is completely liquid-crystalline. This is not intended to indicate fluid-fluid immiscibility of DPPG and DOPC.

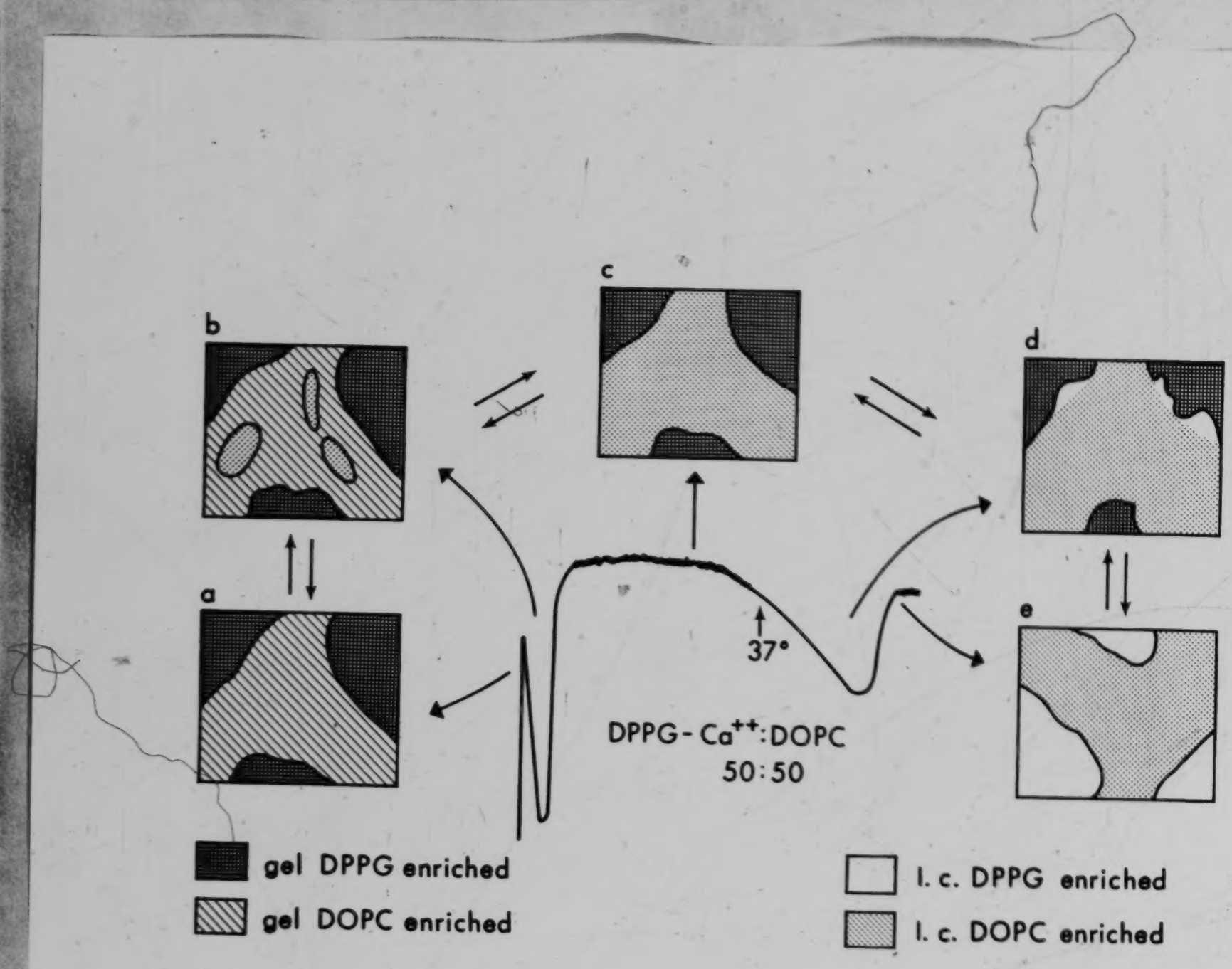
a
b
c
d
e
37°
DPPG - Ca++ : DOPC
50 : 50
gel DPPG enriched
gel DOPC enriched
l. c. DPPG enriched
l. c. DOPC enriched

lower melting DOPC-enriched domains are liquid-crystalline while the DPPG-enriched domains are predominantly gel. The sequence of events from Fig. 44a-c is not intended to imply that the miscibility with DPPG-enriched domains is the same for both the gel and liquid-crystalline DOPC-enriched fraction. Fig. 44e illustrates completion of the gel to liquid-crystalline transition sequence and does not imply fluid-fluid immiscibility.

8. Effects of cholesterol on DMPG-Na^+ and DPPG-Na^+ in the absence of Ca^{++}

The effect of cholesterol in the thermal behaviour of DMPG-Na^+ and DPPG-Na^+ was similar to that reported for the cholesterol effect on PCs (117,143). At a 3:1 ratio of PG:cholesterol, the cooperativity of the gel-liquid crystalline phase transition was reduced (Fig. 24a - DMPG; Fig. 25d - DPPG). A 2:1 ratio of PG:cholesterol resulted in elimination of the gel to liquid-crystalline endotherm.

9. Effects of cholesterol on PG:PC mixtures in the presence of Ca^{++}

Demel et al. (124) have reported that in immiscible mixtures of acidic phospholipids and phosphatidylcholines (DMPG-Na^+:DOPC [50:50]; DMPG-Na^+:DOPE [50:50]), cholesterol preferentially eliminated the transition endotherm of the lower-melting component before decreasing the transition enthalpy of the higher melting phospholipid.

Our results with DPPG-Ca^{++}:DLPC:cholesterol and

DMPG-Ca^{++}:DLPC:cholesterol indicated this preferential interaction did not occur with partially miscible mixtures. Instead, addition of cholesterol to a DPPG-Ca^{++}:DLPC mixture (Fig. 28) resulted in an increase in cooperativity (decrease in transition width) and shifted the transition minimum to a temperature (≈28°C) between the two minima (∿20°C and ∿52°C) observed in the absence of cholesterol (Figs. 24b,c). The phase transition of DPPG-Ca^{++}:DLPC mixtures was eliminated at a phospholipid:cholesterol ratio of 2:1 (Fig. 24d), in agreement with results previously reported for phosphatidylcholines (143) and various phospholipid mixtures (124). Our data for the non-cooperative DPPG-Ca^{++}:DLPC:cholesterol are consistent with the concept that cholesterol is inducing an averaging effect which is manifested in the broad single endotherms. Whether this effect is due to increased miscibility of the PC-enriched and PG-enriched components or to an increase in fluidity of the PG-enriched component concomitant with a decrease in fluidity of the PC-enriched component cannot be determined from our data.

10. Effects of cholesterol on DPPG-Ca^{++} and DMPG-Ca^{++}

The similarity of the DTA heating curves for DPPG-Ca^{++} and DMPG-Ca^{++} in the presence and absence of cholesterol indicated that the Ca^{++}-PG interactions which cause the complex metastable behaviour are essentially unchanged even at a 2:1 ratio of PG:cholesterol. This could occur if:

(a) the binding of Ca^{++} to the PG resulted in exclusion

of the cholesterol from the complex,

(b) cholesterol could be accommodated within the lattice arrangement required for formation of the stable $PG\text{-}Ca^{++}$ complex.

This latter possibility appears unlikely as 2:1 phospholipid:cholesterol ratios normally eliminate any detectable phase transition (124,143). The elimination of the complex, metastable behaviour of $PG\text{-}Ca^{++}$ by relatively small amounts of PC also argues against a mechanism involving inclusion of substantial quantities of a second component within the stable $PG\text{-}Ca^{++}$ complex.

Although the cholesterol-induced changes in the $PG\text{-}Ca^{++}$ heating curves were relatively minor, pronounced changes in the cooling curves were apparent which could not be explained on the basis of complete exclusion of cholesterol.

The following hypothetical mechanism is proposed based solely on the effects of cholesterol on the thermal behaviour of the $PG\text{-}Ca^{++}$ complexes. It cannot be corroborated by data available at this time.

(1) On formation of a $PG\text{-}Ca^{++}$ complex, the cholesterol is excluded into the aqueous medium resulting in a relatively unaltered $PG\text{-}Ca^{++}$ thermogram.

(2) Above the high temperature transition of the stable 'crystal' $PG\text{-}Ca^{++}$, hydrated-liquid crystalline liposomes form which permit inclusion of cholesterol. This results in a decrease in cooperativity of the liquid-crystalline to

gel transition on cooling (Fig. 24d; 25c). At a 2:1 ratio of PG:cholesterol, the rehydration at high temperature is transiently inhibited and the dehydrated lipid undergoes a liquid-crystalline to gel transition at 80-85°C (Fig. 26c, 27b).

(3) The presence of some cholesterol in the PG-Ca^{++} metastable liposomes results in increased fluidity in the gel state, which is manifested in elimination of the low temperature endotherm usually observed in heating thermograms of metastable DPPG-Ca^{++} forms (compare Fig. 18e with Fig. 27c), and a shift of the low temperature exotherm (T_c = 68°C) to approximately 55°C. It is proposed that during the structural rearrangement and/or dehydration events responsible for the exotherm, the cholesterol is excluded from the PG-Ca^{++} complex.

CHAPTER V

COAGULATION ASSAY RESULTS

1. Calibration with a lipid standard

The modified Stypven test (121) described in the methods section was used for all clotting assays as previous use had shown it to be sensitive to physicochemical changes in the lipid component of the assay mixture and to yield similar results using either purified clotting factors or crude reagents (68). Concentrations of the Bell and Alton cephalin (109) used as a standard lipid were expressed as micrograms of lipid phosphorus per ml of buffer. One equivalent of standard lipid was defined as equal to 1 µgP/ml cephalin.

The clotting times obtained for lipid samples were converted to equivalents of standard lipid by determining, from a calibration curve, the number of equivalents of standard lipid required to give a clotting time identical to the test sample.

Fig. 45a shows a typical plot of clotting times obtained at 37°C as a function of standard lipid concentrations with linear coordinates.

Calibration curves were constructed by plotting the logarithms of the clotting times were versus the logarithms of the concentrations of standard lipid. Fig. 45b shows a typical set of calibration curves obtained at 30°C, 37°C and 44°C. The longer clotting times obtained at 30°C probably reflect an overall decrease in enzyme activities

Figure 45. Clotting times as a function of Bell & Alton cephalin concentration.

Clotting assay mixture: 0.1 ml Standard Normal Plasma; 0.1 ml Bell & Alton cephalin in Michaelis buffer at concentration indicated; 0.1 ml Russell viper venom; 0.1 ml $CaCl_2$ (0.025M).

(a) Clotting times at T = 37°C as a function of Bell & Alton cephalin concentration (Linear coordinates).

(b) Logarithm of clotting times as a function of logarithm Bell & Alton concentration at T = 30°C, T = 37°C and T = 44°C.

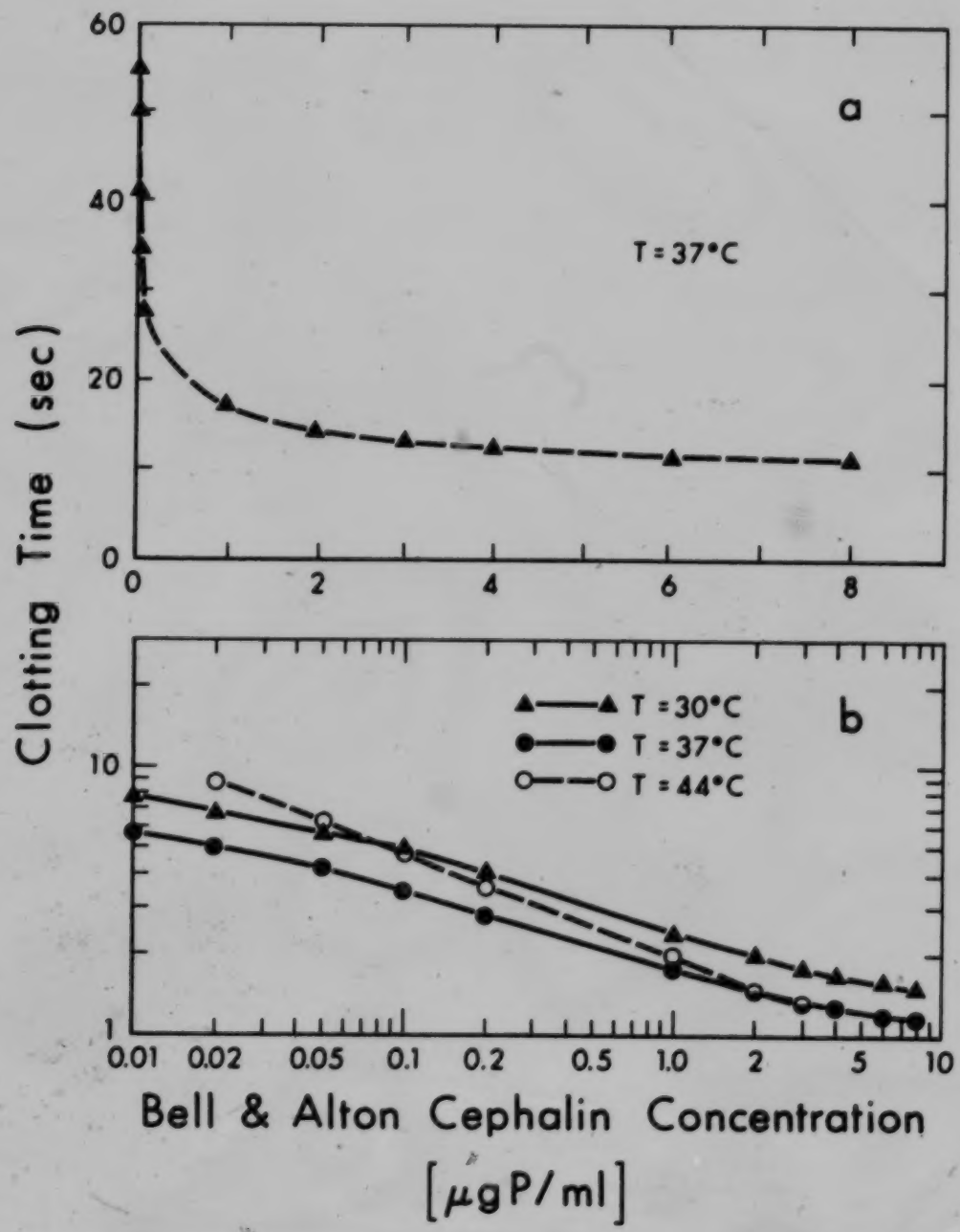
60
40
20
0
a
T = 37°C
0
2
4
6
8
Clotting Time (sec)
10
1
b
T = 30°C
T = 37°C
T = 44°C
0.01
0.02
0.05
0.1
0.2
0.5
1.0
2
5
10
Bell & Alton Cephalin Concentration
[μgP/ml]

at this temperature. At high lipid concentrations (short clotting times) the clotting times at 37°C and 44°C were almost identical. However, as the lipid concentration was decreased (longer clotting times), the difference between the calibration curves at 44°C and 37°C became progressively greater. This decrease in activity as a function of time incubated at 44°C appears to be related to the thermal instability of the SNP and/or RVV reagents. SNP and RVV reagents previously incubated at 44°C produced inordinately long, non-reproducible clotting times. This necessitated using the modified procedure, outlined in the methods section, whereby the reagents were stored at 37°C prior to use in the assay at 44°C.

2. Requirement for an acidic lipid component

Figs. 46, 47, and 48 show profiles of the clotting activity versus lipid composition for the three lipid mixtures at 30°C, 37°C and 44°C respectively. The pure PC components exhibited no coagulant activity. However, increasing the proportion of DMPG (mole %) increased activity to an optimum, beyond which a decrease was manifested.

The proportion of DMPG (mole %) required for optimal activity differed for different chain lengths of the PC component. With DMPG:DMPC and DMPG:DPPC mixtures, the activity profile was shifted toward higher DMPG proportions.

Studies of the correlation between negative surface charge density and coagulant activity of lipid dispersions

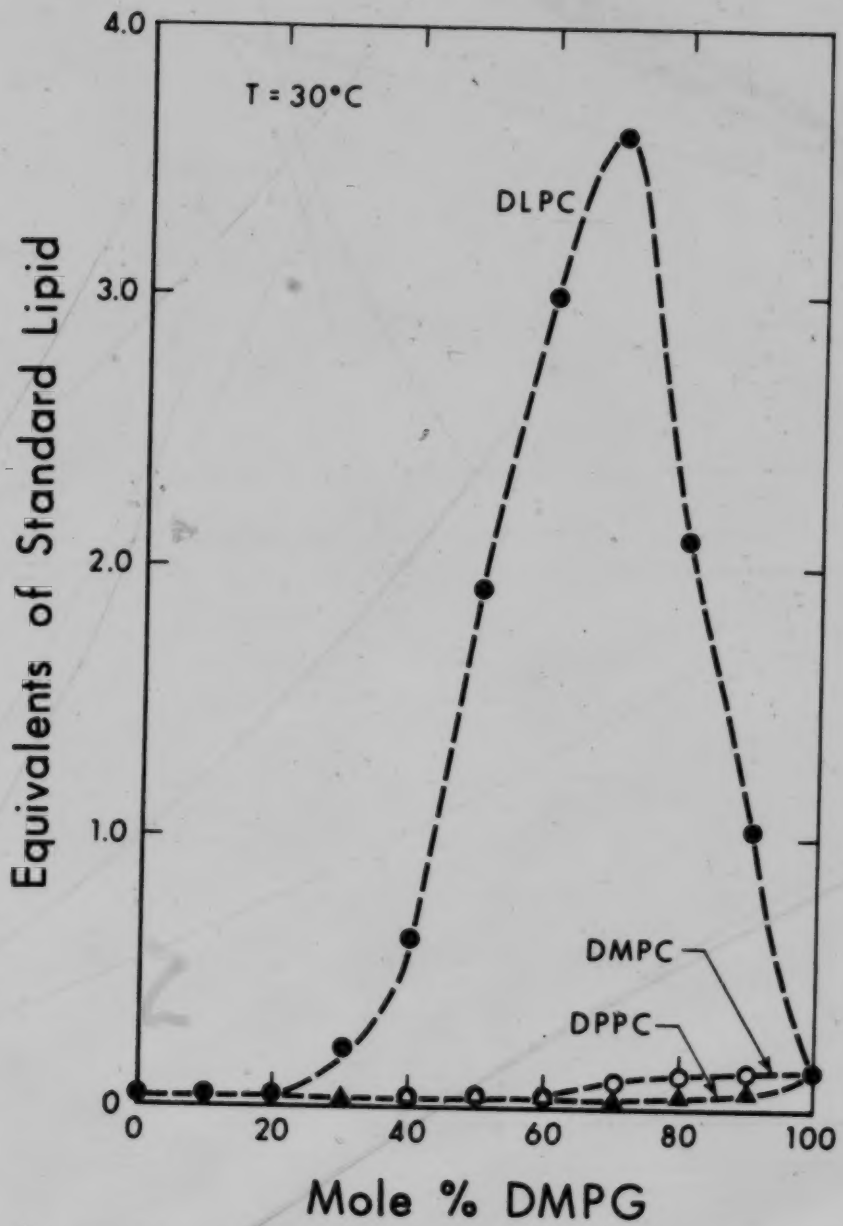

Figure 46. Clotting activity-composition profiles for DMPC:PC mixtures at T = 30°C.

Assay mixtures as in Figure 45.
Lipid mixtures prepared as in Methods (16b).
Lipid mixture concentration: 8 μgP/ml.

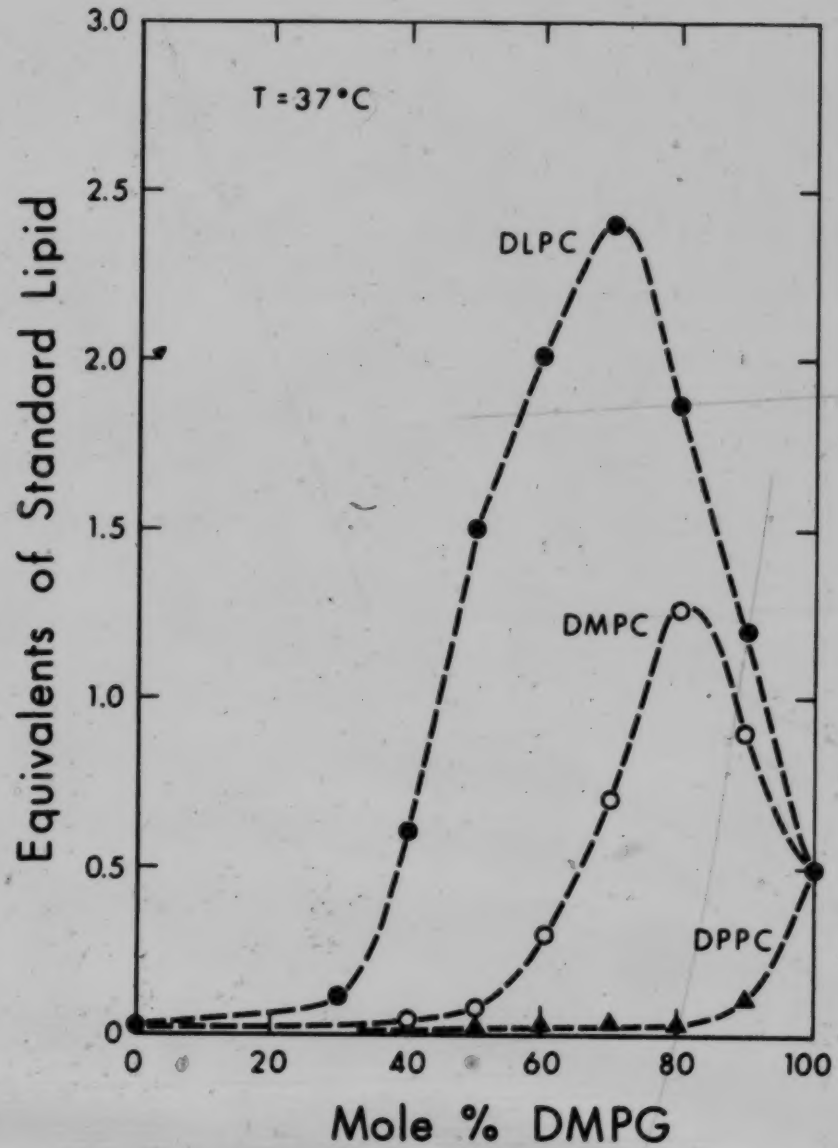

Figure 47. Clotting activity-composition profiles for DMPG: PC mixtures at T = 37°C.

Assay mixtures and lipid mixtures as in Fig. 46. Procedure as outlined in Methods (16c).

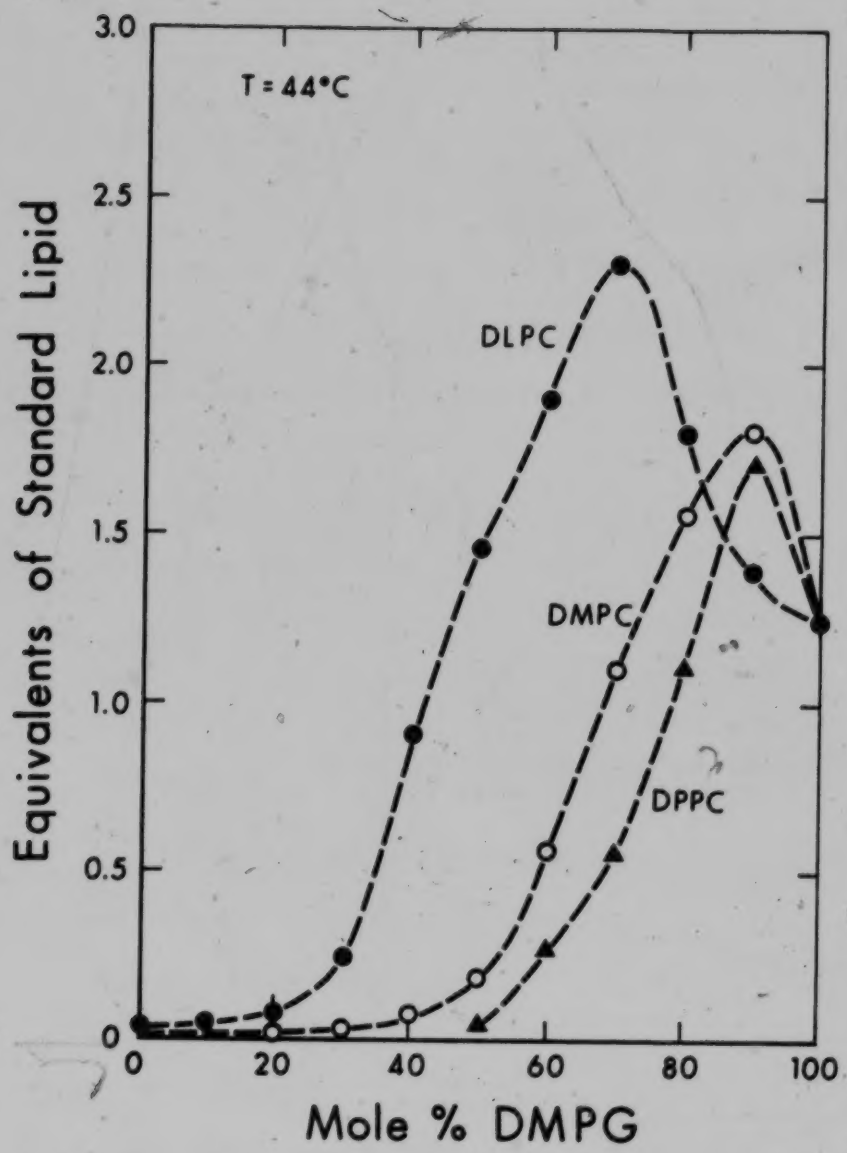

Figure 48. Clotting activity-composition profiles for DMPG:PC mixtures at T = 44°C.

Assay and lipid mixtures as in Fig. 46. Assay procedure as outlined in Methods (16e).

have revealed an apparent requirement for an optimal surface charge (61,62). However, it was later postulated that this requirement might merely reflect the need for interfacial groups capable of binding Ca^{++} in a specified lattice complementary to the spatial arrangement of the γ-carboxyglutamate residues of the coagulant proteins (63).

3. Requirement for a liquid-crystalline (fluid) component

Previous work done in this laboratory using naturally occurring and catalytically hydrogenated bovine brain PS had demonstrated that one physical requirement for high clotting activity was a liquid crystalline lipid phase (68). Catalytically hydrogenated bovine brain PS was found to be inactive at 37°C but activity could be restored by the addition of cholesterol. Cholesterol eliminated the phase transition of the hydrogenated PS (T_c = 72°C) as detected by differential thermal analysis, and presumably 'fluidized' the lipid.

The initial series of clotting assays using the synthetic PG:PC systems was designed to test the proposed requirement for a liquid crystalline lipid state for clotting activity. Clotting assays were done at 30°C, 37°C and 44°C (Figs. 46, 47, 48) using mixtures of DMPG:DLPC, DMPG:DMPC and DMPG:DPPC, and these activities related to the physical state of the various lipid mixtures at each of the three assay temperatures (summarized in Table V). As illustrated by

TABLE V

Physical States of Lipid Mixtures at Different Temperatures

Lipids (% DMPG)	Temperature 30°C	37°C	44°C
DPPC-DMPG (0-100%)	gel	gel*	fl*
DMPC-DMPG (0- 50%)	fl*	fl	fl
(60-100%)	gel*	melt	fl
DLPC-DMPG (0- 40%)	fl	fl	fl
(50- 70%)	ph. sep.	ph. sep.	fl*
(80-100%)	gel	melt	fl

gel = gel phase
fl = "fluid" or liquid crystalline phase
melt = within melting range
ph. sep. = phase separation

* predominant phase

the DMPG:DMPC and DMPG:DPPC mixtures at 30°C (Fig. 46) and the DMPG:DPPC mixtures at 37°C (Fig. 47), lipid mixtures that were completely in the gel phase at the assay temperature showed very little clotting activity. At 37°C (Fig. 47) the DMPG:DMPC mixtures were predominantly liquid crystalline and showed a dramatic increase in activity compared to their activity at 30°C.

At 44°C (Fig. 48) there was a further small increase in the activity of the DMPG:DMPC mixtures and an approximately 15 fold increase in the activity of the DMPG:DPPC above the activity observed at 37°C. At 44°C both the DMPG:DMPC and DMPG:DPPC mixtures are liquid-crystalline and both attain the same maximum activity.

The earlier conclusion concerning a fluid phase requirement for clotting activity was therefore confirmed by these experiments.

4. Cooperative and non-cooperative phase transitions

It can also be seen from Fig. 48 that the maximum activity of the mixtures which show cooperative melting behaviour (DMPG:DMPC, DMPG:DPPC) was not as great as the maximal activity attained by the non-cooperative system of DLPC:DMPG. Furthermore, the DMPG:DLPC mixtures showed a decrease in activity in going from 37°C (within the range of the phase transition) to 44°C (where the mixtures were completely fluid). One explanation for this behaviour is that the co-existence of two phases, one solid and one fluid,

in equilibrium at 37°C provides a more favorable environment than does an entirely fluid phase structure.

To confirm that the greater maximum activity observed with the DMPG:DLPC mixtures was not merely the result of these mixtures being slightly more fluid than the DMPG:DMPC and DMPG:DPPC mixtures at the assay temperatures, a series of experiments was conducted to compare the clotting activity of the DMPG:DLPC with DOPG:DOPC mixtures. At the clotting assay temperatures the DOPG:DOPC mixtures were 40°C to 60°C above their transition temperature. In Fig. 49, the clotting activities of the DMPG:DLPC and DOPG:DOPC mixtures are compared at 30°C, 37°C and 44°C. The DMPG:DLPC mixtures were distinctly more active at all three temperatures than the completely liquid-crystalline DOPG:DOPC mixtures. This result therefore confirmed the conclusion outlined in the previous paragraph.

5. Fluid phase and fluid-fluid phase separation

Fig. 49 also shows that there was a marked decrease in the maximum activity of the DOPG:DOPC in going from 37°C to 44°C. There are several ways to explain this observation. First, it is possible that the increase in entropy of the DOPC:DOPG mixtures at 44°C compared to 37°C may result in an energetically less favourable condition for either the binding or orientation of the coagulant proteins. Secondly, the activity of the lipid may be affected by the presence of the quasicrystalline clusters that have been reported to

Figure 49. Clotting activity-composition profiles for DMPG:DLPC and DOPG:DOPC.

Assay and lipid mixtures as in Fig. 46.
Procedure as in Methods (16).
Assay temperatures as indicated.

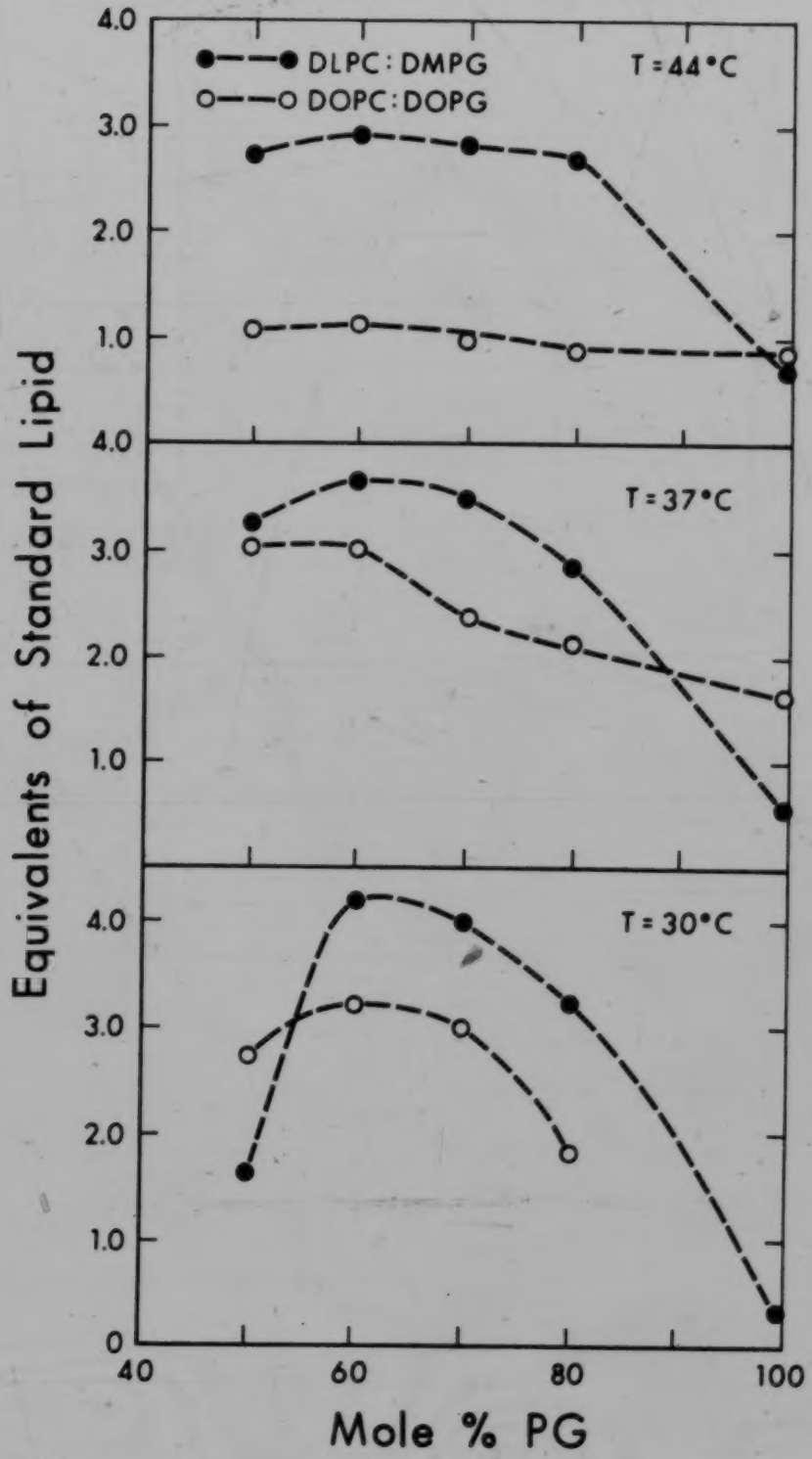
DLPC : DMPG
DOPC : DOPG
T = 44°C
T = 37°C
T = 30°C
Equivalents of Standard Lipid
Mole % PG
4.0
3.0
2.0
1.0
0
40
60
80
100

occur in aqueous dispersions of dioleoyl phospholipids at temperatures well above the gel-liquid crystalline transition (145). These clusters, predicted on the basis of e.s.r studies using Tempo (2,2,6,6-tetramethylpiperidine-1-oxyl) and methyl-12-nitroxidestearate probes, are described as short-lived, more densely packed arrangements of molecules within an environment of freely dispersed molecules. Onset of formation of these clusters at 30°C has been proposed as a possible explanation for the break in Arrhenius plots at 29°C for sarcoplasmic reticulum [Ca^{++}; Mg^{++}] ATPase from rabbit muscle (144).

Similar anomalous behaviour of Tempo probes has been observed in lipid extracts from membranes of E. coli strain L8-2 which are enriched in cis-vaccenate (cis-Δ_{11}-18:1) (145). In this study partition coefficient plots vs. 1/T showed discontinuities at 46°C, some 59°C above the calorimetrically measured gel to liquid-crystalline phase transition. These anomalous discontinuities in Tempo partitioning have only been observed in phospholipids with cis-monoenoic, eighteen-carbon acyl chains and consequently may indicate a specific interaction of the Tempo with this type of acyl substituent rather than an alteration in the fluidity characteristics of the phospholipids. Although these results and the interpretation of them must be viewed with caution, the numerous reports in the literature of membrane-bound or phospholipid-reconstituted enzyme systems which display discontinuities in Arrhenuis plots considerably

above the completion of the calorimetrically determined phase transition suggests that lipid-protein interactions may be sensitive to changes in fluidity that are not detectable by current calorimetric techniques. It is possible that these changes in fluidity of the liquid crystalline lipids are related to the existence of quasicrystalline clusters. The progressive decrease in the clotting activity of the DOPG:DOPC mixtures as the assay temperature is increased from 30°C to 44°C may be related to the disappearance of such clusters over this temperature range (145).

A third possible explanation for the lowered clotting activity of the DOPG:DOPC mixtures at 44°C is that the notorious thermal instability of factor V is more readily manifested in the completely fluid DOPG:DOPC mixtures than in the other mixtures tested. Colman *et al.* (53) have shown that the rate of inactivation of factor V was related to the type of phospholipid associated with the protein. At 37°C in the presence of bovine brain PS, the factor V was 95% inactivated within 2 minutes while under the same conditions in the presence of egg PC there was only 12% inactivation. While there is no data available for the effects of PG:PC mixtures on factor V stability, it is possible that factor V is rapidly inactivated in the presence of DOPG:DOPC mixtures and that this inactivation results in the low clotting activity at 44°C.

6. Gel-fluid phase separation

Further experiments were performed to determine if the mere existence of a phase separation was itself sufficient to promote optimal clotting activity or whether the physical and chemical nature of the resulting individual phases was also important. Three lipid mixtures were therefore selected with a view to obtaining:

(a) Widely separated thermal transitions of the two components with the zwitterionic lipid as the major high-melting component. DOPG:DSPC was selected for this.

(b) Widely separated thermal transitions of the two components with the acidic lipid as the high-melting component. DPPG:DOPC was selected.

(c) An incompletely resolved transition. DMPG:DLPC was selected.

Each of the three lipid mixtures provided, at the assay temperature of 37°C, an equilibrium mixture of gel and liquid-crystalline phases. The mixture DOPG:DOPC, completely liquid-crystalline at 37°C, provided a reference point for this comparison.

As shown in Figs. 50 and 51, the mixtures in which the acidic lipid components were almost entirely in the gel phase at the assay temperature (DPPG:DLPC and DPPG:DOPC) had lower activity than mixtures with fluid acidic lipid components (DOPG:DSPC and DOPG:DOPC).

Figure 50. Clotting activity-composition profiles for DOPG:DOPC and DPPG:DLPC mixtures.

Assay and lipid mixtures as for Fig. 46.
Procedure as in Methods (16c).
T = 37°C.

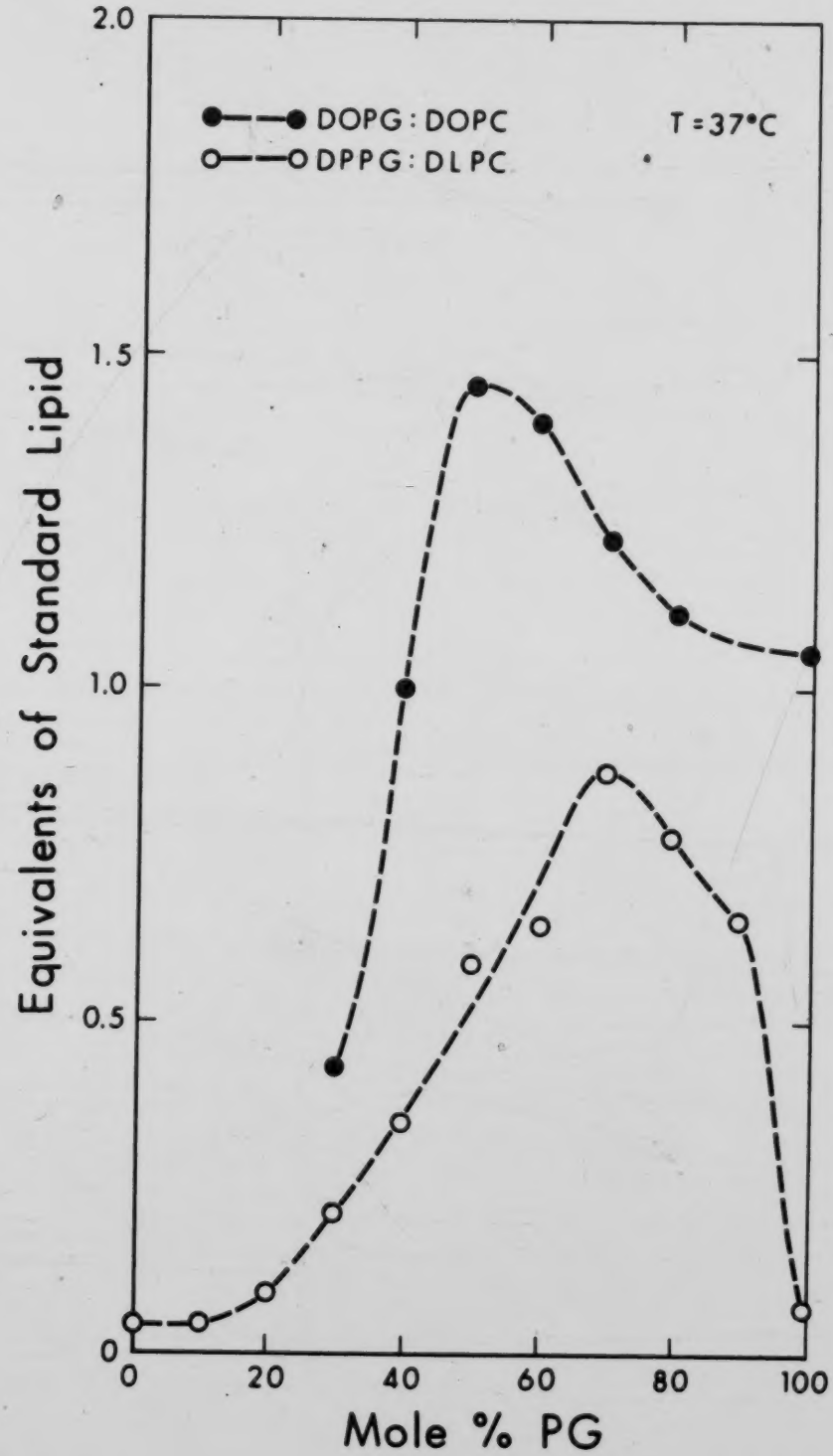
2.0
1.5
1.0
0.5
0
DOPG : DOPC
DPPG : DLPC
T = 37°C
Equivalents of Standard Lipid
0
20
40
60
80
100
Mole % PG

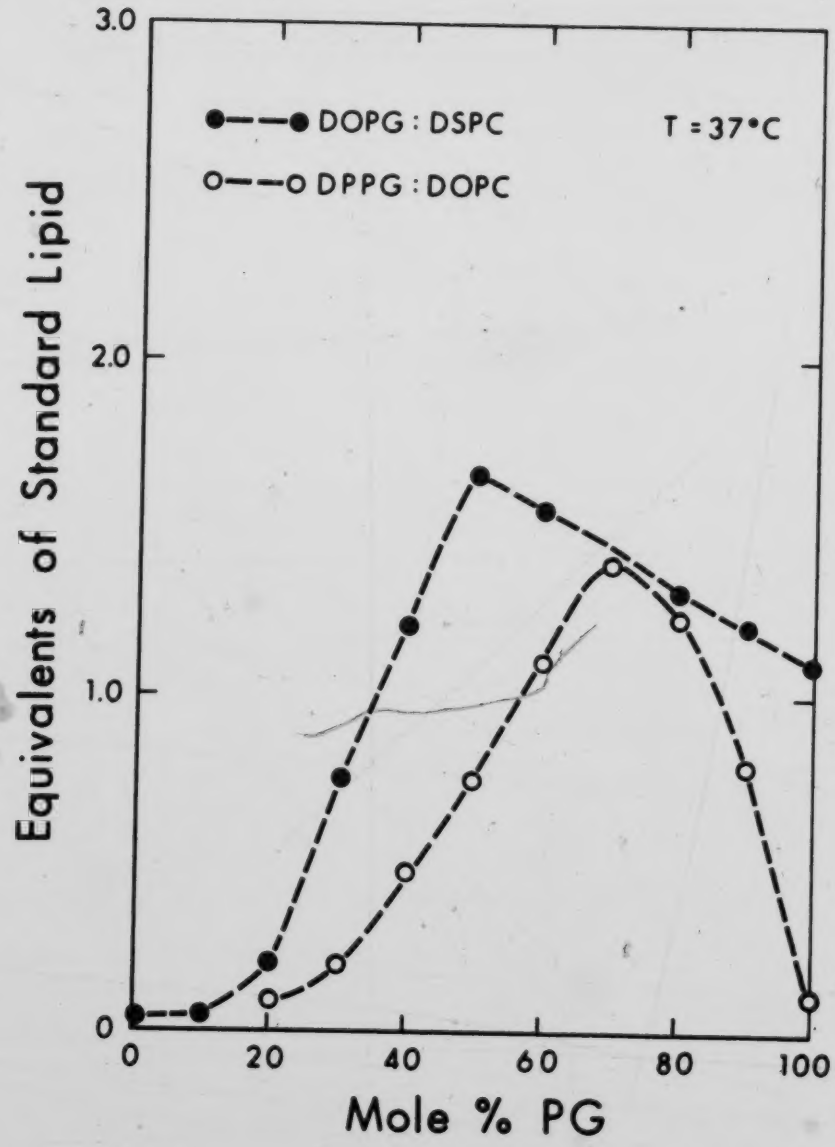

Figure 51. Clotting activity-composition profiles for DOPG:DSPC and DPPG:DOPC mixtures.

Assay and lipid mixtures as for Fig. 46. Procedure as in Methods (16c). T = 37°C.

7. Lipid composition of the active phases

In none of the cases examined in the preceding sections, where phase separations are involved, do the two transition temperatures observed correspond to those of the two pure lipid components. This implies that each of the separating phases is enriched in one or other of the lipid components but to an extent less than 100%. The observed transition temperatures then presumably reflect the mole fraction of each lipid in each of the two phases. Several of the results shown in Figs. 46 to 51 indicate that the clotting activity is dependent on the lipid composition within each of the phases.

For example, mixtures in which the acidic lipid was completely liquid-crystalline and well above its transition temperature had optimal activity at lower mole fractions of acidic component than those observed for mixtures in which the acidic lipid component was partially in the gel phase or only slightly above its transition temperature. DOPG:DOPC mixtures (Fig. 50) and DOPG:DSPC (Fig. 51) mixtures had optimal activity at 50 mole % DOPG. Mixtures of bovine brain PS and egg PC were reported to show maximal activity at 35 mole % PS (15). In contrast, DMPG:DPPC and DMPG:DMPC have optimal activity at 90 mole % DMPG (Fig. 48). In lipid mixtures such as DMPG:DLPC (Fig. 47), DPPG:DLPC (Fig. 50) and DPPG:DOPC (Fig. 51) which demonstrated phase separation behaviour with the acidic lipid as the high-melting component, the overall optimum was approximately 70 mole % PG. In

these mixtures the high-melting component was enriched in acidic lipid and the mole % PG of this high melting component probably approached 90% - the optimum observed with the more ideally miscible lipid mixtures. This was corroborated by the observation that in thermograms of DMPG:DLPC mixtures at 70 mole % DMPG (Fig. 16) the thermographic minimum observed for the high-melting component was at the same temperature as the minimum for the 90 mole % DMPG mixture. As it is unlikely that the geometrical and chemical properties of the lipid lattice directly bound to the coagulant proteins varies appreciably with the various PG:PC mixtures, the different mole fractions of PG required for optimal activity of the various mixtures probably reflects the influence of the lipid fluidity on the formation of an effective protein-binding lipid lattice. Speculatively, with fluid components the necessary lipid lattice for optimal activity can be sequestered from mixtures with relatively low mole fractions of acidic component. When the acidic lipid is gel or only slightly above its transition temperature, it cannot be readily sequestered into the required lattice and consequently requires a much higher ratio of acidic lipid to zwitterionic lipid to provide the negatively charged sites in an array suitable for binding.

A. COMMENT ON THE B & A CEPHALIN CALIBRATION CURVES

Although the calibration curves constructed for the clotting assay experiments were all qualitatively similar,

enough quantitative variation was encountered to preclude direct comparisons of lipid mixture clotting activities determined from different calibration curves.

To determine if the method used to disperse the lipid mixtures (brief sonication ~ 60 sec) was resulting in heterogeneous dispersions which could cause variation in clotting times, the effect of sonication on B & A cephalin and DMPG:DLPC mixtures was examined. Sonication for 30 sec resulted in an increase in the clotting activity (decreased clotting time) compared to non-sonicated (vortexed) dispersions (Fig. 52). Sonication for up to one hour caused no further increase in clotting activity so it is unlikely that heterogeneity of the lipid dispersions was the cause of variation. The fact clotting times could vary using the same synthetic lipid mixture with different lots of SNP and RVV reagents led to the conclusion that the quantitative variation was due to minor variations in the activity of these latter two components. Consequently, a calibration curve was obtained for each individual experiment and clotting activity comparisons were made only if data from the different lipid mixtures could be related, directly, to a single calibration curve.

Figure 52. Effect of sonication on clotting times.

Sonication was performed in a water-cooled cell at T = 20°C. Assay and lipid mixtures as for Figs. 45 and 46. Bell & Alton cephalin [2 µgP/ml].

DMPG:DLPC (50:50) [8 µgP/ml].

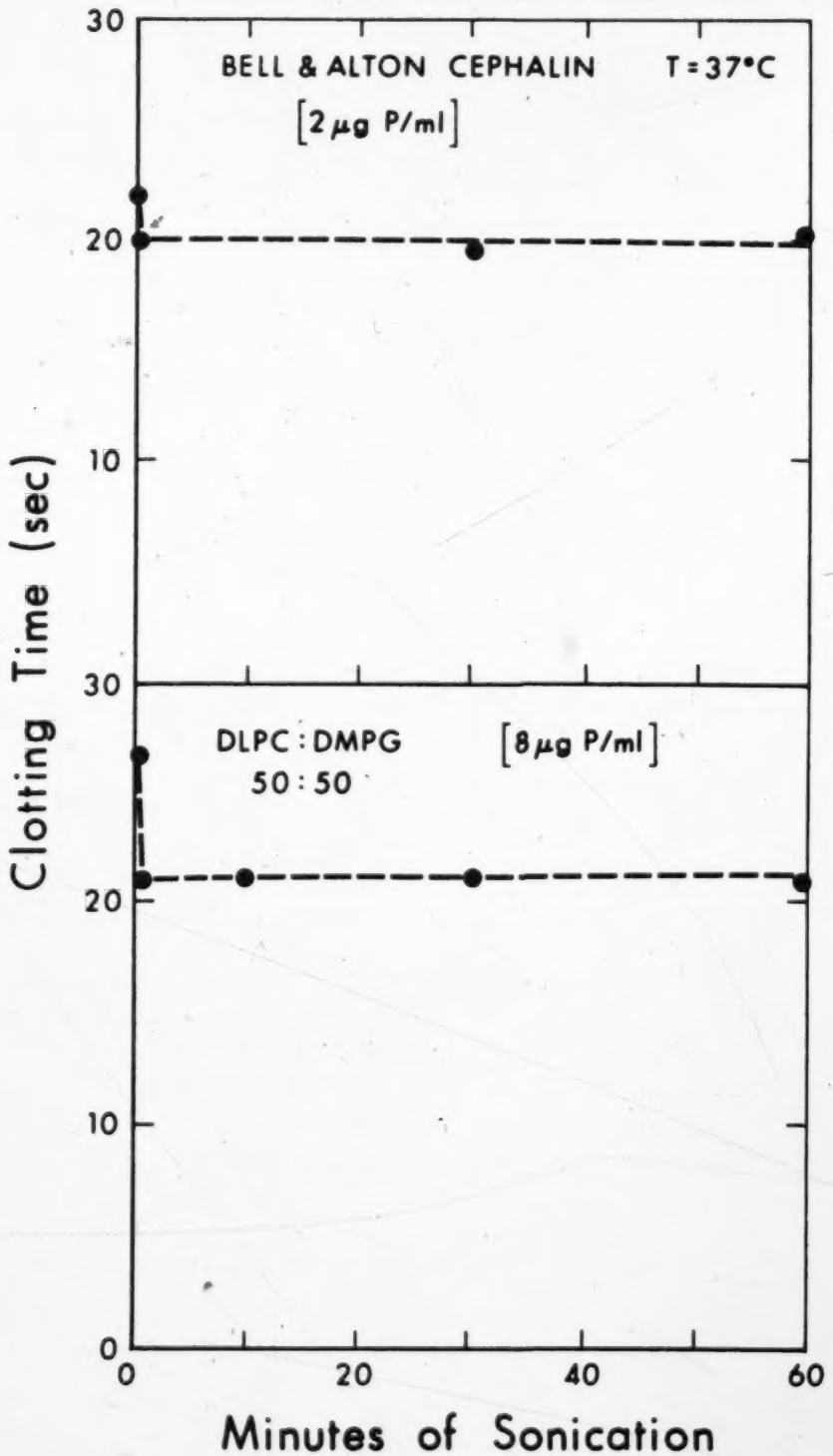
BELL & ALTON CEPHALIN
T = 37°C
[2 μg P/ml]
DLPC : DMPG
50 : 50
[8 μg P/ml]
Clotting Time (sec)
30
20
10
30
20
10
0
0
20
40
60
Minutes of Sonication

CHAPTER VI

DISCUSSION - A LIPID PHASE SEPARATION MODEL FOR PROTHROMBIN ACTIVATION

In order to formulate a model for prothrombin activation, we take into account:

(1) the specific lipid requirement for optimal activation;

(2) the nature of the individual lipid-protein interactions involved in prothrombinase formation and in prothrombin activation. These have been outlined in Chapter I;

(3) current concepts of rotational and translational diffusion of proteins associated with lipid bilayers (147). Such processes may become rate-limiting in the formation of multi-protein complexes such as prothrombinase.

A. DESCRIPTION OF THE MODEL

(1) The reactions of prothrombin activation occur at the lipid-water interface. Adsorption of the proteins produces a local increase in their concentration.

(2) The optimal structure of the lipid-bilayer consists of two lipid phases, one comprising domains rich in acidic lipids the other forming a matrix rich in the zwitterionic components (Fig. 53a).

(3) The Ca^{2+}-mediated binding of prothrombin and factor Xa occurs through Ca^{2+} bridges linking these proteins to the PG-enriched gel phase domains (Fig. 53b).

(4) Increased molecular disorder at the domain-

Figure 53. Schematic illustration of prothrombin activation model.

(a) Phospholipid phase structure during a thermal transition. Adapted from Marsh et al. (101). F indicates fluid or liquid crystalline domains. S indicates solid or gel phase lipid. I indicates phase boundary or interfacial lipid.

(b) Phospholipid phase structure as for (a) incorporating the proteins of the prothrombin activation complex. Prothrombin (II = factor II) and factor X_a bind to anionic phospholipid enriched gel domains. Hydrophobic interaction of Factor V (V) with the lipid is facilitated by liquid crystalline phase and/or interfacial lipids. Mobility of the proteins in liquid crystalline phase and at interface permits orientation into an effective catalytic unit (illustrated at bottom right corner).

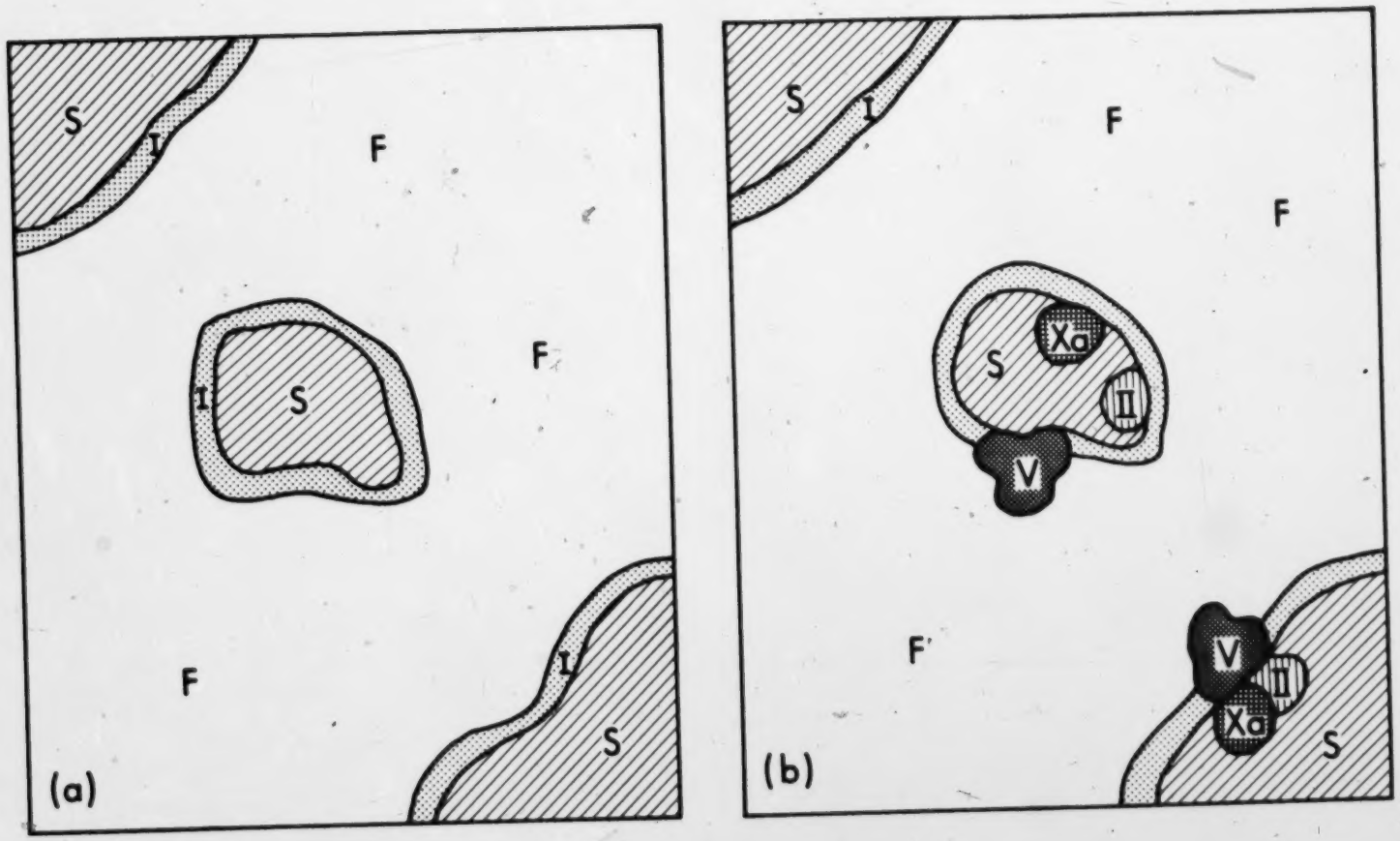
S
I
F
I
S
F
F
I
S
(a)
S
I
F
F
Xa
S
II
V
F
V
II
Xa
S
(b)

boundaries facilitates the accommodation of factor V in the bilayer and permits lateral and/or rotational protein mobility necessary for protein-protein interactions involved in formation of the final complex (Fig. 53b). The reported interaction of factor V with prothrombin (23,60) in a region (fragment 2) adjacent to the phospholipid binding site (fragment 1) is compatible with this model.

B. IMPLICATIONS OF THE MODEL

A primary feature of the model is that the lipid matrix should allow sufficient lateral and possibly rotational mobility to permit orientation of the phospholipid-adsorbed clotting factors in a catalytically effective arrangement. This should be facilitated by a liquid-crystalline lipid phase. However, we have demonstrated that the DMPG:DLPC mixtures which were only partially liquid-crystalline at the clotting assay temperatures were more active than completely liquid-crystalline DOPG:DOPC mixtures. Furthermore, DMPG:DLPC mixtures were less active in a fully liquid-crystalline state (T = 44°C) than at lower temperatures (30, 37°C) where gel and liquid-crystalline domains co-existed (Fig. 49). Since the design of these experiments precludes chemical differences a physical origin of these observations must be sought. As discussed previously, a lipid bilayer at a temperature between the upper and lower limits of a phase transition exhibits anomalous physical properties. These include increased permeability (79,100), increased lateral

compressibility (147) and an increase in the amount of domain boundary lipid (100,101). These properties all imply an enhanced disorder (structural defect) in the hydrocarbon core of the bilayer. A lipid phase separation may, therefore, be more conducive to prothrombin activation than a purely liquid-crystalline phase.

Recent results obtained by Colman et al. (148) may also be consistent with this hypothesis. They observed that factor V showed high activity in combination with bovine PE (liquid-crystalline). Interaction with saturated bovine PE (gel) resulted in greatly reduced factor V activity. Mixtures of saturated PE and naturally occurring PE resulted in factor V activity higher than that achieved with either of the PEs alone. The synergistic effect of saturated PE and naturally occurring bovine PE mixtures could also be interpreted in terms of a lateral phase separation leading to enhanced factor V-lipid interaction.

The inclusion of cholesterol in DPPG vesicles (1:1 m/m) abolished the transient increase in permeability associated with the phase transition (100). This was attributed to elimination of the DPPG phase transition and coincidentally the domain boundaries. On the basis of the proposed model, cholesterol would be expected to decrease the clotting activity of DMPG:DLPC mixtures by altering or eliminating the domain boundaries. Increasing the molar/ratio of cholesterol to DPPG:DLPC and DMPG:DLPC mixtures from (0-0.5) resulted in a progressive decrease in clotting activity (Fig. 54). At a

Figure 54. Effect of cholesterol on the clotting activity of PG:PC mixtures.

Samples of DPPG:DLPC (1:1) or DMPG:DLPC (1:1) in $CHCl_3$ and cholesterol (also in $CHCl_3$) were mixed in amounts required to give the indicated molar ratios of cholesterol: total phospholipid. The chloroform was removed under N_2 and in vacuo at room temperature. The sample was dispersed [in Michaelis buffer] by brief sonication, at a phospholipid concentration of 8 µgP/ml.

(a) Clotting times vs cholesterol:phospholipid ratios. Standard clotting assay at T = 37°C.

(b) Conditions as in (a). Clotting times converted to equivalents of standard lipid.

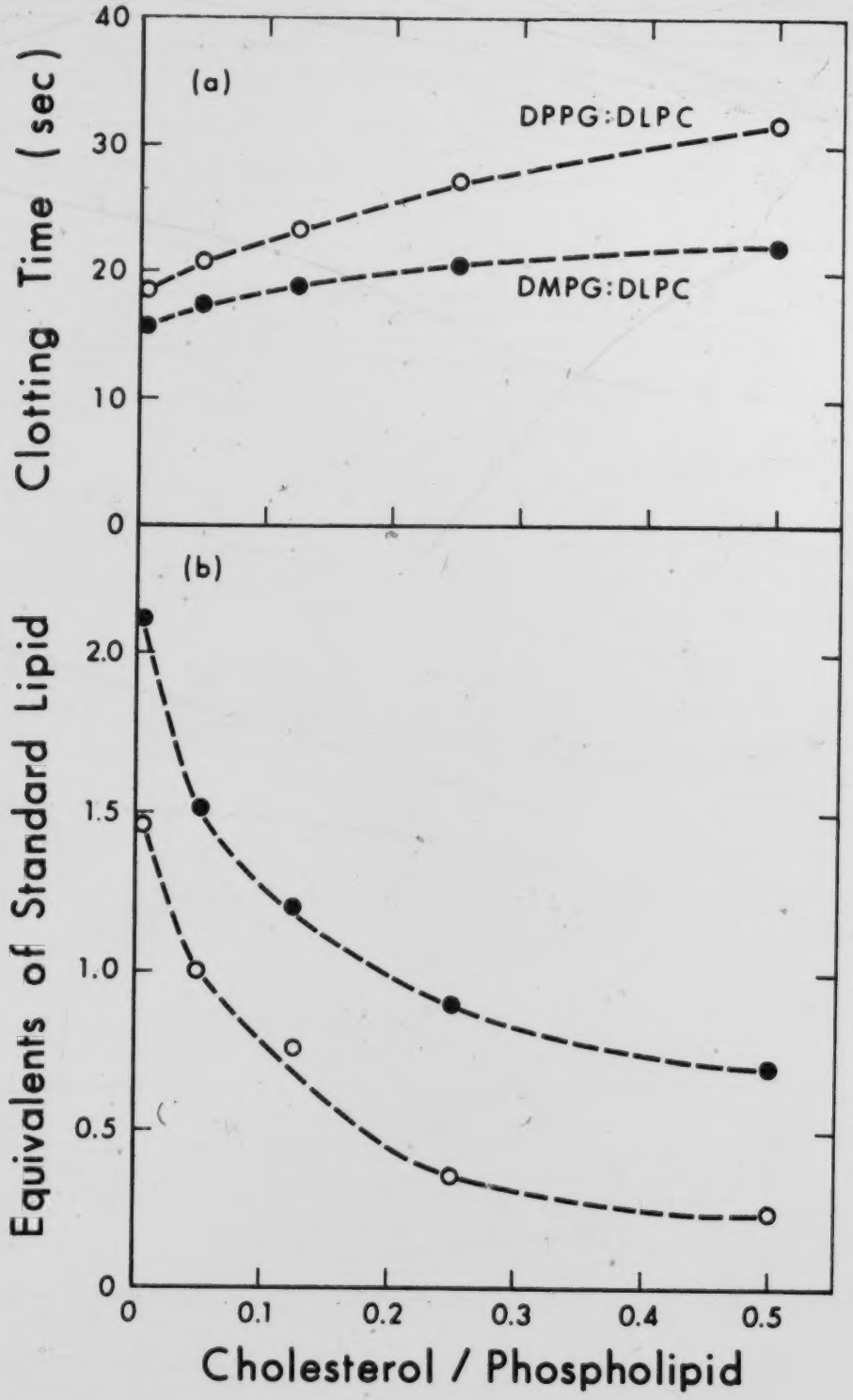
(a)
DPPG:DLPC
DMPG:DLPC
Clotting Time (sec)
40
30
20
10
0
(b)
Equivalents of Standard Lipid
2.0
1.5
1.0
0.5
0
0
0.1
0.2
0.3
0.4
0.5
Cholesterol / Phospholipid

1:1:2 molar ratio of PG:PC:cholesterol all mixtures tested showed extremely low activity (0.1 to 0.2 equivalents of standard lipid). The progressive decrease in clotting activity at low PG:PC:cholesterol ratios is consistent with the observed increase in cooperativity and apparent averaging effect of cholesterol on the thermal behaviour of non-cooperatively melting phospholipid mixtures (Fig. 28).

Although the proposed model lacks detail at the molecular level, it is compatible with the data on the effects of phospholipid physical states on clotting activity and with the properties and interactions reported for the components of the prothrombin activation complex.

BIBLIOGRAPHY

1. Suttie, J.W., and Jackson, C.M. (1977): Physiological Reviews 57, 1-70.

2. Reich, E., Rifkin, D.B., and Shaw, E. (eds.) (1975): Proteases and Biological Control. Cold Spring Harbour Symposium on Cell Proliferation, Vol. 2.

3. Schiffman, S., and Lee, P. (1974): Brit. J. Haematol. 27, 101-114.

4. Schiffman, S., Rapaport, S.I., and Chang, M.M.Y. (1973): Brit. J. Haematol. 24, 633-642.

5. Walsh, P.N. (1974): Blood 43, 597-605.

6. Biggs, R., and Walsh, P.N. (1972): Brit. J. Haematol. 22, 743-760.

7. Davie, E.W., and Fujikawa, K. (1975): Ann. Rev. Biochem. 44, 799-829.

8. Barton, P.G. (1976): PAABS REVISTA 5, 363-374.

9. Milstone, J.H. (1964): Fed. Proc. 23, 742-748.

10. Barton, P.G., Jackson, C.M., and Hanahan, D.J. (1967): Nature 214, 923-924.

11. Hemker, H.C., Esnouf, M.P., Hemker, P.W., Swart, A.C.W., and Macfarlane, R.G. (1967): Nature 215, 248-251.

12. Seegers, W.H., Sakuragawa, N., McCoy, L.E., Sedensky, J.A., and Dombrose, F.A. (1972): Thromb. Res. 1, 293-310.

13. Esmon, C.T., Owen, W.G., and Jackson, C.M. (1974): J. Biol. Chem. 249, 8045-8047.

14. Jobin, F., and Esnouf, M.P. (1967): Biochem. J. 102, 666-674.

15. Ingwall, J.S., Scheraga, H.A. (1969): Biochemistry 8, 1860-1868.

16. Cox, A.C., and Hanahan, D.J. (1970): Biochim. Biophys. Acta 207, 49-64.

17. Hewett-Emmett, D.L., McCoy, L.E., Walz, D.A., Reuterby, J., and Seegers, W.H. (1975): Thromb. Res. 7, 227-234.

18. Magnusson, S., Petersen, T.E., Sottrup-Jensen, L., and Claeys, H. (1975): In: Proteases and Biological Control (Reich, E., Rifkin, D.B., and Shaw, E. eds). Cold Spring Harbor Symposium on Cell Proliferation Vol. 2, 123-149.

19. Owen, W.G., Esmon, C.T., and Jackson, C.M. (1974): J. Biol. Chem. 249, 594-605.

20. Heldebrant, C.M., Butkowski, R.J., Bajaj, S.P., and Mann, K.G. (1973): J. Biol. Chem. 248, 7149-7163.

21. Mann, K.G., Noyes, C., Kingdon, H.S., and Heldebrant, C.M. (1973): Biochem. Biophys. Res. Commun. 54, 155-160.

22. Barton, P.G. (1971): In: Abstracts II Congr. Internat. Soc. Thrombos. Haemostasis, p. 4, Oslo.

23. Mann, K.G., Bajaj, S.P., and Butkowski, R.J. (1975): J. Biol. Chem. 250, 2150-2156.

24. Stenflo, J., and Ganrot, P.O. (1972): J. Biol. Chem. 247, 8160-8166.

25. Bjork, I., and Stenflo, J. (1973): FEBS Lett. 32, 343-346.

26. Henricksen, R.A., and Jackson, C.M. (1975): Arch. Biochem. Biophys. 170, 149-159.

27. Bull, R.K. (1973): Ph.D. Thesis "Studies on Bovine Prothrombin". University of Alberta, Edmonton, Alberta, Canada.

28. Benson, B.J., Kisiel, W., and Hanahan, D.J. (1973): Biochim. Biophys. Acta 329, 81-87.

29. Benson, B.J., and Hanahan, D.J. (1975): Biochemistry 14, 3265-3277.

30. Stenflo, J. (1974): J. Biol. Chem. 249, 5527-5535.

31. Howard, J.B., Nelsestuen, G., and Zytkovicz, T.H. (1974): J. Biol. Chem. 249, 6347-6350.

32. Nelsestuen, G., and Zytkovicz, T.H. (1975): J. Biol. Chem. 250, 2968-2972.

33. Magnusson, S., Sottrup-Jensen, L., Petersen, T.E., Morris, H.R., and Dell, A. (1974): FEBS Lett. 44, 189-193.

34. Stenflo, J., Ferlund, P., Egan, W., and Roepstorff, P. (1974): Proc. Natl. Acad. Sci. U.S.A. 71, 2730-2733.

35. Suttie, J.W., and Nelsestuen, G.L. (1972): J. Biol. Chem. 247, 8176-8182.

36. Nelsestuen, G.L., and Suttie, J.W. (1973): Proc. Natl. Acad. Sci. U.S.A. 70, 3366-3370.

37. Stenflo, J. (1972): J. Biol. Chem. 247, 8167-8175.

38. Nelsestuen, G.L., and Suttie, J.W. (1972): Biochemistry 11, 4961-4964.

39. Esmon, C.T., Suttie, J.W., and Jackson, C.M. (1975): J. Biol. Chem. 250, 4095-4099.

40. Jackson, C.M. (1973): Proc. Natl. Acad. Sci. U.S.A. 70, 1344-1348.

41. Esmon, C.T., Owen, W.G., and Jackson, C.M. (1974): J. Biol. Chem. 249, 7789-7807.

42. Fujikawa, K., Legaz, M.E., and Davie, E.W. (1972): Biochemistry 11, 4882-91.

43. Fujikawa, K., Coan, M.H., Legaz, M.E., and Davie, E.W. (1974): Biochemistry 11, 4892-4899.

44. Barton, P.G., and Radcliffe, R.D. (1973): J. Biol. Chem. 248, 6788-6795.

45. Furie, B.C., and Furie, B.J. (1975): J. Biol. Chem. 250, 601-608.

46. Radcliffe, R.D., and Barton, P.G. (1972): J. Biol. Chem. 247, 7735-7742.

47. Reekers, P.P.M., Lindhout, M.J., Kop-Klassen, B.M.H., and Hemker, H.C. (1973): Biochim. Biophys. Acta 317, 559-562.

48. Howard, J.B., and Nelsestuen, G.L. (1975): Proc. Natl. Acad. Sci. U.S.A. 72, 1281-1285.

49. Jackson, C.M. (1972): Biochemistry 11, 4873-4882.

50. Hanahan, D.J., Subbaiah, P.V., Bajwa, S.S., and Smith, C.M. (1976): Biochim. Biophys. Acta 444, 131-146.

51. Nelsestuen, G.L., Broderius, M., Zytkovicz, T.H., and Howard, J.B. (1975): Biochem. Biophys. Res. Commun. 65, 233-240.

52. Barton, P.G., and Day, W.C. (1972): Biochim. Biophys. Acta 261, 457-468.

53. Kandall, C.L., Shohet, S.B., Akinbami, T.K., and Colman, R.W. (1975): Thrombos. Diathes. Haemorrh. 34, 271-284.

54. Barton, P.G., and Hanahan, D.J. (1967): Biochim. Biophys. Acta 133, 506-518.

55. Kahn, M.J.P., and Hemker, H.C. (1972): Thrombos. Diathes. Haemorrh. 29, 25-32.

56. Day, W.C. (1975): Biochim. Biophys. Acta 386, 352-361.

57. Esmon, C.T., and Jackson, C.M. (1973): Thromb. Res. 2, 509-524.

58. Papahadjopoulos, D., Hougie, C., and Hanahan, D.J. (1964): Biochemistry 3, 264-270.

59. Jackson, C.M., Esmon, C.T., Owen, W.G., and Duiguid, D.L. (1973): Biochim. Biophys. Acta 310, 289-294.

60. Esmon, C.T., and Jackson, C.M. (1974): J. Biol. Chem. 249, 7791-7797.

61. Bangham, A.D. (1961): Nature 192, 1197-1198.

62. Papahadjopoulos, D., Hougie, C., and Hanahan, D.J. (1962): Proc. Soc. Exper. Biol. Med. 111, 412-416.

63. Barton, P.G., and Jevons, S. (1970): Chem. Phys. Lipids 4, 289-310.

64. Bull, R.K., Jevons, S., and Barton, P.G. (1972): J. Biol. Chem. 247, 2747-2754.

65. Hemker, H.C., Kahn, M.J.P., and Devilee, P.P. (1970): Thrombos. Diathes. Haemorrh. 24, 214-223.

66. Hemker, H.C., and Kahn, M.J.P. (1972): Thromb. Diathes. Haemorrh. 29, 33-42.

67. Vroman, L. (1964): Thrombos. Diathes. Haemorrh. 10, 455-493.

68. Sterzing, P.R., and Barton, P.G. (1973): Chem. Phys. Lipids 10, 137-148.

69. Daemen, F.J.M., van Arkel, C., Hart, H.Ch., van der Drift, C., Van Deenen, L.L.M. (1969): Thrombos. Diathes. Haemorrh. 13, 195-217.

70. Yang, S.F., Freer, S., and Benson, A.A. (1967): J. Biol. Chem. 242, 477-484.

71. Joutti, A., and Renkomen, O. (1976): Chem. Phys. Lipids 17, 264-267.

72. Muller, R.J., and Finkelstein, A. (1972): J. Gen. Phys. 60, 285-306.

73. Papahadjopoulos, D., and Ohki, S. (1970): In: Liquid Crystals and Ordered Fluids. Plenum Press, 13-57.

74. Papahadjopoulos, D. (1971): Biochim. Biophys. Acta 241, 254-259.

75. Tocanne, J.F., Ververgaert, P.H.J.Th., Verkleij, A.J., and Van Deenen, L.L.M. (1974): Chem. Phys. Lipids 12, 201-219.

76. Verkleij, A.J., de Kruyff, B., Ververgaert, P.H.J.Th., Tocanne, J.F., and Van Deenen, L.L.M. (1974): Biochim. Biophys. Acta 339, 432-437.

77. Ververgaert, P.H.J.Th., de Kruyff, B., Verkleij, A.J., Tocanne, J.F., and Van Deenen, L.L.M. (1975): Chem. Phys. Lipids 14, 97-101.

78. Mabrey, S., Sturtevant, J.M. (1976): Proc. Natl. Acad. Sci. U.S.A. 73, 3862-3866.

79. Van Dijck, P.W.M., Ververgaert, P.H.J.Th., Verkleij, A.J., Van Deenen, L.L.M., and de Gier, J. (1975): Biochim. Biophys. Acta 406, 465-478.

80. Jacobsen, K., and Papahadjopoulos, D. (1975): Biochemistry 14, 152-161.

81. Papahadjopoulos, D., Vail, W.J., Pangborn, W.A., and Poste, G. (1976): Biochim. Biophys. Acta 448, 265-283.

82. Abramson, M.B., Katzman, R., and Gregor, H.P. (1964): J. Biol. Chem. 239, 70-76.

83. Barton, P.G., and Jevons, S. (1970): Chem. Phys. Lipids 4, 289-310.

84. Hendrickson, S.H., and Fullington, J.G. (1965): Biochemistry 4, 1599-1605.

85. Barton, P.G. (1967): J. Biol. Chem. 243, 3884-3890.

86. Papahadjopoulos, D., and Bangham, A.D. (1966): Biochim. Biophys. Acta 126, 181-184.

87. Hauser, H., Chapman, D., and Dawson, R.M.C. (1969): Biochim. Biophys. Acta 183, 320-333.

88. Papahadjopoulos, D. (1968): Biochim. Biophys. Acta 163, 240-254.

89. Phillips, C.G.S., and Williams, R.J.P. (1966): In: Inorganic Chemistry, Clarendon Press, Oxford, Vol. 2, 80-86.

90. Ohnishi, S., and Ito, T. (1973): Biochem. Biophys. Res. Commun. 51, 132-138.

91. Ohnishi, S., and Ito, T. (1974): Biochemistry 13, 881-887.

92. Ito, T., and Ohnishi, S. (1974): Biochim. Biophys. Acta 352, 29-37.

93. Galla, H.J., and Sackmann, E. (1975): Biochim. Biophys. Acta 401, 509-529.

94. Hauser, H., Finer, E.G., and Darke, A. (1977): Biochem. Biophys. Res. Commun. 76, 267-274.

95. Papahadjopoulos, D., Poste, G., and Schaeffer, B.E. (1973): Biochim. Biophys. Acta 323, 23-42.

96. Papahadjopoulos, D., Vail, W.J., Newton, C., Nir, S., Jacobson, K., Poste, G., and Lazo, R. (1977): Biochim. Biophys. Acta 465, 579-598.

97. Papahadjopoulos, D., Vail, W.J., Jacobson, K., and Poste, G. (1975): Biochim. Biophys. Acta 394, 483-491.

98. Papahadjopoulos, D., and Bangham, A.D. (1966): Biochim. Biophys. Acta 126, 185-188.

99. Papahadjopoulos, D., Poste, G., Schaeffer, B.E., and Vail, W.J. (1974): Biochim. Biophys. Acta 352, 10-28.

100. Papahadjopoulos, D., Jacobson, K., Nir, S., and Isac, T. (1973): Biochim. Biophys. Acta 311, 330-348.

101. Marsh, D., Watts, A., and Knowles, P.F. (1976): Biochemistry 15, 3570-3578.

102. Blok, M.C., van der Neut-Kok, E.C.M., Van Deenen, L.L.M., and de Gier, J. (1975): Biochim. Biophys. Acta 406, 187-196.

103. Tsong, T.Y., Greenberg, M., and Kanehisa, M.I. (1977): Biochemistry 16, 3115-3121.

104. Barton, P.G., and Gunstone, F.D. (1975): J. Biol. Chem. 250, 4470-4476.

105. Lea, C.H., Rhodes, D.N., and Stoll, R.D. (1955): Biochem. J. 60, 353-363.

106. Hanahan, D.J., Dittmer, J.C., and Warashima, E. (1957): J. Biol. Chem. 228, 685-700.

107. Sanders, H. (1967): Biochim. Biophys. Acta 144, 485-487.

108. Rouser, G., Kritchevsky, G., Heller, D., and Leiber, E. (1963): J. Amer. Oil Chem. Soc. 40, 425-453.

109. Bell, W.N., and Alton, H.G. (1954): Nature 174, 880-881.

110. Baer, E., and Buchnea, D. (1958): J. Biol. Chem. 232, 895-901.

111. Cubero-Robles, E., and van den Berg, D. (1969): Biochim. Biophys. Acta 187, 520-526.

112. Le Cocq, J., and Ballou, C.E. (1964): Biochemistry 3, 976-980.

113. Dawson, R.M.C. (1967): Biochem. J. 102, 205-210.

114. Bligh, E.G., and Dyer, W.J. (1959): Can. J. Biochem. and Phys. 37, 911-917.

115. King, E.J. (1932): Biochem. J. 26, 292-299.

116. Brockerhoff, H. (1965): Archives Biochem. and Biophys. 110, 586-592.

117. Ladbrooke, B.D., Williams, R.M., and Chapman, D. (1968): Biochim. Biophys. Acta 150, 333-340.

118. Tocanne, J.F., Verheij, H.M., Op Den Kamp, J.A.F., and Van Deenen, L.L.M. (1974): Chem. Phy. Lipids 13, 389-403.

119. Birdsall, N.J.M., Feeney, J., Lee, A.G., Levine, Y.K., and Metcalfe, J.C. (1972): J.C.S. (Perkins II) 1441-1445.

120. Hjort, P., Rapaport, S.I., and Owren, P.A. (1955): J. Lab. and Clin. Med. 46, 89-97.

121. Bachmann, F., Duckert, F., and Koller, F. (1958): Thrombosis 2, 24-38.

122. Stothers, J.B. (1972): Carbon-13 NMR Spectroscopy, Academic Press, p.49.

123. Phillips, M.C., Williams, R.M., and Chapman, D. (1969): Chem. Phys. Lipids 3, 234-244.

124. Demel, R.A., Jansen, J.W.C.M., Van Dijck, P.W.M., and Van Deenen, L.L.M. (1977): Biochim. Biophys. Acta 465, 1-10.

125. Abramson, M.B., Katzman, R., Wilson, C.E., and Gregor, H.P. (1964): J. Biol. Chem. 239, 4066-4072.

126. Abramson, M.B., Colacicco, G., Curci, R., and Rapport, M.M. (1968): Biochemistry 7, 1692-1698.

127. Finer, E.G., Flook, A.G., and Hauser, H. (1972): Biochim. Biophys. Acta 260, 49-55.

128. Wills, M.C., Tinker, D.O., and Pinteric, L. (1972): Biochim. Biophys. Acta 241, 483-493.

129. Trauble, H., and Eibl, H. (1974): Proc. Natl. Acad. Sci. U.S.A. 71, 214-219.

130. Trauble, H., Teubner, M., Woolley, P., and Eibl, H. (1976): Biophys. Chem. 4, 319-342.

131. Jahnig, F. (1976): Biophys. Chem. 4, 309-318.

132. Yi, P.N., and MacDonald, R.C. (1973): Chem. Phys. Lipids 11, 114-134.

133. Oldfield, E., Marsden, J., and Chapman, D. (1971): Chem. Phys. Lipids 7, 1-8.

134. Sheetz, M.P., and Chan, S.I. (1972): Biochemistry 11, 4573-4581.

135. Gally, H., Neiderberger, N., and Seelig, J. (1975): Biochemistry 14, 3647-3652.

136. Rand, R.P., Chapman, D., and Larsson, K. (1975): Biophys. J. 15, 1117-1124.

137. Janiak, M.J., Small, D.M., and Shipley, G.G. (1976): Biochemistry 15, 4575-4580.

138. Klopfenstein, W.E., de Kruyff, B., Verkleij, A.J., Demel, R.A., and Van Deenen, L.L.M. (1974): Chem. Phys. Lipids 13, 215-222.

139. Chapman, D., Peel, W.E., Kingston, B., and Lilley, T.H. (1977): Biochim. Biophys. Acta 260-275.

140. Bugg, C.E. (1973): J. Amer. Chem. Soc. 95, 908-913.

141. Cook, W.J., and Bugg, C.E. (1973): J. Amer. Chem. Soc. 6442-6446.

142. Balchin, A.A., and Carlisle, C.H. (1965): Acta Crystallogr. 19, 103-109.

143. Hinz, H.J., and Sturtevant, J.M. (1972): J. Biol. Chem. 247, 3697-3700.

144. Lee, A.G., Birdsall, N.J.M., Metcalfe, J.C., Toon, P.A., and Warren, G.B. (1974): Biochemistry 13, 3699-3705.

145. Baldassare, J.J., Rhinehart, K.B., and Silbert, D.F. (1976): Biochemistry 15, 2986-2994.

146. Edidin, M. (1974): Ann. Rev. Biophys. Bioeng. 3, 179-201.

147. Phillips, M.C., Graham, D.E., and Hauser, H. (1975): Nature 254, 154-156.

148. Colman, R.W., Kandall, C.L., Shohet, S.B., and Akinbami, T.K. (1976): Thrombos. Diathes. Haemorrh. 34, 256-270.